TRANSPORTATION RESEARCH RECORD 922

# Improving Estimates from Flood Studies

TRANSPORTATION RESEARCH BOARD

NATIONAL RESEARCH COUNCIL
NATIONAL ACADEMY OF SCIENCES
WASHINGTON, D.C. 1983

**Transportation Research Record 922**
Price $9.20
Edited for TRB by Naomi Kassabian

mode
1 highway transportation
3 rail transportation

subject area
22 hydrology and hydraulics

**Library of Congress Cataloging in Publication Data**
National Research Council. Transportation Research Board.
Improving estimates from flood studies.

(Transportation research record; 922)
1. Flood forecasting—Addresses, essays, lectures. I. National Research Council (U.S.). Transportation Research Board. II. Series.
TE7.H5 no. 922 380.5s [551.48'9] 84-3299 [GB1399.2]
ISBN 0-309-03611-9 ISSN 0361-1981

# Contents

# Authors of the Papers in This Record

Baker, Victor R., Department of Geosciences, University of Arizona, Tucson, Ariz. 85721
Boggess, William R., Laboratory of Tree-Ring Research, University of Arizona, Tucson, Ariz. 85721
Chery, Donald L., Jr., U.S. Nuclear Regulatory Commission, Washington, D.C. 20555; formerly with Dames and Moore
McCuen, Richard H., Department of Civil Engineering, University of Maryland, College Park, Md. 20742
Miller, Norman, Soil Conservation Service, U.S. Department of Agriculture, 10,000 Aerospace Road, Lanham, Md. 20706
Osborn, Herbert B., Southwest Watershed Research Center, U.S. Department of Agriculture, 442 East Seventh Street, Tucson, Ariz. 85705
Shen, Hsieh Wen, Department of Civil Engineering, Colorado State University, Fort Collins, Colo. 80521
Stockton, Charles W., Laboratory of Tree-Ring Research, University of Arizona, Tucson, Ariz. 85721
Taylor, Stewart W., Bechtel Civil and Minerals, Inc., P.O. Box 3965, San Francisco, Calif. 94119
Traille, Leon A., Dames and Moore, 7101 Wisconsin Avenue, Bethesda, Md. 20814
Wahl, Kenneth L., U.S. Geological Survey, Box 25046, Denver Federal Center, Denver, Colo. 80225

# Determining Streamflow Characteristics Based on Channel Cross-Section Properties

KENNETH L. WAHL

Channel dimensions have proved to be valid indicators of streamflow characteristics. Use of channel geometry requires definition of a relation between the desired flow characteristic and stream-channel size based on data at gaging stations; estimates of the flow characteristic can then be made at ungaged sites by obtaining the channel dimensions. Regional analyses have been made in many western states and in some eastern states by the U.S. Geological Survey. These analyses are summarized and some results are compared. Three reference levels have been used to define the channel dimensions. The principal differences between the channel-geometry approach and conventional approaches that use basin characteristics are that (a) the ungaged site must be visited to measure the channel size before an estimate can be made and (b) some field training is required before an individual can identify the channel reference level. Variability among channel measurements by trained individuals effectively increases the error of the estimate over the standard error of the estimate defined during calibration. The increase is dependent on the variability in channel type, but extremely variable conditions could increase a calibration error of 42 percent to an application error of 55 percent.

Engineers and hydrologists frequently are required to estimate flow characteristics at ungaged sites. Conventional techniques have used relations between flow characteristics and physical characteristics of drainage basins, such as size of drainage area, to transfer information to ungaged sites. Flow characteristics in arid and semiarid regions, however, generally are only poorly related to the size of the drainage basin. Relations between flow characteristics and stream-channel size offer a promising alternative.

That streams are the authors of their channels has long been recognized; nevertheless, methods of quantifying the interrelation between flow characteristics of rivers and channel size have developed only in recent years. The regime concept, as originated by Kennedy and Lindley (1) for canals in India and Pakistan, gave empirical relations for the hydraulic properties of stable canals. This concept, however, was not extended to natural rivers in the United States until half a century later.

The initial impetus for the studies of canals stemmed from the need for improved design techniques. Similarly, the early work with rivers was oriented toward expressing channel dimensions as functions of a formative or dominant discharge. In recent years efforts have begun to focus on using the dimensions of the stream channel as indexes of flow characteristics, particularly flood-frequency characteristics. These approaches are not unrelated; nevertheless, the latter approach does not require definition of a dominant discharge.

The purpose of this paper is to examine the evolution of relations between dimensions of river channels and discharge characteristics, to summarize the regional relations that have been developed, and to examine the sources of error. The focus will be on attempts to use these relations as tools in estimating flow characteristics of rivers; the emphasis will be on flood characteristics rather than on use of the information in channel design. Consequently, the regime concept as it relates to canals only will be considered in relation to its bearing on rivers. Because of the emphasis on regional relations, the variation at a station of hydraulic geometry exponents is not included.

## HYDRAULIC-GEOMETRY APPROACH

A channel is considered to be in regime if it can accommodate its flow for 1 yr or more without a net change in hydraulic characteristics (2). Within that period, scour or deposition may occur in either the lateral or vertical direction as long as they are transient phenomena.

The morphology of regime canals has been the subject of many investigations since Kennedy (1) stated his empirical equation of nonscouring velocity for the canals of Punjab in 1895. The basic principle generally was not applied to rivers in the United States, however, until Leopold and Maddock (3) reported their analysis of the relationships between hydraulic properties of the cross section and river discharge. They theorized that the hydraulic geometry of river channels in approximate equilibrium could be expressed as exponential functions of discharge such that

$$W = aQ^b \quad (1)$$

$$D = cQ^f \quad (2)$$

$$V = kQ^m \quad (3)$$

where

W = width,
D = mean depth,
V = mean velocity,
Q = discharge, and
a,c,k,b,f, and m = numerical constants.

The numerical constants for the above relations were developed empirically from data collected on rivers representing a variety of hydrologic conditions. Mean annual discharge was used as the independent variable, because it provided a discharge of approximately the same frequency throughout the area of investigation, which permitted comparison between relations. The values of the exponents b, f, and m were relatively constant, and the average values agreed quite closely with previously defined values for regime canals. The coefficients a, c, and k, however, varied between river systems.

Leopold and Maddock (3) were not the first to apply the regime concept to rivers, although their analysis was one of the first to gain wide acceptance. In 1935 Lacey extended his earlier empirical equations for Punjab canals by including limited data for rivers from the United States, Europe, and Punjab (4); however, he grouped river data by discharge and used averages. Pettis (5) independently developed similar regime equations based on natural streams in the Miami River basin of Ohio. Pettis' relations were intended for use in river channelization; therefore, his discharge was a flood discharge, apparently near the bank-full stage (5, p. 150).

In 1947 Rybkin (6) developed a set of relations based on rivers in the upper Volga and Oka basins of the U.S.S.R. These relations were in terms of long-term average discharge and river gradient but contained a modulus term that permitted computation of the hydraulic properties for discharges other than

the long-term mean. Rybkin's hydraulic-geometry variables, like those of Leopold and Maddock (3), were properties at the particular discharge rather than dimensions based on a specific feature of the channel. In 1950 Altunin confirmed that the general regime equation for width with b = 0.50 was valid for rivers of central Asia. He also concluded that the coefficient a varied with slope to the -0.20 power. Whether the width used in Altunin's analysis is based on a specific channel feature is not clear, but Kondrat'ev (6) gives some insight when he observes, "[Altunin's] formulas are true only for a certain channel-forming discharge, whose value is taken as that of discharges with a 10-20 percent reliability. These discharges are usually accommodated within the height of the channel edges."

Most of the preceding studies, including the 1953 work of Leopold and Maddock, although furthering the status of knowledge, were of limited practical value because the hydraulic-geometry variables used were those of specific discharges and could not be identified with recognizable channel features. Thus the analysis by Wolman (7) of the Brandywine Creek drainage in Pennsylvania, in which he related hydraulic geometry to bank-full discharge, was significant. In addition, he analyzed the hydraulic-geometry relationships with flows of 50, 15, and 2 percent duration. The recurrence interval of flows exceeding the bank-full stage on Brandywine Creek ranged between 1 and 3 yr and averaged 2.2 yr.

Although simple in concept, the bank-full stage may be interpreted in a number of different ways, each associated with different values of width and depth and yielding a different bank-full discharge. Williams (8) gave a comprehensive review of definitions of bank-full stage. He identified and discussed 11 definitions that have been used by investigators. He also concluded (8, p. 1141): "Bank-full discharge does not have a common recurrence frequency among the rivers studied, and the discharge corresponding to the 1.5-year recurrence interval in most cases does not represent the bank-full discharge."

Most later investigations of hydraulic geometry by Wolman (7) were directed at one or more of the following problems:

1. Physically identifying the bank-full stage,
2. Determining the significance (such as the recurrence interval) of bank-full discharge,
3. Determining the exponents in the hydraulic-geometry equations either theoretically or empirically for a specific region or channel type, or
4. Application of the concept to solve practical problems.

Except for the theoretical analyses, many studies involve several of the classifications. The hydraulic-geometry exponents for selected empirical and theoretical studies are summarized in Table 1.

## DISCHARGE RELATED TO CHANNEL DIMENSIONS

Ideally, a channel feature used as an index to discharge should be a unique, recognizable feature of the channel. It should also be active, that is, free to adjust to changes in the flow regime. This thinking, and a need for a reconnaissance technique to estimate discharge characteristics at ungaged sites, led to the recent attempts to relate an active, within-channel feature to discharge characteristics. The approach was apparently first suggested in 1966 by W.B. Langbein of the U.S. Geological Survey.

The concept as well as the feature differed from the earlier work. With the bank-full-stage concept, the emphasis had been on relating the bank-full channel properties (dependent variables) to some formative or dominant discharge (independent variable). Langbein's suggested approach by using the within-channel feature was to empirically relate the average annual discharge, as the dependent variable, to dimensions of recognizable active features of the channel. This permits estimates of the discharge characteristic to be made at ungaged sites on the basis of channel dimensions. The approach infers that the discharge characteristic to be estimated is related directly to the formative discharge of streams in the area of investigation but does not require identification of that formative discharge.

Several reference levels have been used; the levels are referred to in this paper as the section defined by within-channel bars, the active-channel

**Table 1. Exponents of discharge in regime equations for width (b), depth (f), and velocity (m).**

| Region and Literature Reference | b | f | m | Discharge |
|---|---|---|---|---|
| Empirical Study | | | | |
| Indian canals and rivers (4) | 0.50 | 0.333 | 0.167 | Equilibrium |
| Miami River, Ohio (5) | 0.50 | 0.30 | 0.20 | Bank-full |
| Volga and Oka basins, USSR (6) | 0.57 | 0.22 | 0.21 | Mean annual |
| Midwest United States (3) | 0.50 | 0.40 | 0.10 | Mean annual |
| Brandywine Creek, Pennsylvania (7) | 0.58 | 0.40 | 0.02 | 2 percent duration |
| Ephemeral streams in Southwest (9) | 0.50 | 0.30 | 0.20 | Mean annual |
| Rivers in England and Wales (10, 11) | 0.53 | 0.27 | 0.20 | Bank-full |
| Appalachian streams (12, pp. 145-181) | 0.55 | 0.36 | 0.09 | Bank-full |
| Canadian rivers and Colorado canals (13) | 0.50 | 0.40 | 0.10 | 3- to 5-yr flood |
| Illinois rivers (14) | 0.48 | 0.36 | 0.16 | Of measurement |
| Average for Alaska rivers (15) | 0.50 | 0.35 | 0.15 | Bank-full |
| Rivers in central Idaho (16) | 0.54 | 0.34 | 0.12 | Bank-full |
| Colorado gravel-bed streams[a] (17) | 0.480 | 0.374 | 0.146 | Bank-full |
| Theoretical Approach | | | | |
| Leopold and Langbein (18) | 0.55 | 0.36 | 0.09 | |
| Langbein (19, 20) | 0.50 | 0.37 | 0.13 | |
| Acker (21) | 0.53 | 0.35 | 0.12 | |
| Engelund and Hansen (22) | 0.525 | 0.317 | 0.158 | |
| Joering (23) | 0.50 | 0.375 | 0.125 | |
| Smith (24) | 0.6 | 0.3 | 0.1 | |
| Li, Simons, and Stevens (25) | 0.46 | 0.46 | 0.08 | |

[a] Average of values for thick and light bank vegetation.

Figure 1. Commonly used reference levels.

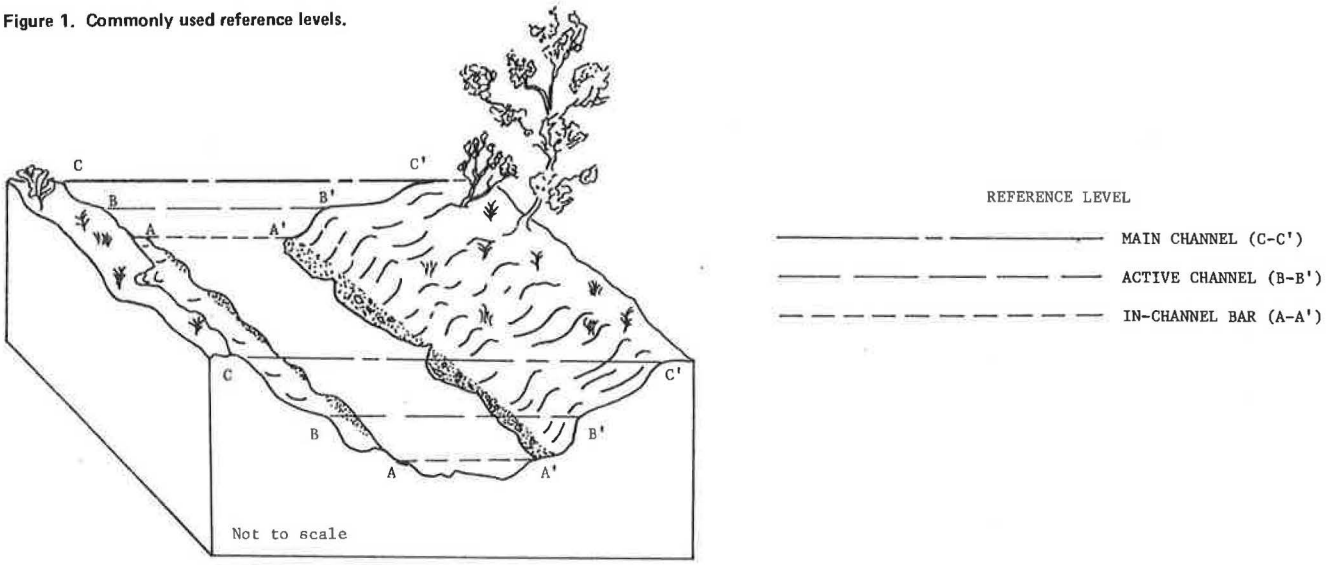


section, and the main-channel section [Figure 1 (26)]. Regional investigations by hydrologists of the U.S. Geological Survey are summarized in Table 2 by the reference level used. Those studies and other investigations are discussed in the sections that follow.

## Within-Channel Bars

Langbein suggested a reference level defined by the tops of point bars that are (a) the highest bed forms of which the particles are subject to annual sediment movement and (b) the lowest prominent bed forms. He also noted that the reference level could be related to vegetation zones if (a) the channel below the reference level generally is free of non-aquatic vegetation; (b) the zone between the tops of the bars and the floodplain is occupied by annuals (forbs and grasses); and (c) the true floodplain is occupied by shrubs. The within-channel bar has been described in more detail by Moore (27); Hedman (28); and Hedman, Moore, and Livingston (29).

Early studies using the within-channel bar defined relations only for mean annual flow. More recent investigations also have defined relations for floods of selected frequency. Relations between the 10-yr flood and within-channel bar width are compared for selected studies in Figure 2.

The first published analysis that used the within-channel feature was that by Moore (27) for streams in Nevada. He graphically related mean annual discharge to the width and average depth of the channel cross section defined by the tops of the channel bars and gave separate results for perennial and ephemeral streams.

In a related study, Hedman (28) equated mean annual flow of 48 California streams to the dimensions of the cross section defined by the within-channel bars. Like Moore (27), he developed separate relations for ephemeral (20 sites) and perennial (28 sites) streams.

Kopaliani and Romashin (31) analyzed relations between the flood-channel width and the 2-yr flood for rivers in western Georgia, U.S.S.R. Based on the following description of the flood channel, the width used seems to be compatible with the within-channel feature treated in this section (31): "The flood channel is that part of the valley which is systematically flooded by high water and within which sediments are continuously redistributed so that there is no vegetation. On mountain rivers it is a wide gravelly-bouldery strip, which dries out during the low-water period. Its relief consists of gentle mobile placer deposits of the side-bar or midstream-bar type." In a logarithmic plot relating 2-yr flood and flood-channel width, the data separate into three distinct but parallel groups. In order of decreasing discharge for a given width, they were braided reaches, reaches with mid-channel and side-channel bars, and meandering reaches. Although Kopaliani and Romashin were defining width as a function of discharge (and gradient), Wahl deduced a relation of

$$Q = aW^{1.5} \quad (4)$$

from a plot of their data. This general relation

Table 2. Summary of regional analyses by U.S. Geological Survey.

| Region and Literature Reference | Characteristic Used: Year Published | Mean Annual Flow | Flood Flows |
|---|---|---|---|
| **Within-Channel-Bar Section** | | | |
| Nevada (27) | 1968 | X | – |
| Coastal and southern California (28) | 1970 | X | – |
| Kansas (29) | 1972 | X | – |
| Colorado (perennial streams) (30) | 1972 | X | X |
| Nevada (31) | 1974 | – | X |
| Utah (32) | 1975 | X | X |
| Missouri River basin[a] (33) | 1977 | X | X |
| **Active-Channel Section** | | | |
| Kansas (34) | 1974 | X | X |
| New Mexico (35) | 1976 | – | X |
| Missouri River basin[a] (33) | 1977 | X | X |
| Western United States (34) | 1982 | X | X |
| Kansas (regulated streams) (35) | 1981 | X | – |
| Ohio (36) | 1981 | – | X |
| Tennessee (Cumberland Plateau) (37) | 1981 | X | X |
| Missouri River basin (26) | 1982 | X | X |
| **Main-Channel Section** | | | |
| Western mountain areas (38) | 1974 | – | X |
| Wyoming (39) | 1976 | X | X |
| Owyhee County, Idaho (40) | 1976 | – | X |
| Idaho (41) | 1980 | – | X |

[a]Includes both the within-channel bar and active-channel section.

Figure 2. Relations between 10-yr flood and within-channel bar width.

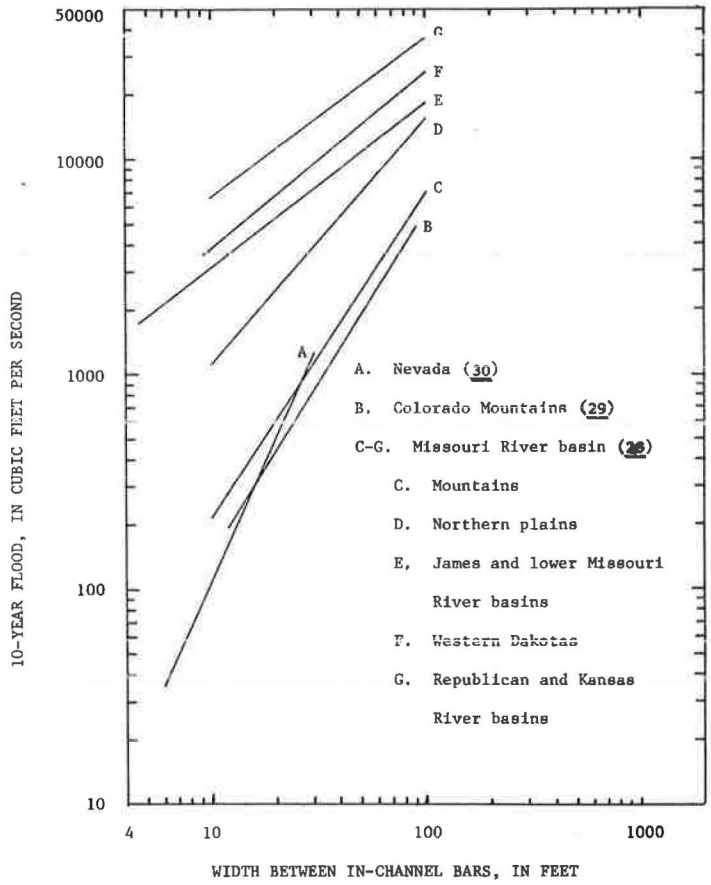


would apply to all three classes of streams, but the constant of proportionality (a) would vary; average standard error of the estimate (graphical) would be in the range of 30 to 40 percent.

Equations for estimating mean annual flow from channel geometry in Kansas were developed by Hedman and Kastner (32). They used the within-channel bar and gave separate results for perennial and ephemeral streams.

One of the first studies to relate flood characteristics to channel dimensions in the United States was done by Hedman, Moore, and Livingston (29). They related mean annual discharge and 2-, 5-, 10-, 25-, and 50-yr flood peaks to width and mean depth of the within-channel cross section for perennial streams in Colorado. The standard errors of the estimate for their flood equations ranged from about 30 to 45 percent and were significantly less than comparable conventional relations between flood characteristics and basin characteristics. Including mean depth and drainage area in the equations did not significantly decrease the standard errors nor did the use of a second-degree polynomial.

DeWalle and Rango (33) used data from 27 small basins (19.59 to 303.44 acres) in Maryland, New Hampshire, New Jersey, Pennsylvania, Vermont, and West Virginia to develop linear relations between the logarithms of mean annual flood and properties of the channel cross section. Their channel width was defined as the horizontal distance from the top of the lowest bank to the opposite bank wall. The description seems to be consistent with that of the within-channel bar based on their statement: "The more obvious upper banks which may be associated with a discharge greater than the mean annual flow were discarded." The results are of limited practical use because only 34 percent of the sample variance was explained by an equation using width; a relation that used only precipitation explained 83 percent of the sample variance. In an earlier study of small drainage areas in the Sleeper's River basin of northern Vermont, Zimmerman, Goodlett, and Comer (34) found that stream width did not increase in the downstream direction for a drainage area less than 0.8 mile$^2$. They attributed this to the effect of vegetation, mostly tree roots, and to relatively small annual peak discharges. This may partly explain the poor results obtained by DeWalle and Rango (33).

Moore (30) extended his earlier study (27) for Nevada to include the 10-yr flood characteristic. He developed separate relations for perennial and ephemeral streams. The 10-yr flood was a function of both width and depth for ephemeral streams but was related only to width for perennial streams.

Fields (34a) developed statewide relations for the mean annual discharge and the 25-yr and 50-yr floods in Utah by using the within-channel bar. The state was divided into three hydrologic areas for floods, and separate relations were developed for the individual areas; flood flows were related to only the width of the section.

In one of the first studies of a large geographical region, Hedman and Kastner (35) related mean annual flow and flood flows for the Missouri River basin to the width of both the within-channel bar and the active channel. Relations also were defined between the flow characteristics and conventional basin characteristics. The basin was divided into six hydrologic areas for both mean annual flow and floods, but the regions for mean annual flow generally differed from those for floods. Standard er-

Figure 3. Relations between 10-yr flood and active-channel width.

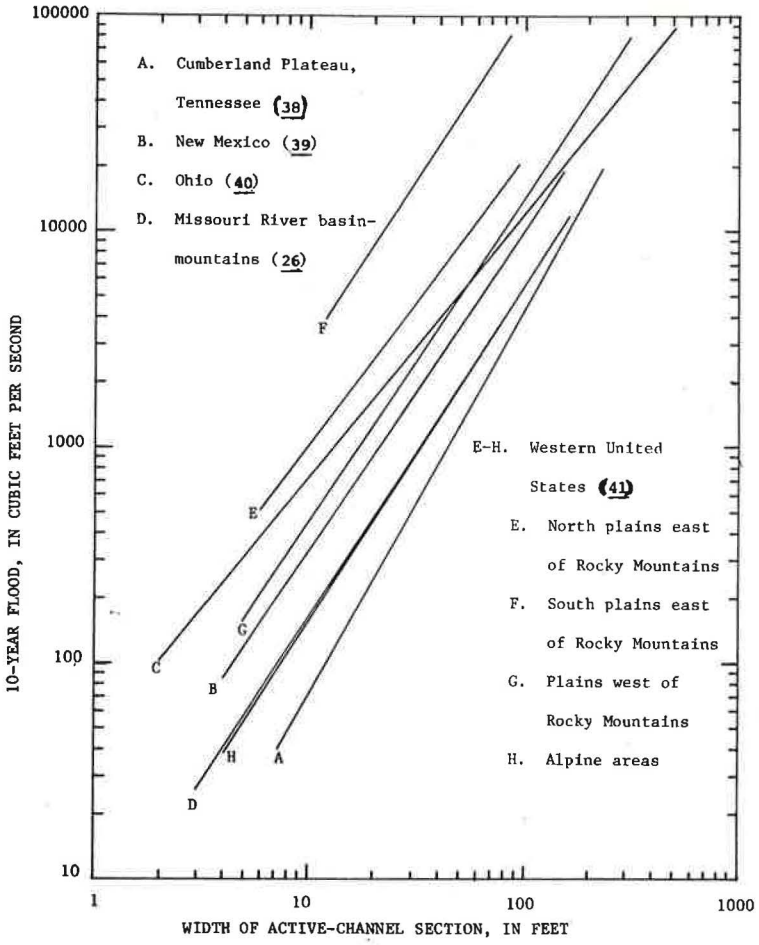


rors of the estimate were comparable for relations that used the width of the within-channel bar and the width of the active channel; however, standard errors of relations based on drainage area and climatic characteristics generally were greater except for mean annual flow in southwestern Iowa and northern Missouri.

## Active-Channel Section

While studying Kansas streams in 1972, E.R. Hedman of the U.S. Geological Survey recognized a channel feature somewhat higher than the within-channel bars that had been used previously. He first referred to this feature as the active floodplain but redefined it as the active channel (36). In effect it is a side bar that would no longer be called a bed feature. Because of annual vegetation, the feature virtually has become a part of the bank, but it is still well within the overall channel. The active channel was described by Osterkamp and Hedman (37, p. 256) as

> a short-term geomorphic feature subject to change by prevailing discharges. The upper limit is defined by a break in the relatively steep bank slope of the active channel to a more gently sloping surface beyond the channel edge. The break in slope normally coincides with the lower limit of permanent vegetation so that the two features, individually or in combination, define the active-channel reference level. The section beneath the reference level is that portion of the stream entrenchment in which the channel is actively, if not totally, sculptured by the normal process of water and sediment discharge.

The active-channel section has since been used in numerous studies to define mean annual and flood flows in the western states and in selected eastern states. These investigations are summarized in Table 2, and 10-yr flood relations are compared for selected studies in Figure 3.

The active-channel section was first used by Hedman, Kastner, and Hejl (36) to define flood-frequency relations in Kansas. They proposed that because the active-channel feature was formed by infrequent flows, the active-channel section was a better descriptor of floods than was the within-channel-bar section.

Scott and Kunkler (39) related the width of the active channel to characteristics of the 2- through 50-yr floods in New Mexico. One set of relations was used for the state; however, an area in the southeastern part of the state was excluded because the channels were actively entrenching. The relations using channel width gave significantly smaller standard errors of the estimate than similar relations that used basin and climatic characteristics.

A similar study for Ohio (40) defined one set of equations that could be used statewide to estimate the 2- through 100-yr floods; the average standard errors of the estimate ranged from 42 to 55 percent.

Glazzard (38) defined relations for the mean annual flow and 2- through 100-yr floods in the Cumberland Plateau, Tennessee, by using the active-

channel width. The average standard errors of estimate were about 60 percent for floods. He also used variables representing stream gradient and percentage of silt, clay, and coal in stream-bank material. Although the additional variables produced some decrease in standard error for mean annual flow, there was no improvement in the flood relations.

Hedman and Osterkamp (41) used the active-channel section in an analysis of mean annual and flood characteristics (2- through 100-yr floods) for the western half of the conterminous United States. Their final equations expressed the flow characteristics as functions of only the active-channel width. For floods, the area was subdivided into four areas based on similarity of climatic conditions. The four areas were (a) alpine and pine forested, (b) northern plains east of the Rocky Mountains, (c) southern plains east of the Rocky Mountains, and (d) plains and intermontane areas west of the Rocky Mountains. Their results are shown in Table 3 (41).

Osterkamp and Hedman (26) expanded on the earlier Missouri River basin study by Hedman and Kastner (35) by considering the effect of channel-sediment properties, channel gradient, and discharge variability. They concluded (35, p. 1): "Results show that channel width is best related to variables of discharge, but that significant improvement, or reduction of the standard errors of estimate, can be achieved by considering channel-sediment properties, channel gradient, and discharge variability." They did not include terms in the regression relations to represent the additional factors; instead, the data were stratified based on those factors, and each group of data was analyzed separately.

Table 3. Equations for determining flood-frequency discharge for streams in western United States.

| Areas of Similar Climatic Characteristics | Equation[a] | Standard Error of Estimate (%) |
|---|---|---|
| Alpine and pine forested | $Q_2 = 1.3W_{AC}^{1.65}$ | 44 |
| | $Q_{10} = 4.4W_{AC}^{1.55}$ | 38 |
| | $Q_{25} = 70W_{AC}^{1.50}$ | 42 |
| | $Q_{50} = 9.6W_{AC}^{1.45}$ | 45 |
| | $Q_{100} = 13W_{AC}^{1.40}$ | 50 |
| Northern plains east of Rocky Mountains | $Q_2 = 4.8W_{AC}^{1.60}$ | 62 |
| | $Q_{10} = 46W_{AC}^{1.35}$ | 40 |
| | $Q_{25} = 61W_{AC}^{1.30}$ | 44 |
| | $Q_{50} = 130W_{AC}^{1.30}$ | 50 |
| | $Q_{100} = 160W_{AC}^{1.25}$ | 58 |
| Southern plains east of Rocky Mountains[b] | $Q_2 = 7.8W_{AC}^{1.70}$ | 66 |
| | $Q_{10} = 84W_{AC}^{1.55}$ | 56 |
| | $Q_{25} = 180W_{AC}^{1.50}$ | 57 |
| | $Q_{50} = 270W_{AC}^{1.50}$ | 59 |
| | $Q_{100} = 370W_{AC}^{1.50}$ | 62 |
| Plains and intermontane areas west of Rocky Mountains | $Q_2 = 1.8W_{AC}^{1.70}$ | 120 |
| | $Q_{10} = 14W_{AC}^{1.50}$ | 60 |
| | $Q_{25} = 22W_{AC}^{1.50}$ | 62 |
| | $Q_{50} = 44W_{AC}^{1.40}$ | 71 |
| | $Q_{100} = 59W_{AC}^{1.40}$ | 83 |

[a] Active-channel width ($W_{AC}$) in feet; discharge ($Q_n$) in cubic feet per second, where n is the recurrence interval in years.
[b] Subject to intensive precipitation events.

## Main-Channel Section

The third and highest reference level used is the main-channel section (also referred to as the whole-channel section). This section was described by Riggs (42, p. 53) as "variously defined by breaks in bank slope, by the edges of the flood plain, or by lower limits of permanent vegetation." He also notes: "In selecting the channel width, one should avoid a high reference level that does not reflect the present flow regime. This is most often a possibility on ephemeral streams."

When the preceding descriptions are compared with the various descriptions of the bank-full stage, it is evident that the main-channel section and the bank-full section are the same for perennial streams. The relationship is less obvious for ephemeral streams where distinct floodplains may not be formed; however, there is no evidence to indicate that the sections are not the same when determined properly.

The study by Riggs (42) presented reconnaissance-level relations between 10-yr flood and main-channel width (whole-channel width) for ephemeral streams in Utah and Wyoming and perennial streams in Alaska. Relations also were compared for the 50-yr flood in the western mountains, Kansas, and Kentucky.

Riggs and Harenberg (43) demonstrated for Owyhee County, Idaho, how channel-geometry measurements could be used to provide estimates of flood characteristics without a visit to the site. The relationship between the 10-yr flood and main-channel width was developed and used to estimate the 10-yr flood at 79 sites in and adjacent to Owyhee County. The resulting estimates and those for 33 gaging stations were plotted on a map of the county; the map can be used for interpolation to make estimates at intermediate sites.

Lowham (44) used the main-channel section to define relations for mean annual flow and 2- through 100-yr flood characteristics for Wyoming. For floods, the state was divided into four hydrologic areas and separate relations were defined for each area. Average standard errors of the estimate for all frequencies ranged from about 34 to 75 percent and were smaller than standard errors for comparable relations that used drainage basin and climatic variables. More recently, Lowham (45) developed a relation between the geometric mean of peak discharges (approximately the 2-yr flood) and main-channel width for Wyoming that had an average standard error of the estimate of 47 percent. The relation applies (45, p. 37) "to all types of streams, including perennial, intermittent, and ephemeral types of either the mountains or plains, provided the channel is stable and has been formed by the hydraulic forces of floodflows."

Harenberg (46) used the bank-full width to define relations for the 1.5- through 100-yr floods for Idaho. He reports that his bank-full width is equivalent to the whole-channel width used in the Owyhee County report. The equations were applicable statewide and had average standard errors of about 70 percent.

The relations between 10-yr flood and main-channel width for these studies are shown in Figure 4.

## USE OF CHANNEL-GEOMETRY RELATIONS

Channel-geometry measurements are proven indexes for use in estimating flood-frequency characteristics at ungaged locations. The technique can be used where relations between flow characteristics and traditional basin and climatic characteristics are poor, or channel measurements may be used to provide virtually independent estimates for comparison with the traditional approaches. Nevertheless, the method may not provide reliable results for areas in which bedrock prevents the channel from adjusting to accommodate the normal regimen of flow. Similarly, the approach is not applicable on braided, sand-channel streams where channels have not stabilized. Where possible, sections should be located in straight reaches where flows are approximately uni-

Figure 4. Relations between 10-yr flood and main-channel width.

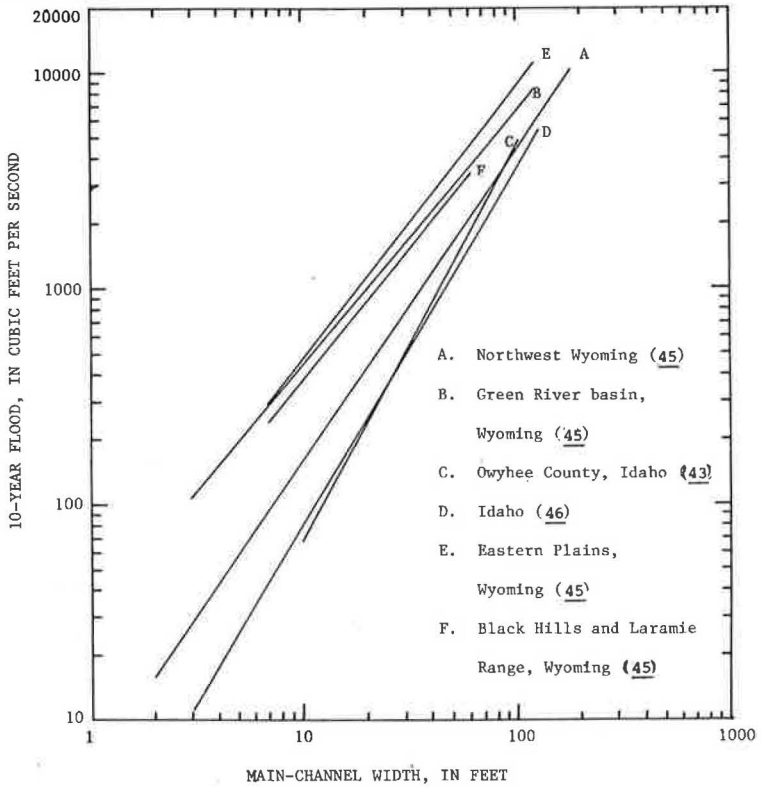


form. In meandering streams, Lowham (44) suggests locating sections in the crossover area, midway between bends. Channel dimensions need to be measured at two or three cross sections separated by at least one channel width, and average values should be used in computations.

Regardless of which of the three sections is used, experience is needed to identify the proper reference level. Before channel measurements are made, a few days of field instruction should be obtained from a person experienced in the technique. Training needs to be done in a hydrologic environment that is similar to that in which the relations will be used; the various sections generally are much easier to identify on perennial streams than on ephemeral streams. In using an existing relation, only those variables contained in the relation need to be measured. If a new relation is being developed, however, other factors such as channel slope and bed and bank material should be obtained in addition to the width and average depth of the section.

## RELIABILITY

The reliability of flow estimates from channel characteristics depends on both the applicability of the regional relation (calibration and model errors) and the ability of different individuals to recognize and measure the channel dimensions used as independent variables (application error).

The calibration and model errors include errors in estimates of the discharge characteristics used to develop the relations and are reflected in the standard errors of the estimate reported for individual studies. At this time, however, the components cannot be separated; that is, the contributions attributed to errors in the calibration discharge estimates, to the use of the power-function relation, and to measurement errors by the individuals developing the relations cannot be identified separately. In most investigations that use channel geometry it has been found that standard errors of the estimate are equal to or less than the standard errors for conventional methods.

The principal difference between the conventional regression relations and those that use channel geometry is in the degree of subjectivity involved in defining the independent variables. For example, there may be numerous maps of an area giving mean annual precipitation, but if a particular map is specified, all users could derive about the same estimated value for a particular basin. With relations based on channel geometry, however, the user needs to be able to both recognize the feature and measure it consistently.

## VARIATION BETWEEN INDIVIDUALS

Wahl (47, pp. 311-319) conducted and reported on a test designed to define the possible variability of channel measurements by individuals. An added objective of the test was to gain insight into potential advantages and disadvantages of the three reference levels. The test was conducted in northern Wyoming. Seven individuals, all experienced in using channel-geometry techniques, independently visited 22 sites and measured channel dimensions in sections of their choosing. Only general reaches of each stream were identified, so the cross sections at which individuals measured channel dimensions were of their own choosing; thus, the variability of measurements between individuals reflected the combined effects of differences in cross-section location within the test reach and differences in identification of the reference levels. This should reflect the variability resulting from having trained individuals measure channel size in an ungaged reach.

A summary of the statistics of cross-correlation coefficients between measurements for width and av-

Table 4. Summary of cross correlations between measurements by individuals.

| Section | Statistics of Correlation Coefficients | | |
|---|---|---|---|
| | Mean | Standard Deviation | Range |
| Low bar | | | |
| Width | 0.95 | 0.055 | 0.74-0.99 |
| Depth | 0.74 | 0.128 | 0.51-0.93 |
| Active channel | | | |
| Width | 0.97 | 0.028 | 0.91-0.99 |
| Depth | 0.59 | 0.164 | 0.27-0.83 |
| Main channel | | | |
| Width | 0.92 | 0.067 | 0.79-0.99 |
| Depth | 0.59 | 0.193 | 0.16-0.89 |

erage depth of the three reference levels is given in Table 4 (47, pp. 311-319). The data in Table 4 show high correlation between width measurements for all three reference levels, but the correlation between depth measurements is low. This can be rationalized by considering that depths are relatively shallow and that slight differences in locating the top of a reference level will have little effect on the overall measurement of width but a significant effect on the average depth. Wahl (47, pp. 311-319) also used analysis of variance to test for differences among individuals in the average values of a given channel-size dimension. The hypothesis of no difference among means for individuals was accepted at the 95 percent level for widths of all three reference levels.

Relations between a discharge characteristic (Q) and channel width (W) usually take the following form:

$$Q = aW^b \quad (5)$$

where a and b are numerical constants. This is a linear relation when expressed in logarithms:

$$\log Q = \log a + b \log W \quad (6)$$

For the Wyoming test, the average standard deviation of log W (base 10 logarithms) for the seven individuals was 0.089. Given a relation of the form of Equation 6, the standard error in log Q produced by variation in estimates of W is b times the standard error of log W. Wahl (47, pp. 311-319) assumed that b averaged about 1.5 and arrived at an estimate of the standard error in log Q of 0.13 log unit due to variation in width measurements alone. This converts to an error of about 30 percent in estimated discharge. In addition, Wahl (47, pp. 311-319) noted an average bias (with respect to the mean) in log W of 0.06 log unit, or about 14 percent.

The effect of the variation in channel-width measurements by individuals is to increase the error of applying a relation to more than that indicated by the standard error of the estimate, which shows the calibration and model error. Assuming that the three errors are independent, the true error would be the square root of the sums of the squares of the individual components. For example, the 25-yr flood for the alpine area from Table 3 shows an average standard error of the estimate of 42 percent, or 0.178 log unit. The true error (in log units) of using this relation, which would account for both variation and possible bias in width measurements, would be

$$[(0.178)^2 + (0.13)^2 + (0.06)^2]^{0.5} = 0.228 \quad (7)$$

This yields an average error of 55 percent compared with the calibration error of 42 percent.

It should be noted, however, that the sites in the Wyoming test were chosen for their diversity. The sites ranged from ephemeral streams in a near-desert environment to perennial streams in a high-mountain environment. The variability of measurements in this test probably is greater than normally would be encountered in applying channel-geometry measurements in a particular hydrologic area.

## SOME COMPARISONS

Comparing published results for different physiographic areas is difficult because the areas have morphological and hydrological differences. In addition, three different reference levels have been used, and some relations include independent variables not used in other studies. Nevertheless, general comparisons are possible for studies that have overlapped or covered similar physiographic regions. For example, agreement shown in Figure 2 between the 10-yr flood results for the mountains of Colorado (29) and those for the mountains of the Missouri River basin (35) is good. Results for the mountains of Nevada (30) also compare with the preceding results.

Similar comparisons in Figure 3 show that for the 10-yr flood and the active-channel width, the relations for the alpine areas of the western United States (41) and for the mountains in the Missouri River basin (35) are almost identical. The relation for New Mexico (39) has about the same exponent but has a different intercept.

Selected relations for the 10-yr flood and the main-channel section are shown in Figure 4. Only the results for Owyhee County, Idaho (43), and the statewide study for Idaho (46) are directly comparable; they are quite similar.

## NEEDED RESEARCH

Studies to date (1982) have clearly shown that stable channel dimensions are valid indexes of the flow characteristics of rivers. Much needs to be done, however, to fully realize the potential of this approach. A number of features, including the within-channel-bar section, active-channel section, and the main-channel or whole-channel section, are now being used to define flow characteristics. Consequently, it is difficult to make comparisons between studies, and the applicability of individual results depends on the ability of a user to identify the feature used in developing the relation.

Research is needed to define relations between the dimensions of the various reference levels and the areas over which the relations apply. Riggs (48) developed the following relation between main-channel width and active-channel width:

$$MC = 1.75AC^{0.96} \quad (8)$$

where MC is the main-channel width and AC is the active-channel width. All units are in feet. He suggested that this relation could be used in semiarid regions to estimate one width from another, but a similar relation developed by Wahl (47, pp. 311-319) for the Wyoming test data produced unusable results. This probably was because of the extreme variation in stream types in the Wyoming test.

Additional work is needed to determine the role of other variables. Several investigators (26,38, 49) have examined the relation between channel size and sediments in the bed and banks. Results to date (1982) have varied from region to region. Andrews (17) examined data for gravel-bed streams in Colorado and separated the data into two groups depending on whether bank vegetation along the study reach

was light or thick. He made width, depth, and velocity dimensionless by dividing each by the median particle diameter in the riverbed surface. Regression relations for hydraulic-geometry exponents showed no significant difference between data for light and thick bank vegetation; nevertheless, the regression coefficients a, c, and k were significantly different. This implies that exponents for gravel-bed rivers are the same, regardless of region.

Examination of the hydraulic-geometry exponents in Table 1 suggests that for a given channel type, a fixed relation should exist between a formative discharge and channel width. There appears to be justification for imposing a slope for width-discharge relations and allowing the constant (intercept) to be determined by the data. This would minimize the variability among relations that is now produced by fitting curves to a limited range of data. Based on the theoretically derived relations for the regime equations, formative discharge should relate to width raised to the 1.8 to 2.0 power. However, this would only be true for the formative discharge; using the same exponent for other discharges would imply that the variability of flows of large streams is as large as that of small streams. Osterkamp and Hedman (37) have attempted this approach, but additional work is needed.

Much of the work to date has dealt with efforts to define regional relations (calibration). Ways should be sought to make the calibration results more useful. Additional work also is needed to refine estimates of the application errors. The application errors estimated by Wahl (47) probably are anomalously large because of the extreme variability designed in the experiment.

REFERENCES


1. S. Leliavsky. An Introduction to Fluvial Hydraulics. Dover Publications, New York, 1955, 257 pp.
2. T. Blench. Mobile-Bed Fluviology. Univ. of Alberta, Edmonton, 1969, 168 pp.
3. L.B. Leopold and T. Maddock, Jr. The Hydraulic Geometry of Stream Channels and Some Physiographic Implications. U.S. Geological Survey, Professional Paper 252, 1953, 56 pp.
4. K. Mahmood and H.W. Shen. The Regime Concept of Sediment-Transporting Canals and Rivers. In River Mechanics (H.W. Shen, ed.), Colorado State Univ., Fort Collins, 1971, 39 pp.
5. C.R. Pettis. Discussion. Transactions of the American Society of Civil Engineers, Vol. 102, 1937, pp. 149-152.
6. N.E. Kondrat'ev and others. River Flow and River Channel Formation. Israel Program for Scientific Translations, Jerusalem, 1962, 172 pp.
7. M.G. Wolman. The Natural Channel of Brandywine Creek, Pennsylvania. U.S. Geological Survey, Professional Paper 271, 1955, 56 pp.
8. G.P. Williams. Bankfull Discharge of Rivers. Water Resources Research, Vol. 14, No. 6, 1978, pp. 1141-1154.
9. L.B. Leopold and J.P. Miller. Ephemeral Streams--Hydraulic Factors and Their Relation to the Drainage Net. U.S. Geological Survey, Professional Paper 282-A, 1956, 36 pp.
10. J.E. Nash. A Study of Bankfull Discharge of Rivers in England and Wales: Discussion. Proc., Institute of Civil Engineers, London, Vol. 14, 1956.
11. M. Nixon. A Study of Bankfull Discharges of Rivers in England and Wales. Proc., Institute of Civil Engineers, London, Vol. 12, 1956, pp. 157-174.
12. L.M. Brush, Jr. Drainage Basins, Channels, and Flow Characteristics of Selected Streams in Central Pennsylvania. U.S. Geological Survey, Professional Paper 282-F, 1961.
13. R. Kellerhals. Stable Channels with Gravel-Paved Beds. Proc. ASCE, Vol. 93, No. WW1, 1967, pp. 63-84.
14. J.B. Stall and Y. Fok. Hydraulic Geometry of Illinois Streams. Illinois State Water Survey, Research Rept. 15, 1968, 47 pp.
15. W.W. Emmett. The Hydraulic Geometry of Some Alaskan Streams South of the Yukon River. U.S. Geological Survey, open-file report, 1972, 44 pp.
16. W.W. Emmett. The Channels and Waters of the Upper Salmon River Area, Idaho. U.S. Geological Survey, Professional Paper 870-A, 1975, 116 pp.
17. E.D. Andrews. Hydraulic Geometry of Gravel-Bed Rivers in Colorado. Bulletin of the Geological Society of America (to be published).
18. L.B. Leopold and W.B. Langbein. The Concept of Entropy in Landscape Evolution. U.S. Geological Survey, Professional Paper 500-A, 1962, 20 pp.
19. W.B. Langbein. Geometry of River Channels. Proc. ASCE, Vol. 90, No. HY2, 1964, pp. 301-312.
20. W.B. Langbein. Geometry of River Channels: Proc. ASCE, Vol. 91, No. HY3, 1965, pp. 297-313.
21. P. Acker. Experiments on Small Streams in Alluvium. Proc. ASCE, Vol. 90, No. HY4, 1964, pp. 1-38.
22. F. Engelund and E. Hansen. A Monograph of Sediment Transport in Alluvial Streams. Teknisk Forlag, Copenhagen, Denmark, 1967, 62 pp.
23. E.A. Joering and H.C. Preul. A Set of Regime Equations for Indirectly Estimating Streamflow Characteristics. Proc., International Water Resources Association, Sept. 24-28, 1973, pp. 411-426.
24. T.R. Smith. A Derivation of the Hydraulic Geometry of Steady State Channels from Conservation Principles and Sediment Transport Laws. Journal of Geology, Vol. 82, 1974, pp. 98-104.
25. R.M. Li, D.B. Simons, and M.A. Stevens. Morphology of Cobble Streams in Small Watersheds. Proc. ASCE, Vol. 102, No. HY8, 1976, pp. 1101-1117.
26. W.R. Osterkamp. Perennial-Streamflow Characteristics Related to Channel Geometry and Sediment in the Missouri River Basin. U.S. Geological Survey, Professional Paper 1242, 1982, 37 pp.
27. D.O. Moore. Estimating Mean Runoff in Ungaged Semiarid Areas. International Association of Scientific Hydrology, Bull. 13, Vol. 1, 1968, pp. 29-39.
28. E.R. Hedman. Mean Annual Runoff as Related to Channel Geometry in Selected Streams in California. U.S. Geological Survey, Water Supply Paper 1999-E, 1970, 17 pp.
29. E.R. Hedman, D.O. Moore, and R.K. Livingston. Selected Streamflow Characteristics as Related to Channel Geometry of Perennial Streams in Colorado. U.S. Geological Survey, open-file report, 1972, 14 pp.
30. D.O. Moore. Estimating Flood Discharges in Nevada Using Channel-Geometry Measurements. Nevada Department of Highways, Reno, Hydrologic Rept. 1, 1974, 43 pp.
31. F.D. Kopaliani and V.V. Romashin. Channel Dynamics of Mountain Rivers. Soviet Hydrology--Selected Papers, Vol. 5, 1970, pp. 441-452.
32. E.R. Hedman and W.M. Kastner. Mean Annual Runoff as Related to Channel Geometry of Selected

Streams in Kansas. Kansas Water Resources Board, Topeka, Tech. Rept. 9, 1972, 25 pp.
33. D.R. DeWalle and A. Rango. Water Resources Application of Stream Channel Characteristics on Small Forested Basins. Water Resources Bulletin, Vol. 8, No. 4, 1972, pp. 697-703.
34. R.C. Zimmerman, J.C. Goodlett, and G.H. Comer. The Influence of Vegetation on Channel Form of Small Streams. International Association of Scientific Hydrology, Symposium of Berne, River Morphology, No. 75, pp. 255-274.
34a. F.K. Fields. Estimating Streamflow Characteristics for Streams in Utah Using Selected Channel-Geometry Parameters. U.S. Geological Survey, Water Resources Investigations 34-74, 1975, 19 pp.
35. E.R. Hedman and W.M. Kastner. Streamflow Characteristics Related to Channel Geometry in the Missouri River Basin. U.S. Geological Survey Journal of Research, Vol. 5, No. 3, 1977, pp. 285-300.
36. E.R. Hedman, W.M. Kastner, and H.R. Hejl, Jr. Selected Streamflow Characteristics as Related to Active-Channel Geometry of Streams in Kansas. Kansas Water Resources Board, Topeka, Tech. Rept. 10, 1974, 21 pp.
37. W.R. Osterkamp and E.R. Hedman. Variation of Width and Discharge for Natural High-Gradient Stream Channels. Water Resources Research, Vol. 13, No. 2, 1977, pp. 256-258.
38. C.F. Glazzard. Streamflow Characteristics Related to Channel Geometry of Selected Streams on the Cumberland Plateau, Tennessee. Univ. of Tennessee System, Knoxville, master's thesis, 1981, 132 pp.
39. A.G. Scott and J.L. Kunkler. Flood Discharges of Streams in New Mexico as Related to Channel Geometry. U.S. Geological Survey, Open-File Rept. 76-414, 1976, 29 pp.
40. E.E. Webber and J.W. Roberts. Floodflow Characteristics Related to Channel Geometry in Ohio. U.S. Geological Survey, Open-File Rept. 81-1105, 1981, 28 pp.
41. E.R. Hedman and W.R. Osterkamp. Streamflow Characteristics Related to Channel Geometry of Streams in Western United States. U.S. Geological Survey, Water Supply Paper 2193, 1982, 17 pp.
42. H.C. Riggs. Flash Flood Potential from Channel Measurements. International Association of Scientific Hydrology, Publ. 112, Proc. of Paris Symposium, 1974, pp. 52-56.
43. H.C. Riggs and W.A. Harenberg. Flood Characteristics of Streams in Owyhee County, Idaho. U.S. Geological Survey, Water Resources Investigations 76-88, 1976, 14 pp.
44. H.W. Lowham. Techniques for Estimating Flow Characteristics of Wyoming Streams. U.S. Geological Survey, Water Resources Investigation 76-112, 1976, 83 pp.
45. H.W. Lowham. Streamflows and Channels of the Green River Basin, Wyoming. U.S. Geological Survey, Water Resources Investigations 81-71, 1982, 73 pp.
46. W.C. Harenberg. Using Channel-Geometry Measurements to Estimate Flood Flows in Idaho. U.S. Geological Survey, Water Resources Investigations 80-32, 1980, 39 pp.
47. K.L. Wahl. Accuracy of Channel Measurements and the Implications in Estimating Streamflow Characteristics. In Modern Developments in Hydrometry, World Meteorological Organization, Padua, Italy, Vol. 2, 1976.
48. H.C. Riggs. Streamflow Characteristics from Channel Size. Proc. ASCE, Vol. 104, No. HY1, 1978, pp. 87-96.
49. S.A. Schumm. The Shape of Alluvial Channels in Relation to Sediment Type. U.S. Geological Survey, Professional Paper 352-B, 1960, 30 pp.

# Tree-Ring Data: Valuable Tool for Reconstructing Annual and Seasonal Streamflow and Determining Long-Term Trends

CHARLES W. STOCKTON AND WILLIAM R. BOGGESS

Two examples are discussed that demonstrate how information derived from the annual growth rings of certain tree species can be used as a proxy source of data to extend hydrologic records back in time. In the first case, tree-ring reconstructions of the annual flow of the upper Colorado River show that the period of record used as a basis for the 1922 Colorado River Compact was anomalously wet, in fact, the wettest comparable period in the entire 450 yr of reconstructed annual discharge at Lee Ferry, Arizona. The full impact of this overestimated flow has yet to be felt. In the second example, data from 13 carefully selected sites were used to reconstruct the annual and seasonal flows of the Salt and Verde Rivers back to 1580. These two rivers, draining some 13,000 miles$^2$ in central Arizona, furnish water for municipal, industrial, and agricultural use as well as hydroelectric power for the metropolitan Phoenix area. Future water supply and flooding potential are both critical problems due to rapid escalation of population. Results show that several periods of prolonged low flows have occurred that were more severe than any comparable period since 1890. These low-flow periods have an apparent recurrence interval of about 22 yr on the Salt River. Also, the gaged records contain an above-average number of high seasonal and annual flows when compared with the entire 400 yr of reconstruction.

Planning and design for controlling and managing water are predicated on the analysis of historic data to determine both the magnitude and the frequency of annual water yields that have been measured over a finite period of time. In general, statistical procedures used to forecast annual flows are hampered by the relatively short time span covered by instrumented records. This is true throughout the Western Hemisphere and especially so in most developing countries, where hydrologic rec-

ords are essentially nonexistent. Even where reliable records are available, there is no assurance that they represent a truly random sample and that the occurrence of hydrologic events throughout the period is based on some probability distribution. As a consequence, statistical descriptions may contain considerable bias and produce erroneous results.

In most instances, probability distributions are uniquely defined by the mean ($\bar{X}$), a measure of central tendency; the variance ($S^2$), a measure of the average spread of events around the mean; and skewness (G), a measure of the asymmetry of the distribution of events around the mean. For many runoff and tree-ring series, the variables are normally distributed (G approaches zero) and the probability distribution is adequately described by $\bar{X}$ and $S^2$.

In developing first-order autoregressive models of runoff time series, the first-order correlation ($r_1$), a measure of short-term persistence, is used along with the mean and variance. The population values of these statistics are usually unknown and must be estimated from existing records. From Monte Carlo simulations involving thousands of trials on each of several probability functions for various values of n and $\gamma$ (the number of observations and the population coefficient of skew), Wallis, Matalas, and Slack (1) demonstrated that the distributions of $\bar{X}$ and $S^2$ and G are functions of n, $\lambda$, and the probability function. Although $\bar{X}$ is an unbiased estimate, both $S^2$ and G are biased estimates of population values, the degree of bias being a function of n, $\gamma$, and the probability distribution.

It follows that errors in estimating population parameters due to short periods of record are preserved in any synthetic series that is generated from the available data. For example, Rodriquez-Iturbe (2) showed that in annual runoff records of 40 yr or less, there may be an error of 2 to 20 percent in estimating the first-order correlation, which is probably related to the inadequacy of short periods of record for estimating the low-frequency persistence in climatologic data.

Another complicating factor is that the possible effects of climatic change in probability distributions are largely ignored. This is due in part to the guidelines for determining flood-flow frequency issued by the Hydrology Committee of the U.S. Water Resources Council (WRC) (3). In the guidelines, it is stated that

> there is much speculation about climatic change. Available evidence indicates that major changes occur in the time scales of thousands of years. In hydrologic analyses it is conventional to assume that flood flows are not affected by climatic trends or cycles. Climatic time invariance was assumed in developing this guide.

Contrary to the WRC statement, there is considerable evidence that climate is nowhere invariant and that the variability is not a random function of time (4). For example, the world has experienced both cooling and warming during the past century. The overall trend has been toward warming; there has been a greater tendency for change in the higher northern latitudes. According to Hansen and others (5), the higher northern latitudes warmed about 0.8°C between 1880 and 1940, whereas the lower southern latitudes increased only 0.3°C. Cooling, especially in the northern latitudes, followed in the 1940s but the trend reversed on a global basis in the mid-1960s. The same authors point out that global temperatures are now about equal to the 1940 peak and suggest that the common misconception that temperatures are cooling is based on experiences in the Northern Hemisphere.

The growing consensus among climatologists is that global temperatures will continue to rise due to the greenhouse effect of increases in atmospheric carbon dioxide caused by man. There is no unanimity of opinion on the magnitude or speed of such changes, but Hansen and others (5) suggest that a rise of about 2.5°C is possible during the next century for a scenario of slow energy growth and a mixture of fossil and nonfossil fuels. Such a rise in global temperatures would be almost unprecedented, and the results would be disastrous for many parts of the world. Any changes that might occur in the next century are well within the time frame for hydrologic planning, and their likely occurrence raises an important question: Can hydrologists and engineers ignore climatic variability as a parameter for planning and design?

Because existing climatic and hydrologic records are not old enough to reflect climatic variability and trends, one must turn to some source of proxy data to document the occurrence and persistence of these changes. The most commonly used sources include layered ice cores; pollen profiles developed from bog, swamp, or lake sediments; stream geometry, stratigraphy, and morphology; and tree rings. The first three sources can generally be extended farther back in time than tree rings, but they cannot be precisely dated and lack the capacity to preserve high-frequency (short-term) variations. In contrast, tree rings can be accurately dated as to the year of formation and preserve both high- and low-frequency (long-term) variations. Also, the climatic information stored in tree rings is annually cumulative, and samples can be replicated to a much greater extent than the other sources.

A disadvantage of tree-ring series is that they rarely extend back in time more than 400-500 yr and the climatic signals by species growing under a wide variety of climatic conditions are not equally strong or clearly defined. The trees most responsive to climatic variation in the United States are some of the relatively long-lived species growing in the West, especially those on arid sites. It is not surprising that the study of tree rings (dendrochronology) developed in the Southwest, and much of the past work pertains to western conditions.

Earlier applications of dendrochronology were largely confined to dating archaelogical materials such as wood or charcoal from ancient Indian dwellings. More recently, much progress has been made in using tree-ring series to reconstruct past climates (dendroclimatology) and hydrologic events (dendrohydrology). Two aspects of our work in dendrohydrology are discussed here. The first illustrates how streamflow records from an anomalously wet period were used as a basis for the 1922 Colorado River Compact. Second, we show how tree-ring data can be used to reconstruct annual and seasonal flows of the Salt and Verde Rivers in Arizona.

## RECONSTRUCTION TECHNIQUES

The techniques used in both climatic and hydrologic reconstructions involve advanced statistics and modeling, especially in the area of time-series analysis. These and the computer techniques involved are not discussed here; they have been described in detail by Stockton (6), Fritts (7), and Stockton and Boggess (8).

It is especially important to recognize two aspects of tree-ring analysis. First, each ring must be precisely dated. This cannot be done by merely counting rings. Instead, a tedious and time-consuming process called crossdating is essential to ac-

count for possible multiple or locally absent rings. Second, measured ring widths cannot be used directly in statistical analyses because rings tend to become narrower as trees senesce and grow older. This growth trend is removed by fitting an appropriate least-squares curve to provide a ring-width index (measured ring widths are divided by corresponding curve values to provide the index). In addition to removing the growth trend, this procedure reduces all ring widths to a uniform mean value (value of 1). When plotted against time, the ring-width indexes form a new stationary time series known as a standardized ring-width chronology. These procedures are discussed in detail by Fritts (7, Chapter 6).

Another analytical problem that must be dealt with in developing tree growth-climate relationships is that of persistence (autocorrelation) in tree-ring series. This results because growth during a particular year is influenced not only by conditions during that year but perhaps also by antecedent conditions during one or more preceding years. For instance, in a favorable year an excess of photosynthate more than that required for growth and other metabolic processes will carry over and produce a positive effect on the next year's growth. Conversely, an unfavorable year will likely represent the opposite. Available food reserves will be depleted for the onset of growth in the following year.

Autocorrelation is estimated in a manner similar to that for the product-moment correlation coefficient, except that instead of determining the relationship between two variables, x and y, the relationship between x and x - i is calculated, where i is the amount of lag. Autocorrelation may be removed from some time series by regressing the response at time t with that at t - 1. The effect of t - 1 is then subtracted from the response at time t (9). Meko (10) discusses in detail how the resulting autoregressive (AR) process can be applied to tree-ring series to remove the effect of soil moisture and biological carryovers. It should be noted that persistence also exists in many climatic time series; there is a tendency for clustering of wet and dry years.

A period of overlap between historic hydrologic or climatic data and the tree-ring series is essential. A part of the overlapping record is used to develop statistical relationships between the two series (calibration). The remaining record provides a basis for verifying the accuracy of the established relationship (verification). If the relationship appears valid, transfer functions are developed to extend the hydrologic series back in time based on the existing tree-ring series.

Because of the nature of tree growth, each annual ring represents an integration of environmental and physiological factors over 1 yr or more. For this reason, streamflow reconstructions are generally limited to annual values. With exceptionally good data collected near runoff-producing sites, seasonal flows can often be successfully estimated. Peak flows can only be inferred in that they might be expected to occur more frequently when annual or seasonal flows are well above the long-term mean.

## COLORADO RIVER STUDY

As pointed out earlier, most statistical analyses involving hydrologic data assume that the period of record adequately represents the infinite number of past events. This assumption of randomness may or may not be correct. That it may not be correct is dramatically illustrated by results of a study reported variously by Stockton (6), Stockton and Jacoby (11), and Stockton and Boggess (8, pp. 266-273) in which the flow of certain streams in the upper Colorado River basin was reconstructed by using tree-ring data.

The Colorado River is the major source of surface water for much of the southwestern part of the United States. Flowing some 1,440 miles from the high mountains of Colorado to the Gulf of Lower California, the river traverses some of the most arid land in the country. Its annual flow of about 14 million acre-ft (maf) is modest when compared with that of the Mississippi (440 maf) or the Columbia (180 maf), yet more water is exported from the basin (about 5 maf) than from any other river basin in the United States. Most of the flow originates in the upper basin where an estimated 85 percent of the flow is generated on 15 percent of the land area.

In 1922 the estimated annual flow of the Colorado River was allocated equally between the upper and lower basins--7.5 maf to each. A later treaty guaranteed a 1.5-maf allotment to Mexico. The compact was based on a sustained flow of 17.5 maf at Lee Ferry, Arizona (12, pp. 79-95). The flow at Lee Ferry was estimated from fragmentary data, dating in part back to 1896, on some of the tributary streams in the upper basin.

The tree-ring reconstructions, dating back to 1564, were based on data collected from up to 30 sites located near runoff-producing areas. The reconstructed average annual flow was about 13.5 maf, far short of the 17.5 maf on which the compact was based. Why the large discrepancy? As stated earlier, the records used for the compact were fragmentary and were extrapolated from tributaries to the main stream at Lee Ferry. More important, the reconstructions show that the period of record was anomalously wet--the wettest indeed for the entire 450 yr covered by the reconstructions [Figure 1 (up-

Figure 1. Long-term hydrograph of annual runoff at Lee Ferry, Arizona, based on average of results of two reconstructions.

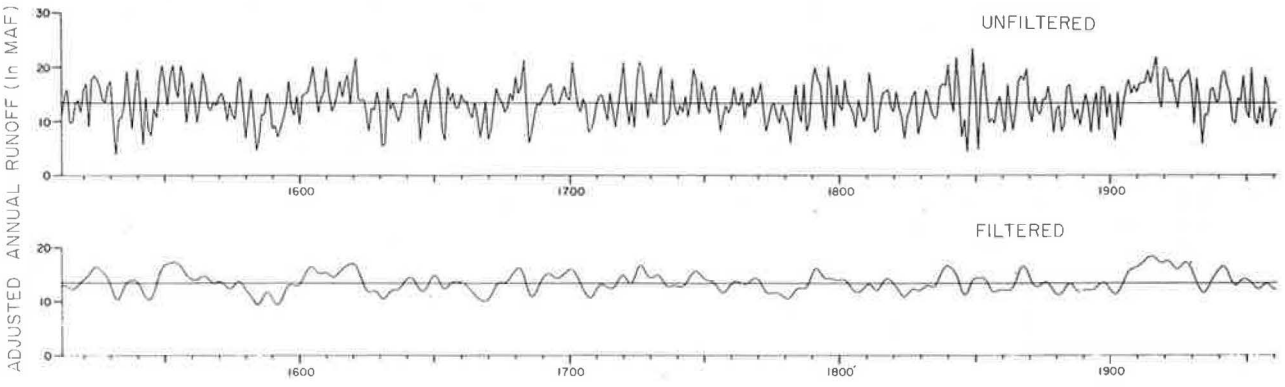

per graph, actual year-by-year values; lower graph, same data but with high-frequency components--those with period less than 10 yr--removed)]. It is of interest to note that the measured flow of the river at Lee Ferry for the period 1930-1974 is 13.78 maf. If the high flows of the early part of the century are included (1906-1974), this increases to an estimated 15.17 maf. Thus the reconstructions appear to be a good representation of the actual behavior of the river as well as to have shown the bias toward wetness in the data used for the compact. The full impact of the overestimated flow has yet to be felt, because the upper basin has not used its full allocation.

## SALT-VERDE RECONSTRUCTIONS

In addition to the Colorado River study, tree-ring data have been used to reconstruct streamflow on the Rio Limay and Rio Neugguen in Argentina (13), eight rivers in western Tasmania (14), and the Salt and Verde Rivers in Arizona (15). Results from the Salt and Verde Rivers are discussed here.

### Basin Characteristics and Water Demand

The basins of the Salt and Verde Rivers include some 13,000 miles$^2$ in central Arizona. The two rivers converge at Granite Reef, north of Phoenix, to form the largest tributary of the Gila, which then flows southwesterly to join the Colorado at Yuma. Both rivers originate in the high mountains at altitudes of approximately 12,000 ft. Precipitation ranges from more than 32 in. in the higher mountains to less than 8 in. in the more arid portions and occurs as winter storms from Pacific frontal systems or as convective thunderstorms during the summer. The latter make minimal contributions to streamflow.

The Salt and Verde Rivers are the main source of water for metropolitan Phoenix as well as for a large area of irrigated agriculture. Six dams, which have a combined storage of about 2.08 maf, have been constructed on the two rivers. Four of these produce hydroelectric power. The water and power resources are managed by the Salt River Project, the oldest multipurpose reclamation project in the country.

The demand for water has escalated since World War II, accompanying the phenomenal population growth of the Phoenix area. Flooding, always a threat in the Salt River Valley, has become an even greater problem because of the conversion of agricultural land to urban developments. Population growth shows no sign of decreasing, and there is increasing concern over both future water supply and flooding potential. A basic tenet in both issues is whether the period of record, although relatively long, adequately represents the long-term flow characteristics of the rivers. Our study, requested and supported by the U.S. Army Corps of Engineers, was designed to provide information on this important point.

### Data Sources

The locations of stream-gaging stations, climatic stations, and tree-ring sites are shown in Figure 2. Data from the gaging station near the town of Roosevelt, operational since 1914, were used to calibrate the streamflow records. Although a gage located about 16 miles downstream from the one near Roosevelt operated during 1901-1913, data from the two could not be combined because such data represented considerably different drainage areas. Nevertheless, the earlier data, along with estimates of flow from data at Arizona Dam for the period

Figure 2. Locations of tree-ring sites, climatic stations, and gaging stations.

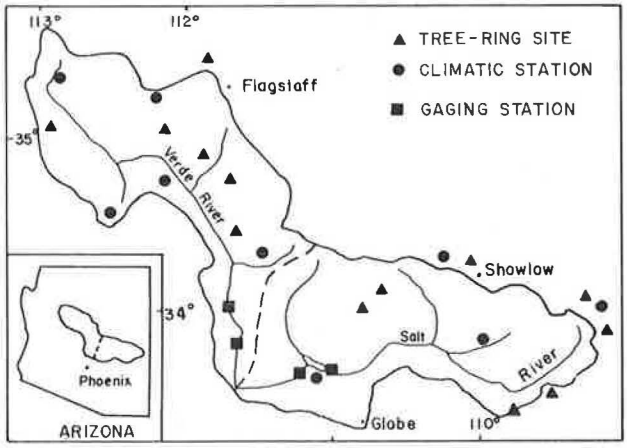


1883-1913, were valuable because they could be used to verify the relative magnitude of flows outside the 1914-1979 calibration period. Also, the period 1883-1913 included some of the largest discharges ever recorded for the two rivers.

The gage below Bartlett Dam on the Verde River was established in 1895. The flow below the dam, however, has been regulated by Bartlett and Horseshoe reservoirs since their completion in 1939 and 1943, respectively. Monthly discharges after 1939 were corrected by adding net monthly changes in reservoir capacity published by the U.S. Geological Survey to the reported monthly flow at the gage. A gaging station was established below Tangle Creek in 1945 that represents the inflow into the Verde reservoir system. The drainage area between the two gages is insignificant, so the Tangle Creek gage was used after 1945 to avoid errors in estimating reservoir contents associated with the gage below Bartlett Dam.

Tree-ring samples were collected from 13 locations, as shown in Figure 2. Each sample consisted of two cores from a least 10 trees per site. Sites were selected to maximize both the climatic sensitivity and the length of the tree-ring series. Generally the most climatically sensitive trees are those growing on open, exposed sites with shallow soils whose moisture supply is solely from precipitation. Tree species sampled included ponderosa pine (Pinus ponderosa Laws) and pinyon pine (Pinus edulis Englm.).

Data from selected climatic stations were analyzed to determine relationships among precipitation, runoff, and tree growth. Stations were chosen for the length and quality of their records. Data from Roosevelt, White River, Springerville, and Pinedale were used to represent the Salt River basin, whereas Jerome, Seligman, Williams, Natural Bridge, and Prescott were chosen for the Verde.

### Analysis of Data

Reconstruction of stream discharge from tree-ring data is based on the generally accepted assumption that both are responding to the same climatic input (temperature, precipitation, evapotranspiration, and so on). To determine the relationships between climate and discharge and climate and tree growth, we used principal-component analysis (PCA), a method that allows a large field of correlated data to be expressed as a smaller number of uncorrelated variables called eigenvectors. A spatial array of M stations each having the same number (N) of data

points will yield the smaller of either M or N eigenvectors. Each eigenvector will contain M components corresponding to the number of stations, or variables, and will account for a portion of the total variance (16). The sum of the products of an eigenvector generated by PCA with the values of its components for a given year yields a value called the amplitude for that year (17).

The amplitudes corresponding to the eigenvectors of monthly climatic data for several stations within the Salt and Verde basins represent modes of temperature and precipitation that are independent in time and weighted spatially over each of the basins. These amplitudes were entered as predictor variables in a multiple-linear-regression (MLR) analysis with the $\log_{10}$ transform of annual discharge to determine water-balance models. A $\log_{10}$ transform was performed because the original discharge data were log normally distributed and their use in an MLR with normalized predictor variables would have resulted in the estimation of negative values for low-flow years. The use of the transform increased the variance explained by a few percent for each model, most likely because of the dampening in variance resulting from the $\log_{10}$ transformation.

Under the general assumption that discharge and tree growth respond to climatic stimuli in a similar manner, the record of past climate contained in the tree-ring series was substituted as proxy data to reconstruct records of annual runoff. Streamflow records were reconstructed by using the tree-ring series as independent predictors in an MLR with the $\log_{10}$ discharge data for the period of gaged record. In all MLRs only those variables that were significant at the 99 percent confidence level and that resulted in an increase in $R^2$, adjusted for the loss of a degree of freedom caused by entering the variable (18), were entered in the prediction equations.

The streamflow reconstructions were analyzed for periodic components by using spectral-analysis methods (19). The series was lagged by 100 yr and the Parzen weighting function was employed, as detailed in the computer program of Aarons and Reagan (20). The confidence limits for the spectral density function were determined in accordance with the technique described by Chatfield (21).

## Results and Discussion

Because the discharge reconstructions for the two rivers are quite similar, and in the interest of brevity, only the results for the Salt River basin are discussed here. Important differences between the two basins will be noted.

The results of the calibration of the Salt River discharge and tree-ring data are summarized in the third column of Table 1. Because the most important precipitation influencing both discharge and tree growth occurs in the winter months, two separate calibrations were used; the discharge for October through April and that for December through March were reconstructed in addition to the total annual flow. Because all of the tree-ring series were not of the same length, separate prediction equations were developed for each of the common data periods to maximize the length of the reconstructed records. The reconstructed annual discharge is plotted along with the actual gaged data in Figure 3 (calibration period is 1914-1979).

The reconstructed values were tested against actual gaged flow by simple linear regression that used both the early independent data from 1895-1907 and that from 1911-1913 and the data from the 1914-1979 calibration period (columns B of Table 1). A reduction in $R^2$ from the original prediction equation occurred in every case. This reduction was due to the underestimation of major flows in 1905 and 1916 and also because the earlier data were from a larger drainage area. The flows predicted for 1908 and 1920 were of the same magnitude as those for 1905 and 1916, respectively, which implied an apparent lag in prediction of 3 to 4 yr for those two high flows. A likely explanation for this lag is that the period 1899-1904 was very dry, as shown by both precipitation and streamflow records. Also, cores from sample trees showed minimal or no measurable diameter growth during portions of the period. Although 1905 was a wet year, the annual ring widths did not show maximum response to this moisture until 1908. This lag was undoubtedly caused by an exhaustion of food reserves in the trees during these 6 yr of hot, dry weather. The 2 yr preceding 1916 were also very dry; many of the sample trees experienced only minimal diameter growth. During such extended dry periods, photosynthesis is inhibited by the lack of moisture and respiration rates are increased by high temperatures. This combination depletes the food reserves available for growth. Once moisture is again available, these depleted food reserves must be replenished before ring widths show a maximum response. The longer period of lag associated with these two high flows was not removed by the time-series analysis because it was unrelated to the autocorrelation structure associated with a more common 1- or 2-yr lag. Instead it appears to be a nonstationarity associated only with very wet years following drier periods.

**Table 1. Results of regressions between actual gaged data and predicted flows for Salt River near Roosevelt.**

| Season | Common Period | Original Regression ($R^2$) | Regression B | | Regression C | | Regression D | |
|---|---|---|---|---|---|---|---|---|
| | | | $R^2$ | SE (acre-ft 000s) | $R^2$ | SE (acre-ft 000s) | $R^2$ | SE (acre-ft 000s) |
| Annual | 1702-1979 | 0.728 | 0.593 | 336 | 0.757 | 260 | 0.730 | 221 |
| | 1630-1979 | 0.666 | 0.435 | 396 | 0.617 | 326 | 0.637 | 257 |
| | 1620-1979 | 0.643 | 0.387 | 413 | 0.558 | 350 | 0.579 | 276 |
| | 1580-1979 | 0.535 | 0.390 | 411 | 0.564 | 348 | 0.534 | 290 |
| Oct.-April | 1702-1979 | 0.717 | 0.586 | 293 | 0.729 | 237 | 0.712 | 191 |
| | 1680-1979 | 0.704 | 0.480 | 328 | 0.673 | 260 | 0.750 | 178 |
| | 1630-1979 | 0.686 | 0.525 | 314 | 0.679 | 258 | 0.708 | 192 |
| | 1620-1979 | 0.641 | 0.425 | 345 | 0.513 | 317 | 0.614 | 221 |
| | 1580-1979 | 0.527 | 0.361 | 364 | 0.540 | 308 | 0.524 | 246 |
| Dec.-March | 1702-1979 | 0.665 | 0.497 | 240 | 0.706 | 184 | 0.724 | 132 |
| | 1680-1979 | 0.633 | 0.342 | 275 | 0.577 | 220 | 0.703 | 138 |
| | 1620-1979 | 0.604 | 0.425 | 257 | 0.522 | 227 | 0.630 | 154 |
| | 1580-1979 | 0.490 | 0.341 | 275 | 0.498 | 240 | 0.517 | 176 |

Notes: SE = standard error of estimation.
$R^2$-values are adjusted for loss in degrees of freedom.

Figure 3. Reconstructed and actual discharge of Salt River near Roosevelt.

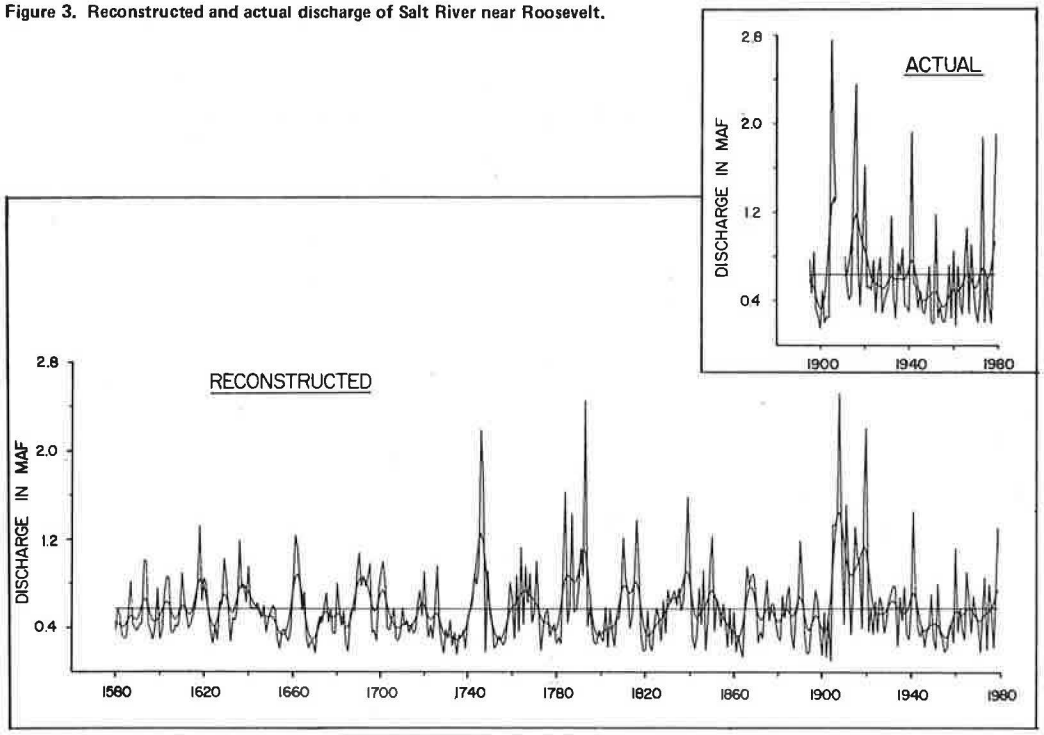


Because the predicted values for 1908 and 1920 most likely represent moisture conditions in 1905 and 1916, respectively, they were substituted for the values for those years, and the regressions were performed again (columns C, Table 1). In each case the value of $R^2$ was much closer to that obtained in the $\log_{10}$ prediction equation for the period 1914-1979. Separate regressions were performed between the gaged and reconstructed data from the period 1921-1979, and the results are shown in columns D of Table 1. The $R^2$-values obtained were in agreement with those derived from the original prediction equation and the regressions with the two high flows transposed, which also indicated that the longer period of lag for the two high flows was responsible for the majority of the reduction in $R^2$.

The standard errors of estimation are also included in Table 1. The values for the 82-yr regression with the high flows transposed (columns C) are probably more representative of the standard errors of the estimated flows themselves. The values obtained without transposing the two high flows (columns B) are more representative of the standard errors associated with the flows predicted for a particular year. Because the magnitude of a high historical flow is more important in terms of design than the year in which it occurred, the standard errors in columns C are probably more realistic estimates of the standard errors in magnitude for flows estimated outside the calibration period.

Statistical analyses performed on the gaged and predicted discharge records and the results for the annual reconstruction are shown in Table 2. The first four moments of the actual and predicted records for the period 1914-1979 were nearly identical for each the models, which indicates that the reconstructions provide reliable estimates of the distribution of annual and seasonal flows. Frequency distributions of both gaged and predicted records for the 1914-1979 period are shown in Figure 4. From a design standpoint, the problems associated with the lag in prediction of certain high seasonal flows are not important when the distributions alone are considered.

Table 2. Results of statistical analyses of reconstructed and actual annual discharge of Salt River near Roosevelt.

| Data | Period | Mean (acre-ft 000s) | Standard Deviation (acre-ft 000s) | Skewness | Kurtosis |
|---|---|---|---|---|---|
| Actual | 1914-1979 | 626.8 | 480.0 | 1.81 | 3.11 |
| Reconstructed | 1914-1979 | 588.1 | 371.9 | 1.89 | 5.01 |
| | 1580-1979 | 576.6 | 343.9 | 2.02 | 9.64 |
| | 1580-1659 | 547.4 | 227.4 | 1.12 | 4.29 |
| | 1660-1739 | 514.9 | 249.1 | 0.84 | 3.12 |
| | 1740-1819 | 623.3 | 431.3 | 2.01 | 8.12 |
| | 1820-1899 | 544.4 | 274.3 | 0.94 | 4.74 |
| | 1900-1979 | 639.1 | 451.4 | 1.81 | 7.21 |

Figure 4. Frequency distributions of actual (open bars) and reconstructed (hachured bars) stream flow of Salt River near Roosevelt.

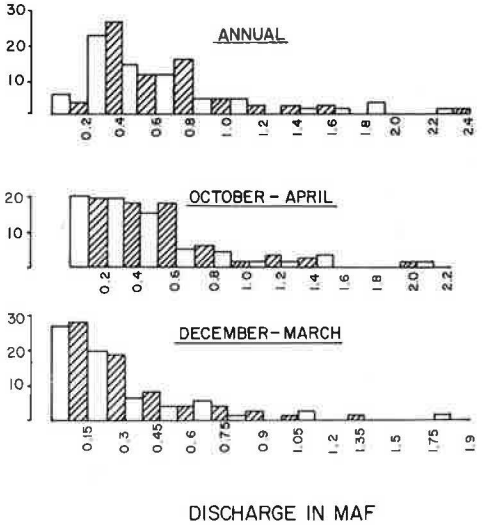

Figure 5. Spectral density function for October-April discharge of Salt River near Roosevelt.

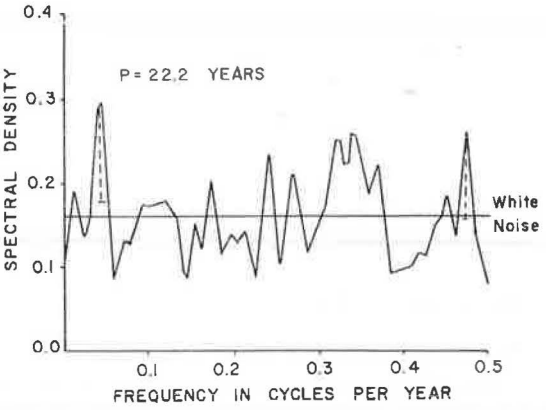


Table 3. Comparison of selected actual and reconstructed flows of Salt River near Roosevelt.

| Flow Year | Season | Actual (maf) | Avg Actual Occurrence | Reconstructed (maf) | Avg Reconstructed Occurrence |
|---|---|---|---|---|---|
| 1905 | Annual | 2.76[a] | 1 in 80 | 2.52 | 1 in 400 |
| | Oct.-April | 2.28[a] | 1 in 80 | 2.17 | 1 in 200 |
| | Dec.-March | 1.51[a] | 1 in 40 | 1.39 | 1 in 400 |
| 1916 | Annual | 2.36 | 1 in 40 | 2.21 | 1 in 133 |
| | Oct.-April | 2.08 | 1 in 40 | 1.88 | 1 in 100 |
| | Dec.-March | 1.78 | 1 in 80 | 1.26 | 1 in 200 |
| 1941 | Annual | 1.93 | 1 in 27 | 1.45 | 1 in 40 |
| | Oct.-April | 1.42 | 1 in 20 | 1.38 | 1 in 57 |
| | Dec.-March | 1.08 | 1 in 16 | 0.99 | 1 in 100 |
| 1979 | Annual | 1.91 | 1 in 20 | 1.30 | 1 in 22 |
| | Oct.-April | 1.59 | 1 in 27 | 1.12 | 1 in 31 |
| | Dec.-March | 1.08 | 1 in 20 | 0.80 | 1 in 57 |

Notes: Average occurrence is the number of times the flow was equaled or exceeded divided by the period of record. Actual period of record is 1900-1979; reconstructed period is 1580-1979.

[a]Includes the discharge of Tonto Creek.

The means for the 80-yr periods 1740-1819 and 1900-1979 were significantly greater than those for the three remaining periods at the 80 percent (or better) confidence level, yet they were not significantly greater than the 400-yr mean. This has important implications for water supply planning because it suggests that although the mean from the period of gaged record (1914-1979) was not significantly different from the 400-yr mean, it may not be a reliable estimator of the dependable annual supply. The mean annual flow from the three 80-yr periods of lower flow (1580-1659, 1660-1739, 1820-1889) may represent a more realistic value.

Several periods of sustained high and low flows are evident throughout the 400-yr reconstructions. The period 1905-1920 was the wettest in the entire reconstruction; almost all of the predicted flows were above the 400-yr mean. The only other period that approached the early 1900s in magnitude was from the mid-1780s through the mid-1790s.

Moving averages of 2, 5, 10, 25, and 50 yr were calculated in order to analyze the short- and long-term trends in the reconstructions. High flows in the early 1900s dominated the short- and long-term means of each seasonal reconstruction. The driest 5-yr period ended in 1670. This drought is known to have occurred over the entire Southwest and resulted in severe hardship for the Pueblo Indians living in the area (22). A sustained low-flow period lasting from 1728 until 1739 dominated the long-term low-flow means. During this period the average annual discharge was only 43 percent of the 400-yr mean, and in no year did the discharge exceed the mean value. The recurrence of such an extended dry period would have devastating consequences.

The spectral density function for the October-April reconstruction is shown in Figure 5. The lower 90 percent confidence level is plotted for two of the frequencies. The white-noise line is the spectral density function of a normally distributed random variable. The only significant value occurred at 22.2 yr and reflects the return of extended low flows. This is important from the standpoint of water supply because it implies that there is a tendency toward deficient streamflow every 22 yr. Mitchell and others (23, pp. 125-143) found a 22-yr periodicity in the occurrence of drought in the western United States and related it to the Hale solar cycle. A similar periodic component in gaged streamflow records for the entire United States has been noted by Langbein and Slack (24). This periodic low-flow tendency for the Salt River should be incorporated into future water supply planning efforts. It should be noted that the reconstructed discharge for the Verde River showed no significant periodicity. This most likely relates to the low-flow characteristics of the Verde, which is controlled by discharge from springs rather than climatic variations.

In terms of high-discharge events, water year 1979 was particularly troublesome to the city of Phoenix; the gaged October-April discharge of 1.59 maf for 1979 had been equaled or exceeded only three times since 1900. A high-discharge value was predicted for 1979 in all of the reconstructions. The predicted discharge was 1.12 maf and was equaled or exceeded 12 times during the past 400 yr. On the average, then, a seasonal flow of this magnitude was recorded in the actual data once every 30 yr, which indicated that the 1979 gaged flow was not anomalous. In general, there was an above-average number of high seasonal flows during the period 1900-1979 when it was compared with the long-term reconstruction. A summary of comparisons between flows from the periods of gaged and reconstructed records is shown in Table 3.

## CONCLUSIONS

In the absence of gaged records, proxy data sources such as tree rings can be used to reconstruct hydrologic events back in time. Among the several sources of proxy data, tree rings are the most widely used and have the advantage of precise dating, site replication, and the preservation of both high- and low-frequency information. The chief disadvantage is that tree-ring reconstructions rarely extend back more than 500 yr.

Tree-ring reconstructions are particularly useful in determining whether a known period of record truly represents the infinite number of events that have occurred in the past. Planning models based on anomalously wet or dry periods are likely to produce erroneous results.

Climatically sensitive tree-ring series can be used to reconstruct annual and, in some instances, seasonal flows. Periods of above- or below-normal flows as well as long-term trends are quite evident in reconstructed hydrologic series. Because an individual tree ring integrates climatic and site factors for an entire year or more, peak flows cannot be reconstructed.

In general, ring widths reflect dry conditions better than wet ones. In a wet season, moisture in excess of that held in the soil profile is not

translated into growth. This point is important in hydrologic reconstructions and also explains why narrow rings are better for diagnostic and crossdating purposes than wide rings.

Hydrologic information derived from tree rings has had limited use in water resources planning. Yet, in lieu of gaged records, there is at present no better source of information on both short- and long-term climatic variations. The development of an expanded, worldwide tree-ring data base could provide a valuable planning tool for hydrologists. This is especially true for parts of the world where gaged records are essentially nonexistent.

## ACKNOWLEDGMENT

The continuing support of our research by the Atmospheric Sciences Division of the National Science Foundation has made it possible to develop the methods and procedures used in hydrologic reconstructions. The U.S. Army Corps of Engineers supported the Salt-Verde Basin Study. We gratefully acknowledge the support from both agencies. The American Water Resources Association has given us permission to use much of the material on the Salt and Verde Rivers that was published in the Water Resources Bulletin.

## REFERENCES

1. J.R. Wallis, N.C. Matalas, and J.R. Slack. Just a Moment! National Technical Information Service, Springfield, Va., 197 pp. NTIS: PB-231816.
2. I. Rodriquez-Iturbe. Estimation of Statistical Parameters for Annual River Flows. Water Resources Research, Vol. 5, No. 6, 1969, pp. 1418-1426.
3. Guidelines for Determining Flood Flow Frequency. Hydrology Committee, U.S. Water Resources Council, Washington, D.C., Bull. 17-A, 1977.
4. P.R. Julian. An Application of Rank-Order Statistics to the Joint Spatial and Temporal Variations of Meteorological Elements. Monthly Weather Review, Vol. 98, No. 2, 1970, pp. 142-153.
5. J. Hansen, D. Johnson, A. Lacis, S. Lebedeff, P. Lee, D. Rind, and G. Russell. Climate Impact of Increasing Carbon Dioxide. Science, Vol. 213, No. 28, 1981, pp. 957-966.
6. C.W. Stockton. Long-Term Streamflow Records Reconstructed from Tree Rings. Univ. of Arizona Press, Tucson, Ariz., Papers of Laboratory of Tree-Ring Research, No. 5, 1975, 111 pp.
7. H.C. Fritts. Tree Rings and Climate. Academic Press, London, England, 1976, 567 pp.
8. C.W. Stockton and W.R. Boggess. Augmentation of Hydrologic Records Using Tree Rings. In Improved Hydrologic Forecasting--Why and How (Proc., Engineering Foundation Conference, Asilomar, Calif., March 25-30, 1979), ASCE, New York, NY, 1980.
9. G.E.P. Box and G.M. Jenkins. Time Series Analysis: Forecasting and Control, rev. ed. Holden-Day, San Francisco, Calif., 1976, 576 pp.
10. D.M. Meko. Applications of Box-Jenkins Methods of Time Series Analysis to the Reconstruction of Drought from Tree Rings. Department of Hydrology, Univ. of Arizona, Tucson, Ph.D. thesis, 1981 (available from University Microfilms, Ann Arbor, Mich.).
11. C.W. Stockton and G.C. Jacoby. Long-Term Surface Water Supply and Streamflow Levels in the Upper Colorado River Basin. Institute of Geophysics and Planetary Physics, Univ. of California at Los Angeles, Lake Powell Research Project Bull. 18, 1976.
12. N.W. Plumer and E. Hinds. Management of the Upper and Lower Colorado River Basins--An Integrated Effort. In Unified River Basin Management (R.M. North, L.B. Dworsky, and D.L. Allee, eds.), American Water Resources Association, Minneapolis, Minn., Tech. Publ. TPS 81-3, 1980.
13. R.L. Holmes, C.W. Stockton, and V.C. LaMarche, Jr. Extension of River Flow Records in Argentina from Long Tree-Ring Chronologies. Water Resources Bulletin, Vol. 15, No. 4, 1979, pp. 1081-1085.
14. D. Campbell. The Feasibility of Using Tree-Ring Chronologies to Augment Hydrologic Records in Tasmania, Australia. School of Renewable Resources, Univ. of Arizona, Tucson, master's thesis, 1980.
15. L.P. Smith and C.W. Stockton. Reconstructed Stream Flow for the Salt and Verde Rivers. Water Resources Bulletin, Vol. 17, No. 6, 1981, pp. 939-947.
16. W.W. Cooley and P.R. Lohnes. Multivariate Data Analysis. Wiley, New York, 1971, 364 pp.
17. J.E. Kutzbach. Empirical Eigenvectors of Sea-level Pressure, Temperature and Precipitation Complexes Over North America. Journal of Applied Meteorology, Vol. 6, No. 5, 1967, pp. 791-802.
18. J.E. Kutzbach and P.J. Guetter. On the Design of Paleoenvironmental Data Networks for Estimating Large-Scale Patterns of Climate. Quaternary Research, Vol. 14, No. 2, 1980, pp. 169-187.
19. G.M. Jenkins and D.G. Watts. Spectral Analysis and Its Applications. Holden-Day, San Francisco, Calif., 1968, 525 pp.
20. D. Aarons and M. Reagan. SPSS Subprogram Spectral--Spectral Analysis of Time Series. Northwestern Univ., Evanston, Ill., Vogelback Computer Center Manual 434, 1977, 23 pp.
21. C. Chatfield. The Analysis of Time Series: Theory and Practice. Chapman and Hall, London, England, 1975, 263 pp.
22. J.K. Page. Rebellious Pueblos Outwitted Spain Three Centuries Ago. Smithsonian, Sept. 1980, pp. 86-95.
23. J.M. Mitchell, Jr., C.W. Stockton, and D.M. Meko. Evidence of a 22 Year Rhythm of Drought in the Western United States Related to the Hale Solar Cycle Since the 17th Century. In Solar-Terrestrial Influences on Weather and Climate (B.M. McCormac and T.A. Seliga, eds.), D. Reidel Publishing Co., Boston, Mass., 1979.
24. W.B. Langbein and J.R. Slack. Patterns in Regional and National Streamflow. U.S. Geological Survey, Washington, D.C., Open-File Rept., 1980.

# Paleoflood Hydrologic Techniques for the Extension of Streamflow Records

VICTOR R. BAKER

Paleoflood hydrology includes geomorphic-botanic studies of the effects of ancient floods on the landscape and the study of ancient slack-water deposits. Slack-water deposits consist of sand and silt that accumulated relatively rapidly from suspension during major floods. Useful slack-water sediment accumulations occur along bedrock canyons at the mouths of tributaries and at other protected localities. Where individual flood-sedimentation units can be recognized, various dating techniques are used to assign ages to the responsible flood events. Problems with incomplete flood records at any one slack-water site, the relating of deposit heights to paleoflood stages, and the age relationships of dated materials to flood ages require the analysis and correlation of numerous sites and flood layers along a given river reach. Paleostage determinations and flood ages can be converted to discharge and recurrence-interval estimates for the large, rare floods recorded in a slack-water sequence. Flood-frequency curves can then be constructed by combining the paleoflood data with shorter-term stream-gage data.

Conventional engineering approaches encounter considerable difficulty in assessing the risks from rare, large flood events. The problem is especially difficult if the true return period of an event of extremely high magnitude is much larger than the period of existing records of streamflow and precipitation. Paleoflood hydrologic techniques have been developed to extend flood-frequency records into the geologic past (1, pp. 3-9; 2) and thereby to assess the true return periods of extreme events.

A significant design problem for large floods arises during the interpretation of hydrologic outliers. Outliers are data points that depart from the trend of the rest of the data on a flood-frequency curve (3). If an especially large flood outlier occurs in a given historic flow record, its inclusion in the analysis could result in the overdesign of flood-control works. An excellent example is the 1954 flood on the Pecos River, which exceeded all events in the previous 54 yr by about an order of magnitude. By paleoflood hydrologic analysis it was recently established that the return period of the 1954 flood event is at least 2,000 yr (4). However, without these data, expensive overdesign might result from overemphasis of the outlier in risk analysis. Alternatively, outliers may be underemphasized, which results in dangerous underdesign of flood-control works. Even the adjustment of outliers for historical data, as recommended by the U.S. Water Resources Council (3), can lead to underdesign when the length of the historical record is particularly short relative to the true recurrence interval of a catastrophic flood event.

## PALEOFLOOD HYDROLOGY

The underlying assumptions in hydrologic risk analysis are the subjects of continual research and scientific debate. Paleoflood hydrology has been developed not to answer questions about theoretical distributions of floods in time but simply to extend the length of hydrologic records by the use of stratigraphic geology and geomorphology (5, pp. 109-117). In this paper, therefore, two pragmatic questions will be addressed: What techniques are available for extending flood records into the geologic past? How can these techniques be moved from the realm of the geologist to that of the field engineer?

### Geomorphic-Botanic Methods

The morphologies of stream channels and their adjacent floodplains can be profoundly influenced by large floods. The effects of such catastrophic floods on the landscape and on vegetation may persist for extremely long periods, and these effects can be preserved by burial with flood debris. Soil formation is a useful indicator of flood frequency, because maturely developed soils can develop on a floodplain only when long time intervals occur between the influxes of new flood debris burying the land surface. Because floodplain soils may be rich in organic matter, radiocarbon dating of specific soil samples has proven useful in dating the past floods that deposited them or their precursor parent materials (6, pp. 189-217). Figure 1 shows a field example; radiocarbon dating of the insoluble residue fraction from soil humus yielded an age of 710 ± 50 yr BP for this ancient organic soil (6).

Because major floods can also erode older landforms on a floodplain, the truncation of dated landforms also can be a useful indicator of flood frequency. For example, Costa (7) found that an alluvial fan eroded by the Big Thompson Canyon flood in 1976 had remained intact for at least 10,000 yr before the flood. In geomorphic flood studies the investigator should attempt to find the youngest surface that has been either buried by the largest known flood or eroded by that flood. The age of that surface is then equivalent to the minimum recurrence interval of the flood. Examples of this relatively simple paleoflood technique are provided by Costa and Baker (8).

### Slack-Water Deposits

Slack-water deposits consist of sand and silt that accumulate relatively rapidly from suspension during major floods. Deposition is localized where the flow boundaries for the peak flood discharges result in sufficiently reduced current velocities relative

Figure 1. Buried soil (center) exposed in the eroded floodplain of Elm Creek, central Texas.

to the channel-center velocities. Confined bedrock canyons or relatively narrow valleys are ideal for slack-water deposition because large floods transform the whole canyon or valley bottom into a temporary flood channel. As discharge increases, the stage rises relatively rapidly because of the narrow valley (channel) walls. This situation is in contrast to that of a broad floodplain valley in which overbank flood flows spread over a wide valley bottom, which results in a relatively slow rise of stage with increasing discharge.

At the high stages achieved by floods in narrow gorges, sufficiently high velocities and shear stresses develop that allow sand and silt to be easily carried in suspension. The relatively coarse suspended load will have a high settling velocity and can easily settle in local zones of reduced flood-flow velocity. Thus, a requirement for useful slack-water flood records is that sufficiently coarse sediment be available in abundance for suspended transport by rare, high-magnitude floods. Figure 2, an aerial photograph taken at maximum flood stage, 3:00 p.m., August 3, 1978, shows the formation of a flood slack-water deposit. Note the prominent slack-water zone in the center, where flow has expanded below a constriction. Flood stage was approximately 10 m.

The local sites of slack-water deposition are of several common varieties. Abrupt channel expansions result in deposition because of flow separations (eddies) that develop downstream of a constriction.

Figure 2. Pedernalles River at Pedernalles Falls, central Texas, August 3, 1978.

Figure 3. Same reach of Pedernalles River as that in Figure 2, August 17, 1978.

Figure 4. Slack-water deposit (covered by trees at center) developed at mouth of tributary (lower center) to Pecos River in western Texas.

Figure 3 shows the slack-water sand accumulation at the former position of the flood eddy shown in Figure 2. Deposition may also occur upstream from channel constrictions because of backwater effects during large floods. Tributary mouths (Figure 4) are also common sites of slack-water deposition because the tributary valleys can be backflooded by large floods in the main channel. The eddies and slack-water zones at the tributary mouths result in flood deposition. Tributary valleys or canyons that join the main valley at an angle close to 90° appear to have the optimum geometry to generate slack-water deposition. Obstructions in the channel, such as large boulders and bedrock knobs, lead to accumulations of flood debris on their downstream ends. Bedrock caves along channel or valley walls can be especially important sites because (a) long-term preservation is likely for deposits and (b) the possibility exists that aboriginal human occupation has left datable material.

The long-term preservation of slack-water deposits may also be important for paleoflood hydrologic studies. Sites that hydraulically favor slack-water sediment accumulation at high flood stage may become eroded by low-stage flows. Thus, the meandering low-flow channel may cut into flood slack-water accumulations at meander bends and downstream of flood-flow channel obstacles. In this way, given sufficient time, low-level slack-water deposits may be completely removed from a canyon or valley. The field investigator must then search for locally preserved high-level remnants of the flood deposits. Even these may be difficult to find if valley-wall and slope processes have removed them. Protected sites near large boulders, in bedrock niches and caves, and in depressions on valley-side benches have been found to preserve flood deposits for the longest periods after extreme events. Deposits at tributary mouths are protected from main-channel low flows, but they are vulnerable to erosion by floods on the tributaries themselves. The optimum tributaries for slack-water deposit preservation are those with relatively small drainage areas or relatively low efficiencies for concentrating runoff or both. That is, the peak discharge per unit area generated by floods on these tributaries does not reach the levels necessary to completely remove slack-water sequences from the tributary mouths. Distinguishing tributary alluvium from the main-channel slack-water deposition is a related problem but usually poses little difficulty. Main-channel alluvium is often lithologically distinct,

Table 1. Localities of slack-water flood paleohydrology studies.

| Location | Investigator | Summary of Results |
|---|---|---|
| Pecos River, West Texas | R.C. Kochel, P.C. Patton, V.R. Baker | Recurrence interval of 1954 flood has been established as >2000 yr |
| Central Texas | P.C. Patton, V.R. Baker | Recurrence intervals of catastrophic floods have been established as several hundred years |
| South-central Utah | P.C. Patton, V.R. Baker | Flood-recurrence intervals of several hundred years have been established |
| Connecticut | P.C. Patton | Slack-water deposits document Holocene floods larger than the largest historic event |
| Central Virginia | R.C. Kochel | Tropical storms have left Holocene record of geomorphic flood effects |
| Central and North Australia | V.R. Baker, G. Pickup | Catastrophic floods have left spectacular accumulations of slack-water sediments |
| Eastern Idaho | V.R. Baker | Late Pleistocene and Holocene slack-water sequences record major floods |
| Skagit River, Washington | J.E. Stewart, G.L. Bodhaine | Paleoflood magnitudes of 1815 and 1856 floods have been reconstructed |
| Northern California | E. Helley, V.C. LaMarche | Radiocarbon and tree-ring studies of floods with recurrence intervals of hundreds of years have been made |

and the fines are deposited in the tributary valley, whereas the tributary alluvium is usually much coarser bedload, which is deposited downstream.

Despite the various limitations on slack-water site development and long-term preservation, a large number of paleoflood studies have now been carried out (Table 1). The relatively narrow valleys and canyons of the western conterminous United States; the dissected plateaus, hills, and piedmonts of the eastern states; and the various dissected uplands of the midcontinent are all favorable areas for the type of analysis reported in this paper.

## ANALYZING PALEOFLOOD STRATIGRAPHY

The study of flood slack-water deposits uses the tools of the stratigraphic geologist: sediment analysis, description of soil profiles, dating techniques, and correlation. Extended discussions on stratigraphic techniques are available in textbooks on Quaternary stratigraphy (9,10); this background cannot be reviewed here. Rather, this section will list some specific techniques that the field experience to date (Table 1) has shown to be most useful.

### Recognizing Individual Flood Sedimentation Units

A slack-water depositional site will often preserve the sedimentation units of numerous individual flood events, as shown in Figure 5 (note the laminated units of flood-deposited sand, each capped by fine-grained organic detritus). Distinguishing the individual floods is accomplished by a number of sedimentological techniques. Flood layers may be capped by indicators of subaerial exposure that followed recession of the flood hydrograph. Such indicators include relict mudcracks, cultural layers indicating aboriginal human occupation of the surface, and ancient soil profiles (paleosols). Layers of colluvium from the valley sides or layers of tributary alluvium may also indicate time breaks in the slack-water sedimentation corresponding to time intervals between flood events.

Properties of the individual flood layers themselves can be useful. Certain flood events may impart distinctive lithologic or textural properties or colors to their deposits. These properties result from variations in the locations of flood-generating storms over the drainage basin or variations in the flood hydrographs at the depositional site or both. Stratigraphic breaks between individual flood units may be marked by abrupt reversals in the vertical grain size trends of the deposit because of hydrograph influences. Cappings of silt, clay, or organic detritus commonly mark the top layer of an individual sandy flood-sedimentation unit (Figure 5). These fine particles are transported near the surface of the flood water and are normally the last materials to be deposited by a flood at a site.

Figure 5. Slack-water sediments in the Katherine River Gorge, Northern Territory, Australia.

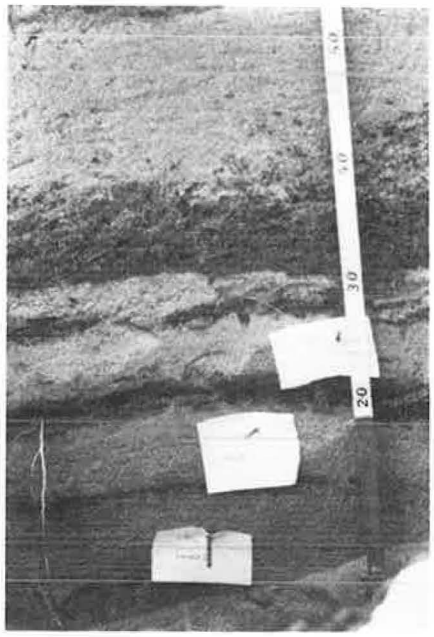


Several difficulties must be kept in mind when flood sedimentology is studied. Bioturbation of slack-water sediments may destroy the depositional structures and textures that permit the recognition of individual flood units. Bioturbation is more common in humid regions and local climatic settings favoring lush vegetation and soil organisms. Abundant roots, insect burrows, worm tubes, and so on are clues to bioturbation of older slack-water deposits. Even where an undisturbed sequence is found, however, the possibility remains that the record may be incomplete. Erosion by tributary

floods, deflation, and slope processes are among the actions that may remove part of the flood record at any one site. The way to minimize the error introduced by an incomplete record at one slack-water site is to study numerous sites along a given river reach and then to correlate flood layers between individual sites.

## Correlation

Correlation of the flood layers that correspond to individual flood events may be accomplished by lithologic or temporal means. The latter approach attempts to date individual layers or the intervals between those layers. In the next subsection dating techniques will be discussed in some detail. Unlike temporal correlations, lithologic correlation does not require datable materials and can be used at all localities.

Floods originating from different subbasins may be labeled by the distinctive source terrains of their sediments. This results in a recognizable lithology and mineralogy for some individual flood units. The duration and recession of flood hydrographs also exert an important control such that thicknesses, grain-size characteristics, and sedimentary structures may also be distinctive in given flood units. Also, the nature and duration of the time intervals between floods can be important in dictating the soil development properties, color, degree of induration, and colluvial burial of individual units. Finally, the stratigraphic positions of units of known age with respect to one another can be guides to what may be missing or present at any given study site.

## Dating Techniques

Slack-water deposits may be dated by both relative and absolute means. Absolute techniques allow a specific age to be assigned to the dated material, whereas relative techniques allow a qualitative comparison of ages between separate dated materials. Relative ages of units can be assessed by their degrees of alteration, soil formation, and burial position.

The occurrence of buried paleosols in slack-water sequences provides an important dating opportunity. Soils in floodplain alluvial settings are cumulative, continuously buried by new additions of alluvium. Generally soils are weakly developed because the rate of soil formation, such as the development of an organic-rich horizon, is simply too slow relative to the burial process. For a slackwater deposit that is high above the river-bed elevation, however, only rare floods can inundate the surface and thereby bury the developing A horizon (11). The result is a preserved paleosol the degree of development of which is a measure of the time interval between flood events. In the Pecos River region of western Texas, Kochel (12) found that at least 500 yr was required between flood events to generate a recognizable buried soil.

Radiocarbon dating is the most commonly employed absolute dating tool in paleoflood hydrology, although several other techniques are also available (Table 2). The method yields an age and standard deviation based on various laboratory procedures (13). Suitable materials for radiocarbon dating include various types of organic matter intercalated with the slack-water deposits. The organics may have been transported directly by the flood water. Litter, such as twigs, seeds, and leaves, may yield nearly synchronous ages to the flood events, because these materials decay rapidly on the ground surface and must be buried for preservation. Flood-transported logs and wood fragments, however, provide only maximum ages of the deposits because wood can be redeposited by floods that have eroded older deposits or it can be stable on the ground for many years, especially in arid climates. Water-transported charcoal poses a similar difficulty (14). Nevertheless, the charcoal and organic detritus associated with aboriginal human occupation can be synchronous with the interval between flood events, especially if the materials are buried by a subsequent flood. Tree stumps buried in their living position and burn zones from ground fires are also useful in marking a time zone, but such features are much less common than more problematic organic materials.

Organic soil horizons pose some difficulty for radiocarbon-dating procedures. The usual assumption in the technique is that the laboratory-determined date is a measure of elapsed time since the death of the organisms responsible for the analyzed organic matter. In soils, however, the accumulation of dead organic matter is a cumulative process. Radiocarbon dates on soils may therefore vary in age, and they will not necessarily represent the initial time of soil formation (15, pp. 77-88). Nevertheless, the oldest date obtained from a soil is the minimum age of soil formation. Because soluble humic acid is the most likely source of contamination in soil humus, the insoluble residue from soil humus is thought to represent the mean residence time of humus in a soil (16, pp. 63-75). Correlation of buried soils on paleoflood deposits is therefore best accomplished by comparing dates on insoluble organic residues. Comparison of these residue dates with dates on humic acid and on the total soil humus are likewise useful in interpreting the time interval over which the soil was developing before its burial by a subsequent flood. Patton and Baker (6, pp. 189-217) give an example of this application of paleosol study in evaluating ancient floods.

In general, the dating and time-stratigraphic correlation of individual flood deposits from one

**Table 2. Datable materials and dating techniques for flood slack-water sediments.**

| Type of Material | Dating Technique | Problem Encountered |
|---|---|---|
| Aboriginal artifacts | Archeological studies | Cultural time transgression |
| Buried trees | Dendrochronology | Cross-dating sequences need to be established |
| Organic matter in buried soils | Radiocarbon | Soils form and are contaminated until subsequent burial |
| Charcoal | Radiocarbon | Allochthonous (water-transported) charcoal may be much older than strata |
| Fine-grained flood-transported organics | Radiocarbon | Decay and contamination by younger roots |
| Flood-transported logs and wood fragments | Radiocarbon (and some dendrochronology) | Wood may be much older than strata |

locality to another are best accomplished by multiple sampling and by multiple techniques. A strategy should be developed so that this multiple approach yields independent checks on evolving hypotheses concerning flood ages and correlations of flood layers.

## HYDROLOGIC ANALYSIS

The transformation of geologic studies of flood sediments to useful design data for flood-hazard management requires a closely knit set of assumptions and procedures. Most critical for establishing past flood magnitudes is the correlation of slack-water elevations to the responsible flood paleostages. Because even the deepest slack-water deposits will have had some water above them at peak stage, the deposit elevations themselves are minimum paleostage indicators. Two procedures can be used to minimize the errors introduced by this situation. The first is to study the deposits of a given flood event at numerous sites. Local conditions will generally allow preservation of the flood sediments at higher levels at some sites relative to others. In this way the maximum flood stage may be approached, but its actual value is always known to be somewhat larger.

A second procedure is to develop empirical correlations between the measured high-water surfaces of historic floods and the depths of deposits that they emplaced. These correlations are then used to correct the paleostage estimates from ancient slack-water deposits. The actual flood levels of historic floods can be determined from gage records, the observations of local residents, or from studies of isolated sediment pockets and drapes on hillsides that are temporarily preserved after a major event.

Another important assumption in paleoflood hydrology is that significant aggradation or degradation of the channel or both have not occurred in the time span represented by the slack-water sedimentary sequence. Generally the use of bedrock canyons and valleys will limit the influence of this factor, but any slack-water study of a long time span should document evidence for bed elevation changes that would alter the discharge calculations obtained from slack-water deposit elevations. Similarly a bedrock channel will minimize the occurrence of scour and fill during an individual flood event, which could complicate the interpretation.

### Slope-Area Calculations

Once paleoflood stages have been established for each of the various slack-water deposit layers corresponding to individual floods, the investigator must transform those data into discharge estimates. This is accomplished by standard slope-area hydraulic calculations (17), which are easily performed on hand calculators (18). The necessary input data are as follows:

1. Cross sections at two (preferably three) locations (determine flow areas and hydraulic radii for stages up to the tops of flood slack-water accumulations),
2. Roughness coefficients (Manning n),
3. Slope of the flood-water surface (approximated as the fall in elevation for the tops of the slack-water sediment accumulations divided by the length of the reach between the cross sections), and
4. Energy coefficients (range 1.15 to 1.5 for natural streams).

### Determining Flood Recurrence Intervals

When only one paleoflood event is recognized, the age of the youngest surface buried or eroded by the flood is the minimum recurrence interval of that event. When multiple events are recognized in a slack-water sequence, the magnitude of each should be determined as described above. Each event is then ranked; the ranking M = 1 is assigned to the largest, M = 2 to the second largest, and so on. The age of the oldest known flood in the sequence is assumed equivalent to the number of years of record (n). Each event can then be assigned a recurrence interval, calculated as (n + 1)/M. The probability that a flood of a given magnitude will be equaled or exceeded in any one year is simply the reciprocal of this recurrence interval. Because only the largest events, and therefore the longest recurrence intervals, are recorded in slack-water sequences, recur-

Figure 6. Comparison of various techniques for estimating flood frequency in the lower Pecos River region of western Texas.

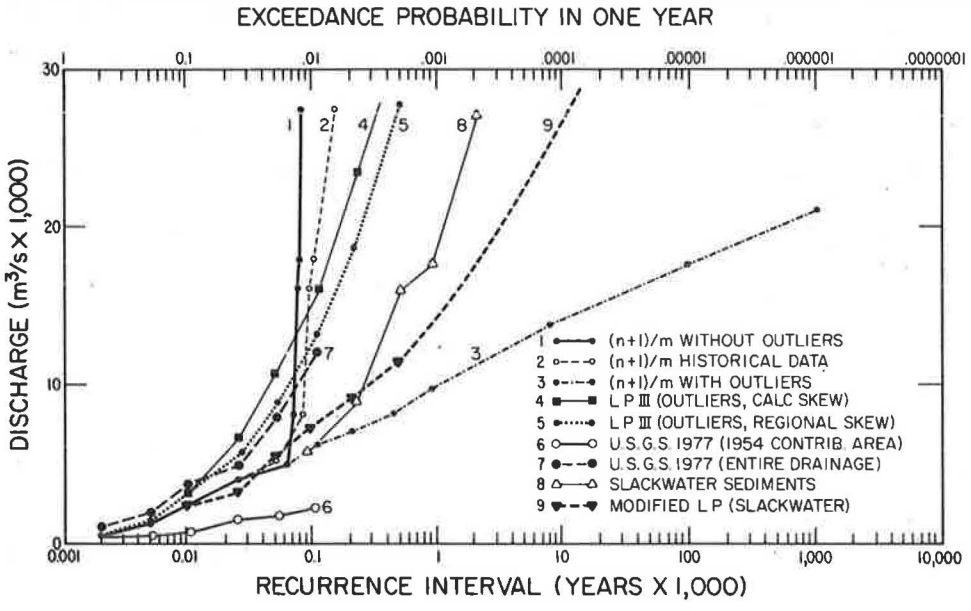

rence intervals for low-magnitude, high-frequency events must be obtained from gage records.

Flood recurrence intervals determined from slack-water sediments or from geomorphic-botanic analysis of ancient floods are generally plotted on flood-frequency curves by assuming various statistical distributions. Kochel and Baker (2) illustrate several plotting approaches for their study of the Pecos River paleohydrology in western Texas. In Figure 6, curves 1-7 illustrate techniques that rely only on gage data and historic data. Note that these curves assign either long recurrence intervals (>1 million yr) or short ones (100 to 500 yr) for the largest flood of record. Curves 8 and 9 incorporate slack-water data and show that the recurrence interval for the great flood of 1954 was between 2,000 and 10,000 yr. The standard procedure is to treat the slack-water data in the same way as historic flood data, which are incorporated along with stream-gage data into a log Pearson type III analysis according to Appendix 6 of U.S. Water Resources Council Bulletin 17B (3).

## CONCLUSIONS

The following conclusions have been determined:

1. Despite the special locations necessary for the accumulation and long-term preservation of slack-water deposits, numerous regions have been found to preserve these records of past floods.
2. Problems in the dating of individual flood layers and in relating slack-water deposit heights to paleoflood stages require that numerous sites be analyzed and correlated along a river reach of interest.
3. Multiple dating of different layers and materials is necessary to properly assign flood age estimates.
4. Flood slack-water deposits in areas of minimal aggradation or degradation will always provide minimum paleostage estimates unless corrected for depths of flood water above deposits.
5. Once the stratigraphic geologic interpretation has been accomplished for paleostage and age estimation, the calculation of paleoflood discharges and recurrence intervals is relatively straightforward.

## ACKNOWLEDGMENT

Research on the paleoflood hydrologic techniques reported in this paper was supported by the Division of Earth Sciences of the National Science Foundation. Peter C. Patton of Wesleyan University and R. Craig Kochel of the University of Virginia worked closely with me in developing the techniques.

## REFERENCES

1. V.R. Baker, R.C. Kochel, and P.C. Patton. Long-Term Flood Frequency Analysis Using Geological Data. International Association of Hydrological Sciences, London, England, Publ. 128, Dec. 1979.
2. R.C. Kochel and V.R. Baker. Paleoflood Hydrology. Science, Vol. 215, Jan. 22, 1982, pp. 353-361.
3. Guidelines for Determining Flood Flow Frequency. Hydrology Committee, U.S. Water Resources Council, Washington, D.C., Bull. 17B, Sept. 1981.
4. P.C. Patton and D.S. Dibble. Archeologic and Geomorphic Evidence for the Paleohydrologic Record of the Pecos River in West Texas. American Journal of Science, Vol. 282, Feb. 1982, pp. 97-121.
5. V.R. Baker. Geology, Determinism, and Risk Assessment. In Scientific Basis of Water Resource Management, National Academy Press, Washington, D.C., 1982.
6. P.C. Patton and V.R. Baker. Geomorphic Response of Central Texas Stream Channels to Catastrophic Rainfall and Runoff. In Geomorphology in Arid and Semi-Arid Regions. Allen and Unwin, Boston, Mass., 1977.
7. J.E. Costa. Holocene Stratigraphy in Flood-Frequency Analysis. Water Resources Research, Vol. 14, 1978, pp. 626-632.
8. J.E. Costa and V.R. Baker. Surficial Geology: Building with the Earth. Wiley, New York, 1981, 498 pp.
9. R.F. Flint. Glacial and Quaternary Geology. Wiley, New York, 1971, 892 pp.
10. P.W. Birkeland. Pedology, Weathering, and Geomorphological Research. Oxford Univ. Press, New York, 1974, 285 pp.
11. P.C. Patton. Geomorphic Criteria for Estimating the Magnitude and Frequency of Flooding in Central Texas. Univ. of Texas, Austin, Ph.D. dissertation, Aug. 1977, 221 pp.
12. R.C. Kochel. Interpretation of Flood Paleohydrology Using Slackwater Deposits, Lower Pecos and Devils Rivers, Southwestern Texas. Univ. of Texas, Austin, Ph.D. dissertation, Dec. 1980, 364 pp.
13. G. Fauré. Principles of Isotope Geology. Wiley, New York, 1977, 464 pp.
14. R.J. Blong and R. Gillespie. Fluvially Transported Charcoal Gives Erroneous $^{14}C$ Ages for Recent Deposits. Nature, Vol. 271, 1978, pp. 739-741.
15. H.W. Scharpenseel. Radiocarbon Dating of Soils: Problems, Troubles, Hopes. In Paleopedology: Origin, Nature, and Dating of Paleosols. Israel Univ. Press, Jerusalem, 1971.
16. M.A. Geyh, J.H. Benzler, and G. Roeschmann. Problems of Dating Pleistocene and Holocene Soils by Radiometric Methods. In Paleopeodology: Origin, Nature, and Dating of Paleosols. Israel Univ. Press, Jerusalem, 1971.
17. V.T. Chow. Open-Channel Hydraulics. McGraw-Hill, New York, 1959, 680 pp.
18. T.E. Croley II. Hydrologic and Hydraulic Computations on Small Programmable Calculators. Iowa Institute of Hydraulic Research, Univ. of Iowa, Iowa City, 1979, 837 pp.

# Storm-Cell Properties Influencing Runoff from Small Watersheds

HERBERT B. OSBORN

In much of the western United States, runoff from small watersheds is dominated by occasional short-duration, extremely variable, high-intensity thunderstorm rainfall. These runoff-producing events are important in highway-culvert and small-bridge design, erosion and sedimentation studies, evaluations of range management and renovation programs, and studies on urbanizing watersheds. A kinematic-cascade model (KINEROS) was adapted in this study for use on a small rangeland watershed to determine the influences of thunderstorm rainfall variability in time and space on peak discharge and runoff volume. Model parameters were developed with existing rainfall and runoff data, and the hydrographs were generated from simulated rainfall distributions. The study showed that for small rangeland watersheds (less than 1 mile$^2$), spatial and temporal rainfall distributions exert approximately equal influences on peak discharge and the influences tend to be additive. Further studies on the interrelationship between rainfall variability and watershed size are indicated, because where the storm is centered becomes increasingly important with increasing watershed size.

In much of the western United States, and particularly in the Southwest, runoff from small watersheds is dominated by occasional short-duration, extremely variable, high-intensity thunderstorm rains (1,2). These runoff-producing events are important in highway-culvert and small-bridge design, erosion and sedimentation studies, evaluations of range management and renovation programs, and studies on urbanizing watersheds, but expected peak discharges and runoff volumes for such events are difficult to estimate accurately. In this paper, a kinematic-cascade model (KINEROS) was adapted for use on a small (560-acre) rangeland subwatershed to investigate the influence of thunderstorm rainfall variability in time and space on peak discharge and runoff volume. The model parameters were developed with existing rainfall and runoff data, and hydrographs were generated from simulated rainfall distributions. The influence of temporal and spatial variability was examined through comparison of the generated peak discharges and runoff volumes.

## WATERSHED DESCRIPTION

The Walnut Gulch Experimental Rangeland Watershed, operated by the Agricultural Research Service (ARS) of the U.S. Department of Agriculture (USDA), is located near Tombstone in southeastern Arizona (Figure 1). The lower two-thirds of the 58-mile$^2$ watershed is primarily brush covered (whitethorn, creosote bush, tar bush, and burroweed); the upper one-third is primarily grass covered (grama grasses). Tombstone is centrally located on the watershed. The 560-acre study subwatershed (63.004) lies north of Tombstone on the Walnut Gulch watershed boundary (Figure 1). Slopes of the study subwatershed vary up to 14 percent; the average is 9 percent. The subwatershed is drained by well-defined sand-bottomed channels in the lower portion and broad swales with poorly defined shallow meandering channels in the upper portion. Headcuts separate the sand-bottomed channels and swales on the two major branches of the drainage system. The subwatershed is brush covered, and the soils are primarily gravelly and silty loams.

## RAINFALL-RUNOFF MODELING

Many different mathematical models have been used to estimate drainage runoff peaks or volumes or both for small watersheds (3,4), but few models are sensitive enough to separate the influences on runoff of rainfall variability and critical watershed characteristics. In some cases, such definition is not needed, and the model can be quite simple (the ra-

Figure 1. Location of Walnut Gulch Experimental Rangeland Watershed and study subwatershed 63.004.

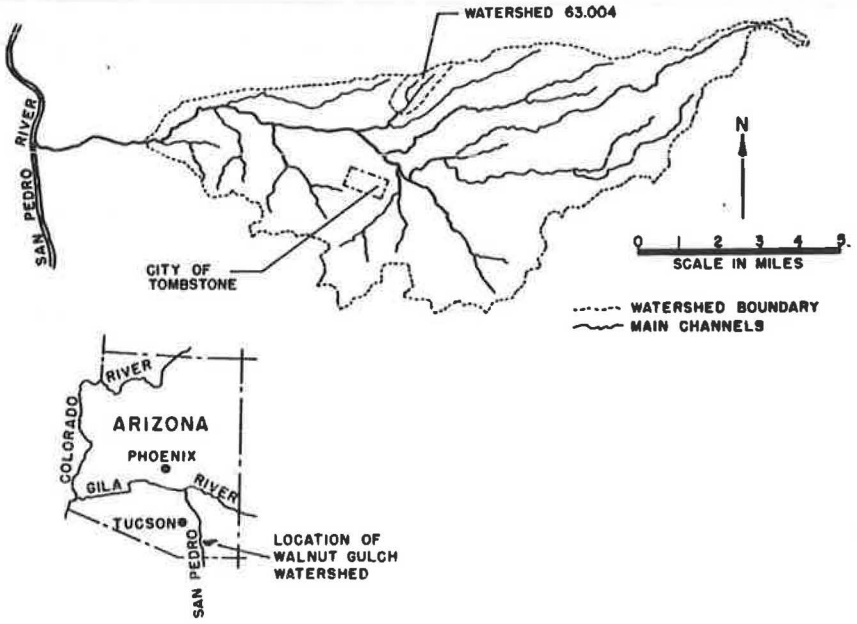

tional formula, for example). Nevertheless, to identify the significant thunderstorm-cell rainfall properties that influence runoff, critical watershed characteristics must be modeled so that their effect can be eliminated when rainfall is varied. It must be possible to isolate the watershed influences on runoff so that variations in runoff can be attributed directly to the rainfall input to the system. In the past, efforts to model the influences of rainfall variability on watershed runoff have been handicapped by the lack of a sensitive (and uncomplicated) rainfall-runoff model.

Several rainfall-runoff models were suggested for this study, and from these a kinematic-cascade model (KINEROS) (5-8) was chosen because it was versatile and sensitive to both rainfall and watershed characteristics.

## Model Description

KINEROS is a well-tested nonlinear, deterministic, distributed-parameter model (6). Inputs are (a) the hyetograph of actual or simulated rainfall, (b) the watershed surface geometry and topography, (c) parameters for surface roughness, (d) infiltration parameters, and (e) the channel networks, including slope, cross-sectional area, cross-sectional shape, and hydraulic roughness. The model also includes a subroutine for erosion, which was not used in this study. A more detailed description of the model is given elsewhere (8). For this study, a subroutine was added to account for channel abstractions.

The watershed was segmented into a series of 21 representative rectangular planes and 9 trapezoidal channel segments (Figures 2 and 3). Because all planes of the watershed were pervious, with relatively homogeneous soils and cover, the same infiltration and roughness characteristics were used throughout. Surface geometries were determined separately for each plane and channel reach (Figure 3). The numbers indicate the order in which each plane was entered into the program. Runoff from the uppermost plane along a slope can be calculated independently of that for all other planes. Because the runoff from the upper plane provides the upper boundary condition for lower planes, sequential calculation is required for complex slopes such as planes 27 and 28 in Figure 3. Flows were routed through each channel segment by using the kinematic approximation to the equations of unsteady, gradually varied flow.

Variables such as infiltration and surface roughness were adjusted based on comparisons of hydrograph simulations and actual runoff hydrographs. Particular attention was paid to surface rock cover (erosion pavement) and roughness, the initial water-holding capacity of the soils, and initial and final infiltration rates. Once the model had been adjusted, it was used to generate a series of hydrographs from simulated rainfall inputs.

## Rainfall Input

The storm-cell properties that would be expected to influence runoff are the rainfall amount and duration and the rainfall variability in time and space. These properties were examined through a series of selected inputs.

Several investigators (2,9) reported strong correlations for small watersheds between peak discharge and maximum rainfall for 30 min. On the other hand, 60-min rainfall is a more common unit used in modeling of rainfall and runoff, so both 30- and 60-min rainfall durations were used in the simulations. Also, commonly used 2-, 5-, 10-, and 100-yr expected rainfall amounts (0.9, 1.2, 1.5, and 2.3 in. for 30-min durations, and 1.2, 1.5, 1.9, and 2.9 in. for 60-min durations) were selected (1).

Temporal and spatial rainfall variabilities were considered next. Maximum intensities were concentrated early and late in the event given for each of the expected 30- and 60-min amounts (Table 1). Early events are characterized by concentration of two-thirds of the rainfall in the first one-third of the storm; in late events, two-thirds of the rainfall was concentrated in the last one-third of the

Figure 2. Detailed map of subwatershed 63.004, Walnut Gulch.

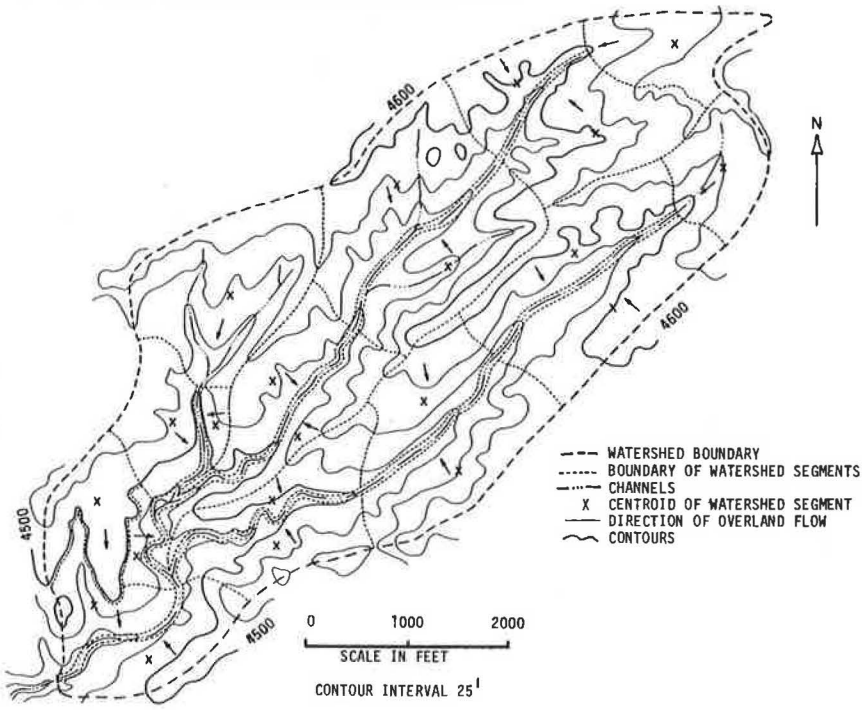

Figure 3. Schematic representation of planes and channels of subwatershed 63.004 for KINEROS.

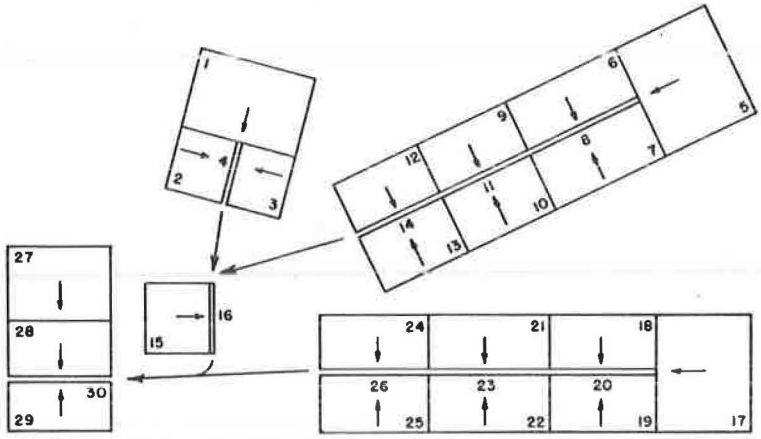


Table 1. Simulated early maximum rainfall intensities for selected frequencies for rainfall and runoff modeling, subwatershed 63.004, Walnut Gulch.

| Duration of Storm | Portion of Storm (min) | Rainfall (in./hr) by Frequency (yr) 2 | 5 | 10 | 100 |
|---|---|---|---|---|---|
| 30 min | 0-3 | 2.3 | 3.0 | 4.0 | 6.0 |
| | 3-6 | 3.1 | 4.2 | 5.2 | 8.0 |
| | 6-9 | 3.1 | 4.2 | 5.2 | 8.0 |
| | 9-12 | 2.3 | 3.0 | 4.0 | 6.0 |
| | 12-15 | 2.3 | 3.0 | 4.0 | 6.0 |
| | 15-18 | 2.0 | 2.6 | 3.2 | 5.0 |
| | 18-21 | 1.7 | 2.0 | 2.6 | 4.0 |
| | 21-24 | 0.8 | 1.0 | 1.3 | 2.0 |
| | 24-27 | 0.5 | 0.6 | 0.8 | 1.2 |
| | 27-30 | 0.2 | 0.3 | 0.4 | 0.6 |
| 60 min | 0-6 | 2.5 | 3.0 | 4.0 | 6.0 |
| | 6-12 | 3.3 | 4.2 | 5.2 | 8.0 |
| | 12-18 | 2.5 | 3.0 | 4.0 | 6.0 |
| | 18-24 | 1.7 | 2.0 | 2.6 | 4.0 |
| | 24-30 | 0.8 | 1.0 | 1.3 | 2.0 |
| | 30-36 | 0.5 | 0.6 | 0.8 | 1.2 |
| | 36-46 | 0.2 | 0.3 | 0.4 | 0.6 |
| | 46-48 | 0.2 | 0.3 | 0.4 | 0.6 |
| | 48-54 | 0.1 | 0.2 | 0.2 | 0.3 |
| | 54-60 | 0.1 | 0.2 | 0.2 | 0.3 |

Note: Late storms are mirror images of early storms.

storm. Spatial variability was modeled by centering each of the simulated events at three locations on the subwatershed--near the outlet, in the middle, and at the head of the subwatershed. Point-to-point reductions in rainfall amounts were based on earlier evaluations of Walnut Gulch rainfall data (10), and rainfall volume varied with storm location.

Finally, as a test of the effect of spatial variability on runoff, the event with the maximum observed rainfall in 25 yr of record on Walnut Gulch was centered on the study subwatershed at three different locations (Figure 4 and Table 2).

## Model Output

Hydrographs were generated from spatially varied rainfall for all 30- and 60-min simulated events. Peaks and volumes were compared (Tables 3 and 4). Storms that were spatially centered on the subwatershed produced significantly greater peaks than those centered near the outlet or at the head of the watershed (Figure 5). For events of all frequencies, rainfall centered near the subwatershed outlet produced slightly greater peaks than that centered at the head of the subwatershed (Figure 6). All

Figure 4. Maximum recorded 60-min point rainfall on Walnut Gulch (1956-1982) for adjacent gages superimposed on subwatershed 63.004.

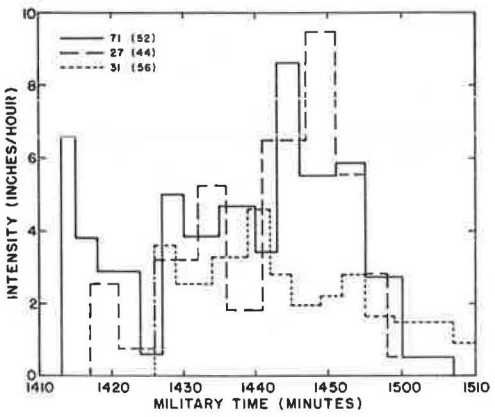


30- and 60-min events were similar in that peak discharges were greater when rainfall was centered on the subwatershed rather than centered either near the outlet or at the head of the subwatershed. All 30- and 60-min simulations in which maximum rainfall was concentrated late in the event produced greater peak discharges than those with rainfall concentrated early in the event (Figure 7), primarily because the maximum intensities were recorded on a saturated subwatershed.

Runoff volumes were significantly higher for those events centered on the subwatershed, whereas runoff volume from the late events was only slightly greater than that from the early events (Figures 8 and 9).

The maximum recorded peak discharge from the subwatershed has been 1,250 $ft^3/sec$. Although there were insufficient data from the subwatershed to plot a peak-discharge frequency curve, the estimated $Q_{100}$ based on the 25-yr record at other Walnut Gulch stations would be 1,660 $ft^3/sec$ (11). The simulated 60-min, 100-yr event with maximum rainfall centered on the subwatershed, and occurring late in the event, produced a peak discharge of 1,900 $ft^3/sec$--400 $ft^3/sec$ higher than a similar simulated event with maximum rainfall concentrated early in the event (Figure 5 and Table 3). Interestingly, the record Walnut Gulch storm when superimposed in time near the outlet, in the center, and at the head of the subwatershed, was so oriented in time and space that it produced peak discharges varying from only 1,814 to 1,871 $ft^3/sec$ (Figure 10). Peak

**Table 2. Maximum-rainfall event superimposed on subwatershed 63.004 with maximum point rainfall centered at rain gages 27, 71, and 31.**

| Military Time | Rainfall (in.) by Rain Gage (RG) | | | | | | | | |
|---|---|---|---|---|---|---|---|---|---|
| | Centered at RG 27 | | | Centered at RG 71 | | | Centered at RG 31[a] | | |
| | 27 | 71 | 31 | 27 | 71 | 31 | 27 | 71 | 31 |
| 1413 | 0 | 0 | 0 | 0 | 0 | 0 | 0 | 0 | 0 |
| 1415 | 0.22 | 0 | 0 | 0 | 0.22 | 0 | 0 | 0 | 0.22 |
| 1416 | – | 0 | 0 | 0 | – | 0 | 0 | 0 | – |
| 1417 | – | 0 | – | 0 | – | 0 | – | 0 | – |
| 1418 | 0.41 | – | 0.08 | – | 0.41 | 0 | 0.08 | – | 0.41 |
| 1421 | – | 0.17 | – | 0.17 | – | 0 | – | 0.17 | – |
| 1423 | – | – | 0.15 | – | – | 0 | 0.15 | – | – |
| 1424 | 0.70 | – | – | – | 0.70 | 0 | – | – | 0.70 |
| 1426 | – | 0.23 | 0.19 | 0.23 | – | 0 | 0.19 | 0.23 | – |
| 1427 | 0.73 | – | – | – | 0.73 | – | – | – | 0.73 |
| 1429 | – | – | – | – | – | 0.18 | – | – | – |
| 1430 | 0.98 | – | – | – | 0.98 | – | – | – | 0.98 |
| 1431 | – | – | 0.23 | – | – | – | 0.23 | – | – |
| 1432 | – | 0.55 | – | 0.55 | – | – | – | 0.55 | – |
| 1434 | – | – | – | – | – | 0.39 | – | – | – |
| 1435 | 1.30 | – | 0.25 | – | 1.30 | – | 0.25 | – | 1.30 |
| 1436 | – | 0.90 | – | 0.90 | – | – | – | 0.90 | – |
| 1439 | – | – | – | – | – | 0.66 | – | – | – |
| 1440 | 1.69 | – | 0.58 | – | 1.69 | – | 0.58 | – | 1.69 |
| 1441 | – | 1.05 | – | 1.05 | – | – | – | 1.05 | – |
| 1442 | – | – | – | – | – | 0.89 | – | – | – |
| 1443 | 1.86 | – | – | – | 1.86 | – | – | – | 1.86 |
| 1445 | – | – | 1.01 | – | – | 1.03 | 1.01 | – | – |
| 1446 | 2.29 | – | – | – | 2.29 | – | – | – | 2.29 |
| 1447 | – | 1.70 | – | 1.70 | – | – | – | 1.70 | – |
| 1449 | – | – | – | – | – | 1.16 | – | – | – |
| 1450 | – | – | 1.29 | – | – | – | 1.29 | – | – |
| 1451 | 2.73 | 2.33 | – | 2.33 | 2.73 | – | – | 2.33 | 2.73 |
| 1452 | – | – | – | – | – | 1.27 | – | – | – |
| 1455 | 3.12 | 2.70 | 1.47 | 2.70 | 3.12 | 1.41 | 1.47 | 2.70 | 3.12 |
| 1458 | – | 2.84 | 1.51 | 2.84 | – | – | 1.51 | 2.84 | – |
| 1459 | – | – | – | – | – | 1.52 | – | – | – |
| 1500 | 3.35 | – | – | – | 3.35 | – | – | – | 3.35 |
| 1501 | – | – | 1.54 | – | – | – | 1.54 | – | – |
| 1504 | – | 2.89 | 1.57 | 2.89 | – | – | 1.57 | 2.89 | – |
| 1507 | 3.41 | | – | | 3.41 | 1.72 | – | | 3.41 |
| 1511 | | | – | | | 1.78 | – | | |
| 1512 | | | 1.60 | | | – | 1.60 | | |
| 1515 | | | | | | 1.86 | | | |

[a]The same as storm centered on RG 27, but amounts at RG 27 and RG 31 are reversed.

**Table 3. Peak discharge from simulated rainfall on subwatershed 63.004, Walnut Gulch.**

| Type of Storm | Location of Event on Subwatershed | Peak Discharge ($ft^3$/sec) by Frequency (yr) | | | |
|---|---|---|---|---|---|
| | | 2 | 5 | 10 | 100 |
| 30-min | | | | | |
| Early | Outlet | 2 | 125 | 201 | 692 |
| | Middle | 1 | 147 | 261 | 1,021 |
| | Head | 0 | 90 | 169 | 743 |
| Late | Outlet | 16 | 159 | 243 | 858 |
| | Middle | 16 | 174 | 304 | 1,185 |
| | Head | 3 | 114 | 207 | 883 |
| 60-min | | | | | |
| Early | Outlet | 70 | 237 | 361 | 1,188 |
| | Middle | 78 | 304 | 499 | 1,492 |
| | Head | 37 | 207 | 355 | 1,248 |
| Late | Outlet | 137 | 339 | 544 | 1,536 |
| | Middle | 154 | 445 | 703 | 1,896 |
| | Head | 92 | 315 | 526 | 1,591 |

**Table 4. Runoff volume from simulated rainfall on subwatershed 63.004, Walnut Gulch.**

| Type of Storm | Location of Event on Subwatershed | Runoff Volume (in.) by Frequency (yr) | | | |
|---|---|---|---|---|---|
| | | 2 | 5 | 10 | 100 |
| 30-min | | | | | |
| Early | Outlet | <0.01 | 0.08 | 0.15 | 0.57 |
| | Middle | <0.01 | 0.13 | 0.22 | 0.79 |
| | Head | 0.00 | 0.07 | 0.14 | 0.54 |
| Late | Outlet | 0.02 | 0.10 | 0.16 | 0.60 |
| | Middle | 0.01 | 0.14 | 0.24 | 0.79 |
| | Head | <0.01 | 0.09 | 0.15 | 0.57 |
| 60-min | | | | | |
| Early | Outlet | 0.04 | 0.18 | 0.30 | 0.99 |
| | Middle | 0.07 | 0.25 | 0.40 | 1.19 |
| | Head | 0.03 | 0.17 | 0.28 | 0.97 |
| Late | Outlet | 0.08 | 0.25 | 0.39 | 1.06 |
| | Middle | 0.13 | 0.33 | 0.50 | 1.26 |
| | Head | 0.07 | 0.24 | 0.38 | 1.04 |

discharges of 1,800 to 1,900 $ft^3$/sec from centered 60-min, 100-yr late-occurring simulated rainfall and from the maximum observed Walnut Gulch rainfall seemed reasonable.

To investigate the effect of spatial variability of rainfall on runoff, average rainfall depths were assumed over the subwatershed for each storm duration and frequency; temporal variability was retained. Hydrographs were generated from the full range of 30- and 60-min simulated rainfall amounts and compared with similar peaks based on spatially and temporally varied rainfall (Tables 3 and 5). The differences were meaningful for the 10-yr events but relatively small for the 100-yr events (generally about 10 percent smaller). Runoff volumes were also less for the spatially uniform rainfall (Tables 4 and 6).

To determine the influence of a constant rainfall rate versus a variable one, hydrographs were generated from simulated spatially varied, constantrate, 30- and 60-min events (Tables 7 and 8). When peak discharges for the 30-min events were compared,

Figure 5. Hydrographs from simulated 60-min, 10- and 100-yr storms centered at three locations with rainfall intensities occurring early and late in the event.

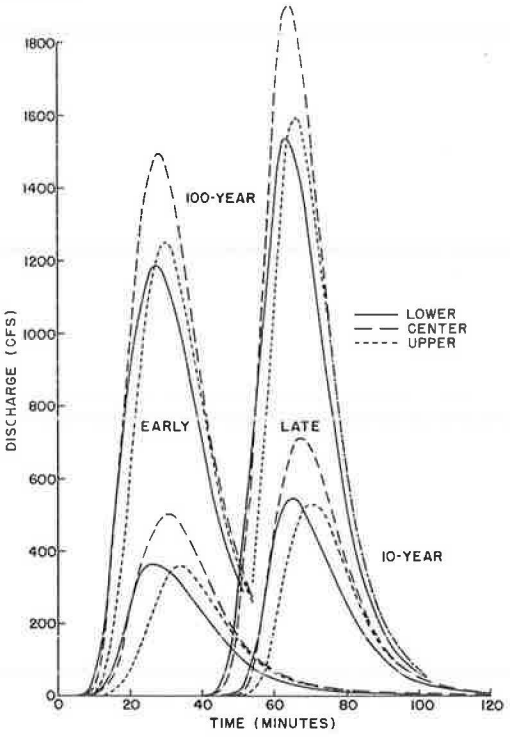


Figure 6. Peak discharge from simulated storms that were centered versus those that were not centered on the subwatershed.

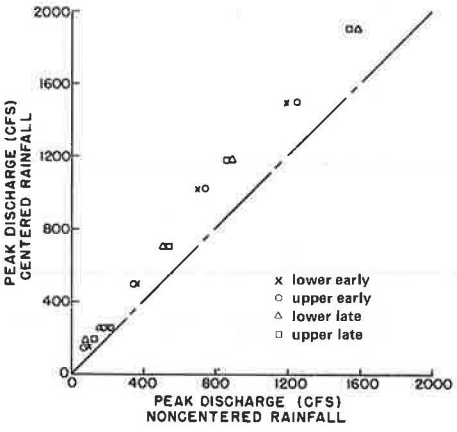


those generated from constant inputs were considerably lower than those generated from time-variable inputs (Tables 5 and 7). When rainfall was spread uniformly over a 60-min period, the differences between constant and varied time inputs were much more striking (Tables 5 and 7). Simulated peaks were reduced by more than 50 percent for events of all frequencies with 60-min constant rainfall rates.

## EVALUATION

Quantitative differences in hydrograph peaks and volumes generated from spatially and temporally varied rainfall patterns were apparent when runoff peaks and volumes were compared. There was a strong linear relationship between storms centered on the

Figure 7. Peak discharge from simulated storms with maximum intensities concentrated early and late in the event.

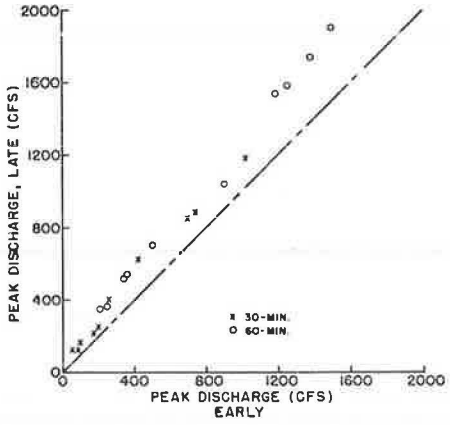


Figure 8. Runoff volume from simulated storms that were centered versus those that were not centered on the subwatershed.

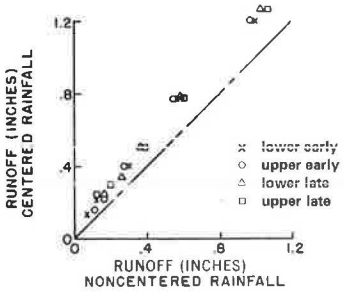


Figure 9. Runoff volume from simulated storms with intensities concentrated early and late in the event.

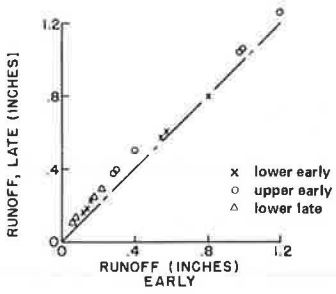


subwatershed and those centered near the outlet or at the head of the subwatershed for peak discharges up to 800 $ft^3$/sec and runoff volumes up to 0.6 in. (Figures 6 and 8). Peak discharges and volumes were 35 to 40 percent higher for events centered on the subwatershed. Rainfall volumes were 10 to 15 percent greater for the events centered on the subwatershed, so higher peaks and volumes were not due entirely to more rainfall. Above 800 $ft^3$/sec and 0.6 in., events centered on the subwatershed produced constant increases in peak discharge of 300 $ft^3$/sec and runoff volume of 0.22 in. The relationships were as follows:

$$Q_{Pc} = 1.375Q_{Pnc} \quad (0 < Q_{Pnc} < 800) \tag{1}$$

$$Q_{Pc} = Q_{Pnc} + 300 \quad (Q_{Pnc} > 800) \tag{2}$$

$$Q_c = 1.375Q_{nc} \quad (0 < Q_{nc} < 0.6) \tag{3}$$

$$Q_c = Q_{nc} + 0.22 \quad (Q_c > 0.6) \tag{4}$$

where

$Q_{Pc}$ = peak discharge from simulated rainfall centered on subwatershed,
$Q_{Pnc}$ = peak discharge from simulated rainfall not centered on subwatershed,
$Q_c$ = runoff volume from simulated rainfall centered on subwatershed, and
$Q_{nc}$ = runoff volume from simulated rainfall not centered on subwatershed.

Figure 10. Hydrographs from the maximum observed Walnut Gulch storm superimposed at three locations on subwatershed 63.004.

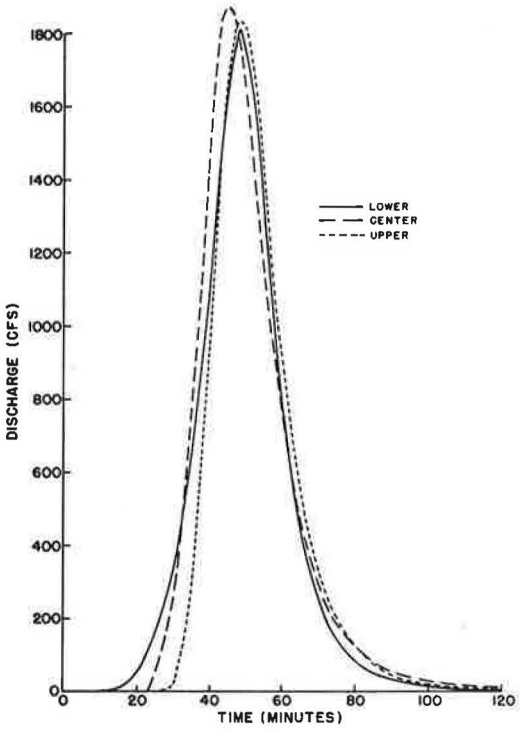


Table 5. Peak discharge for selected frequencies and durations of spatially uniform rainfall on subwatershed 63.004, Walnut Gulch.

| Type of Storm | Peak Discharge ($ft^3$/sec) by Frequency (yr) | | | |
|---|---|---|---|---|
| | 2 | 5 | 10 | 100 |
| 30-min | | | | |
| Early | 0 | 119 | 195 | 908 |
| Late | 2 | 146 | 293 | 1,040 |
| 60-min | | | | |
| Early | 24 | 257 | 422 | 1,380 |
| Late | 78 | 363 | 626 | 1,745 |

Table 6. Runoff volume for selected frequencies and durations of spatially uniform rainfall on subwatershed 63.004, Walnut Gulch.

| Type of Storm | Runoff Volume (in.) by Frequency (yr) | | | |
|---|---|---|---|---|
| | 2 | 5 | 10 | 100 |
| 30-min | | | | |
| Early | 0 | 0.11 | 0.16 | 0.71 |
| Late | <0.01 | 0.13 | 0.21 | 0.72 |
| 60-min | | | | |
| Early | 0.02 | 0.22 | 0.35 | 1.12 |
| Late | 0.07 | 0.29 | 0.46 | 1.19 |

There were also good linear correlations for both peak discharge and runoff volume for the full range of values given by

$$Q_{Pc} = 1.25Q_{Pnc} \quad (5)$$

$$Q_c = 1.25\ Q_{nc} \quad (6)$$

Either Equations 1 and 2 together or Equation 5 alone would give an acceptable estimate of peak discharge for this small watershed, but the suggestion of a limit to the linear relationship could become important with increasing watershed size. Extrapolation of Equation 5 could possibly lead to costly overestimates for peak discharges from larger watersheds.

There was also a strong linear relationship between peak discharges when maximum rainfall intensities occurred early or late in the event (Figure 8). The relationship was as follows:

$$Q_{Pl} = 1.25Q_{Pe} \quad (7)$$

where $Q_{Pl}$ is the peak discharge from maximum intensities occurring late in the event, and $Q_{Pe}$ is the peak discharge from maximum intensities occurring early in the event. Again, however, there was a suggestion that there may be a limit on the linear relationship, which could lead to overestimates for larger watersheds. Because rainfall amounts were the same for each selected storm event, runoff volumes were only slightly greater for the late-occurring events (Figure 9).

The influences of temporal and spatial rainfall variability on peak discharge tended to be additive. The 60-min, 100-yr, late-occurring, centered peak discharge was 60 percent higher than the 60-min, 100-yr, early-occurring, noncentered peak discharge. The maximum peak discharges for the lower-frequency events were up to 100 percent higher than the minimums for storm units of the same frequency. Obviously, both storm location and temporal variability of rainfall can significantly affect peak discharge.

Assuming spatially uniform rainfall on the 560-

Table 7. Peak discharge for selected frequencies and durations of constant rainfall rates on subwatershed 63.004, Walnut Gulch.

| Type of Storm | Location of Event on Subwatershed | Peak Discharge ($ft^3$/sec) by Frequency (yr) | | | |
|---|---|---|---|---|---|
| | | 2 | 5 | 10 | 100 |
| 30-min | Outlet | 0 | 20 | 153 | 677 |
| | Middle | 0 | 20 | 200 | 980 |
| | Head | 0 | 3 | 123 | 714 |
| 60-min | Outlet | 0 | 3 | 108 | 622 |
| | Middle | 0 | 0 | 163 | 795 |
| | Head | 0 | 0 | 90 | 640 |

Table 8. Runoff volume for selected frequencies and durations of constant rainfall rates on subwatershed 63.004, Walnut Gulch.

| Type of Storm | Location of Event on Subwatershed | Runoff Volume (in.) by Frequency (yr) | | | |
|---|---|---|---|---|---|
| | | 2 | 5 | 10 | 100 |
| 30-min | Outlet | 0 | 0.01 | 0.10 | 0.52 |
| | Middle | 0 | 0.02 | 0.16 | 0.72 |
| | Head | 0 | <0.01 | 0.09 | 0.50 |
| 60-min | Outlet | 0 | <0.01 | 0.08 | 0.66 |
| | Middle | 0 | 0 | 0.14 | 0.86 |
| | Head | 0 | 0 | 0.07 | 0.63 |

acre subwatershed reduces peak discharges by only about 10 percent. For larger watersheds and therefore decreasing rainfall averages, however, assuming spatially uniform rainfall could lead to significant underestimates of peak discharge, especially when runoff-producing rainfall does not cover the entire watershed.

As long as assumed rainfall durations are kept relatively short, assuming a constant rainfall rate does not greatly decrease generated peak discharges. However, for durations longer than about 30 min, assuming a constant rainfall rate can lead to greatly underestimating peak discharge. For example, for a duration of 60 min, assuming a constant rainfall rate would reduce the simulated peak discharge by more than 50 percent.

Rainfall versus runoff relationships for simulated storms that were centered and not centered and maximum intensities concentrated early and late in the event are shown in Tables 9-11. Both linear regression and exponential curves were fitted for the four sets of events (Figures 11-14). The exponential curves were only a slight improvement over linear regression. Nevertheless, the differences could be significant at runoff thresholds or for large events. The expressions for combined data were as follows:

$$Q = -0.622 + 0.654P \quad (SEE = 0.070) \tag{8}$$

$$Q = 0.236P^{1.82} - 0.180 \quad (SEE = 0.047) \tag{9}$$

where Q is the storm runoff in inches and P is the storm rainfall in inches. There was slightly more runoff from equal amounts of rainfall for centered events as opposed to those that were not centered. The differences were not significant. There was an average increase of 0.07 in. in runoff volumes from equal amounts of late-occurring, maximum-rainfall intensities as opposed to early concentrations of rainfall. In many situations, the increase would be important.

Relationships between frequency and peak discharge for each classification tend to plot as straight lines on log-normal paper for 5- to 100-yr expected rainfall amounts (Figures 15 and 16). Because the 5-, 10-, and 100-yr events plotted as straight lines, it was assumed that storms for any frequency greater than 5 yr would plot on the same lines. The influence of within-storm variations is clearly evident and well defined for 5- to 100-yr

**Table 9. Rainfall and runoff for simulated early and late 2-, 5-, 10-, and 100-yr storms by location on subwatershed 63.004, Walnut Gulch.**

| Frequency and Type of Storm | Location of Event on Subwatershed | Duration of Storm: 30 min P (in.) | 30 min Q (in.) | 60 min P (in.) | 60 min Q (in.) |
|---|---|---|---|---|---|
| 2 yr, early | Outlet | 0.77 | <0.01 | 1.10 | 0.04 |
| | Middle | 0.84 | <0.01 | 1.19 | 0.07 |
| | Head | 0.77 | 0 | 1.09 | 0.03 |
| 2 yr, late | Outlet | 0.77 | 0.02 | 1.10 | 0.08 |
| | Middle | 0.84 | 0.01 | 1.19 | 0.13 |
| | Head | 0.77 | <0.01 | 1.09 | 0.07 |
| 5 yr, early | Outlet | 1.03 | 0.08 | 1.36 | 0.18 |
| | Middle | 1.12 | 0.13 | 1.49 | 0.25 |
| | Head | 1.02 | 0.07 | 1.35 | 0.17 |
| 5 yr, late | Outlet | 1.03 | 0.10 | 1.36 | 0.25 |
| | Middle | 1.12 | 0.14 | 1.49 | 0.33 |
| | Head | 1.02 | 0.09 | 1.35 | 0.24 |
| 10 yr, early | Outlet | 1.25 | 0.15 | 1.60 | 0.30 |
| | Middle | 1.36 | 0.22 | 1.75 | 0.40 |
| | Head | 1.24 | 0.14 | 1.59 | 0.28 |
| 10 yr, late | Outlet | 1.25 | 0.16 | 1.60 | 0.39 |
| | Middle | 1.36 | 0.24 | 1.75 | 0.50 |
| | Head | 1.24 | 0.16 | 1.59 | 0.38 |
| 100 yr, early | Outlet | 1.80 | 0.57 | 2.46 | 0.97 |
| | Middle | 2.05 | 0.78 | 2.69 | 1.19 |
| | Head | 1.79 | 0.54 | 2.43 | 0.97 |
| 100 yr, late | Outlet | 1.80 | 0.60 | 2.46 | 1.06 |
| | Middle | 2.05 | 0.79 | 2.69 | 1.26 |
| | Head | 1.78 | 0.57 | 2.43 | 1.04 |

Note: P = storm rainfall; Q = storm runoff.

**Table 10. Rainfall and runoff for simulated early and late 2-, 5-, 10-, and 100-yr storms with spatially uniform rainfall.**

| Frequency and Type of Storm | 30-min Storm P (in.) | 30-min Storm Q (in.) | 60-min Storm P (in.) | 60-min Storm Q (in.) |
|---|---|---|---|---|
| 2 yr | | | | |
| Early | 0.78 | 0 | 1.09 | 0.02 |
| Late | 0.78 | <0.01 | 1.09 | 0.07 |
| 5 yr | | | | |
| Early | 1.09 | 0.11 | 1.42 | 0.22 |
| Late | 1.09 | 0.13 | 1.42 | 0.29 |
| 10 yr | | | | |
| Early | 1.28 | 0.16 | 1.70 | 0.35 |
| Late | 1.28 | 0.21 | 1.70 | 0.46 |
| 100 yr | | | | |
| Early | 1.95 | 0.71 | 2.62 | 1.12 |
| Late | 1.95 | 0.72 | 2.59 | 1.19 |

Note: P = storm rainfall; Q = storm runoff.

**Table 11. Rainfall and runoff for simulated early and late 2-, 5-, 10-, and 100-yr storms with constant rainfall.**

| Frequency of Storm | Location of Event on Subwatershed | 30-min Storm P (in.) | 30-min Storm Q (in.) | 60-min Storm P (in.) | 60-min Storm Q (in.) |
|---|---|---|---|---|---|
| 2 yr | Outlet | 0.70 | 0 | 1.00 | 0 |
| | Middle | 0.80 | 0 | 1.10 | 0 |
| | Head | 0.70 | 0 | 1.00 | 0 |
| 5 yr | Outlet | 1.00 | 0.01 | 1.23 | <0.01 |
| | Middle | 1.10 | 0.02 | 1.35 | 0 |
| | Head | 1.00 | <0.01 | 1.22 | 0 |
| 10 yr | Outlet | 1.26 | 0.10 | 1.61 | 0.08 |
| | Middle | 1.37 | 0.16 | 1.75 | 0.14 |
| | Head | 1.24 | 0.09 | 1.59 | 0.07 |
| 100 yr | Outlet | 1.81 | 0.52 | 2.41 | 0.66 |
| | Middle | 2.05 | 0.72 | 2.64 | 0.86 |
| | Head | 1.79 | 0.50 | 2.38 | 0.63 |

Note: P = storm rainfall; Q = storm runoff.

**Figure 11. Rainfall versus runoff for simulated centered 2-, 5-, 10-, and 100-yr storms.**

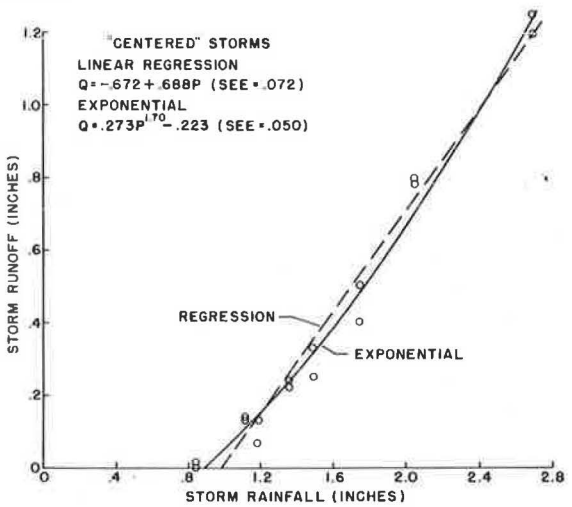

Figure 12. Rainfall versus runoff for simulated 2-, 5-, 10-, and 100-yr storms that were not centered.

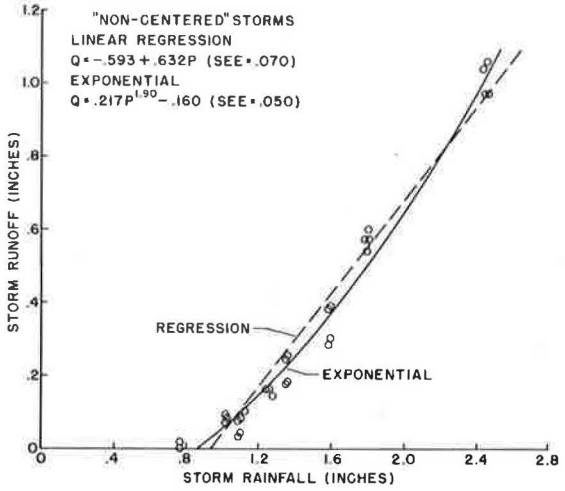


Figure 13. Rainfall versus runoff for simulated early 2-, 5-, 10-, and 100-yr storms.

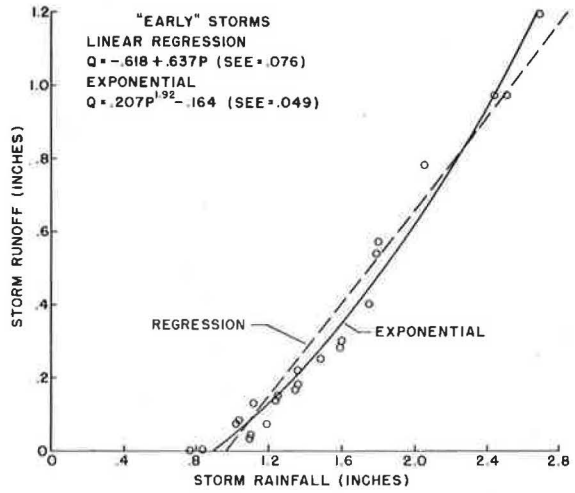


Figure 14. Rainfall versus runoff for simulated late 2-, 5-, 10-, and 100-yr storms.

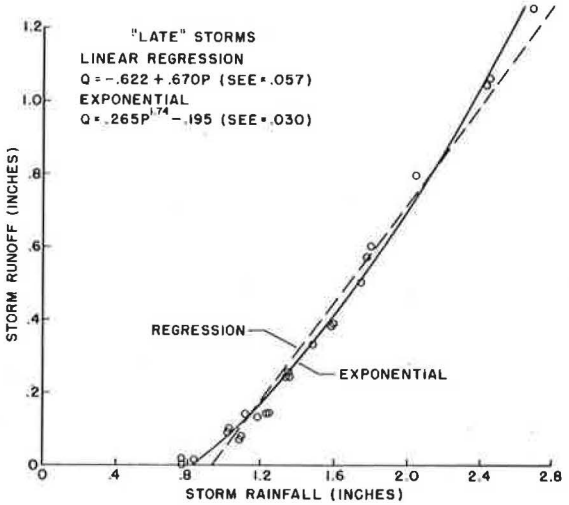


Figure 15. Peak discharge for rainfall frequencies of 2, 5, 10, and 100 yr for selected durations and storm patterns.

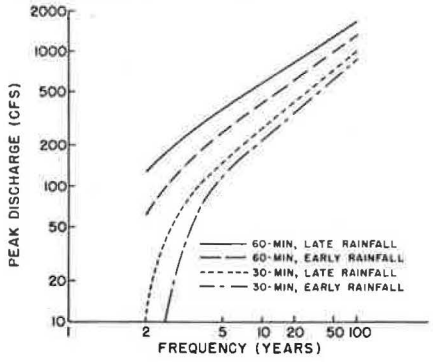


Figure 16. Peak discharge for rainfall frequencies of 2, 5, 10, and 100 yr for selected durations and constraints.

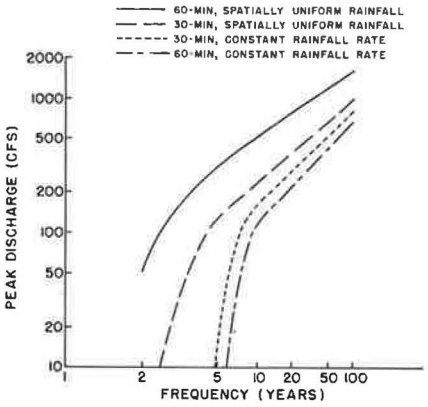


storms. Even for spatially uniform rainfall, the relationships are clearly defined. For more frequent events, however, peak discharges fall off rapidly. For constant rainfall rates, there was no runoff for 5-yr events with 60-min duration and no runoff for 2-yr events with 30-min duration. The curve for peak discharge versus frequency for a 560-acre subwatershed, based on Walnut Gulch data, would plot near the upper curve in Figure 13.

## RECOMMENDATIONS

The results of this study indicated that for a small semiarid rangeland watershed (560 acres), the spatial and temporal distributions of thunderstorm rainfall exert an approximately equal influence on peak discharge from the watershed and that the influences tend to be additive. There are, however, two areas where further research is needed.

First, storm-runoff frequencies as opposed to rainfall frequencies need to be established. In this study, the 30- and 60-min, 2-, 5-, 10-, and 100-yr point rainfall amounts were used to generate peak discharge (Figures 13 and 14). However, these expected rainfall amounts were determined independently from the thunderstorm-cell properties, and a wide range of peak discharges was generated from only eight point-rainfall depths. Furthermore, the relationships between peak discharge and spatial and temporal variability may not be linear.

Second, and equally as important, the relative importance of storm-cell properties with increasing watershed size must be established. The runoff-producing areal extent of thunderstorm cells is

limited, and runoff-producing rainfall will cover a smaller fraction of the watershed as the size of the watershed increases. Therefore, where the storm is centered should become increasingly important with increasing watershed size.

On the other hand, the influence of varying the occurrence of maximum intensity within the storm duration is more or less a function of watershed size and becomes relatively less important with increasing watershed size.

Quantitative analysis of the relationships between thunderstorm rainfall and runoff illustrated here is extremely difficult for several reasons. One reason is that rainfall is not uniform in time or space, and rainfall input can only be estimated from rainfall measurements within certain limits of accuracy and precision. Also, channel abstractions may account for much, or all, of on-site runoff. For example, annual runoff from the 58-mile$^2$ Walnut Gulch watershed is only about 5 percent of summer rainfall (2).

The next step, therefore, would be to model a larger watershed (several square miles) by using KINEROS and simulated rainfall input. In a step-by-step process, by increasing watershed size and complexity, it should be possible to define the interrelationships between storm-cell properties and watershed characteristics. The test of these interrelationships, in each case, would be the comparison of simulated peak discharges and runoff volumes.

REFERENCES

1. H.B. Osborn and L.J. Lane. Point-Area-Frequency Conversion for Summer Rainfall in Southeastern Arizona. In Hydrology and Water Resources of Arizona and the Southwest, Volume 11, Univ. of Arizona, Tucson, 1981.
2. H.B. Osborn and E.M. Laursen. Thunderstorm Runoff in Southeastern Arizona. Journal of Hydraulics Division of ASCE, Vol. 99, 1973, pp. 1129-1145.
3. V.T. Chow. Hydrologic Determination of Waterway Areas for Design of Drainage Structures in Small Basins. Univ. of Illinois, Urbana, Engineering Experiment Station Bull. 462, 1962.
4. C.T. Haan and H.P. Johnson. Hydrologic Modeling of Small Watersheds. American Society of Agricultural Engineers, St. Joseph, Mich., ASAE Monograph, 1982.
5. D.F. Kibler and D.A. Woolhiser. The Kinematic Cascade as a Hydrologic Model. Colorado State Univ., Fort Collins, Hydrology Paper 39, 1970.
6. E.W. Rovey, D.A. Woolhiser, and R.E. Smith. A Distributed Kinematic Model of Upland Watersheds. Colorado State Univ., Fort Collins, Hydrology Paper 93, 1977.
7. L.J. Lane and D.A. Woolhiser. Simplifications of Watershed Geometry Affecting Simulation of Surface Runoff. Journal of Hydrology, Vol. 35, 1977, pp. 173-190.
8. R.E. Smith. A Kinematic Model for Surface Mine Sediment Yield. Trans., ASAE, Vol. 24, No. 6, 1981, pp. 1508-1519.
9. B.M. Reich and L.A.V. Hiemstra. Tacitly Maximized Small Watershed Flood Estimates. Journal of Hydraulics Division of ASCE, Vol. 91, 1965, pp. 217-245.
10. H.B. Osborn, L.J. Lane, and V.A. Myers. Two Useful Rainfall/Watershed Relationships for Southwestern Thunderstorms. Trans., ASAE, Vol. 23, No. 1, 1980, pp. 82-87.
11. B.M. Reich, H.B. Osborn, and M.C. Baker. Tests on Arizona's New Flood Estimates. In Hydrology and Water Resources of Arizona and the Southwest, Vol. 9, Univ. of Arizona, Tucson, 1979.

# Conceptual and Empirical Comparison of Methods for Predicting Peak-Runoff Rates

RICHARD H. McCUEN

A wide variety of hydrologic methods have been proposed by hydrologic design. Because peak-discharge methods are the most widely used, it is instructive to compare the methods that are used most frequently. The methods compared include the rational formula, the U.S. Geological Survey urban peak-discharge equations, and the Soil Conservation Service peak-discharge methods. In addition to a comparison of the methods by using data from 40 small urban watersheds, the methods are compared on the basis of their input requirements and the means by which channel systems are accounted for. These latter two comparison criteria appear to be more important in selecting a method than accuracy.

The adverse hydrologic effects of land-cover changes and the different design solutions that have been proposed to overcome these effects have led to a diverse array of hydrologic methods. Many state and local policies on floodplain management, erosion control, watershed planning, and storm-water management (SWM) require a specific hydrologic method for design. Such policies usually generate considerable controversy among hydrologists and design engineers because each hydrologic method has one or more disadvantages. More important, the different methods lead to different designs at the same location. The failure to specify a specific design method in the design component of a drainage or SWM policy often leads to significant difficulties in the review and approval process.

A number of studies have been undertaken to identify the best method (1,2). Most of the comparisons were limited in some respect. For example, some publications involved data obtained for a limited region, whereas others were based on a limited sample size. In some cases, the criteria for comparison were limited. In all cases, the comparisons were limited to empirical analyses. McCuen and others (3) concluded that (a) there is a noticeable lack of consistency in the structure and presentation of results of comparisons of hydrologic methods, (b) the literature does not accurately reflect the methods that are most frequently used in hydrologic design, and (c) the literature is often defi-

cient in the description of the procedure and its accuracy, reproducibility, and the effort that is required to apply the method.

The most comprehensive comparison of hydrologic methods for predicting peak-flow frequencies was undertaken by the Hydrology Committee of the U.S. Water Resources Council (1); the study was undertaken as a pilot test, however, which was designed and conducted to aid in the design of and provide guidance for performing a conclusive nationwide test. The report concluded that a study involving considerably more data would be necessary to make conclusive statements about the accuracy of the methods. The sample size was much larger than the data base for any previous study involving a comparison of procedures. This suggests that until the funds are available to conduct a nationwide test, results based entirely on empirical analyses cannot be considered conclusive.

The objective of this paper is to compare hydrologic methods that are used for predicting peak-flow rates on the basis of structure, input, and calibration requirements as well as on the basis of the accuracy measured by fitting with data. A comparison of methods based on criteria such as structure and input requirements may be as valuable as a comparison based on measured data. After all, the studies involving a comparison of hydrologic methods based on a comparison of computed peak discharges with estimates obtained from flood-frequency analyses have not been conclusive.

## CLASSIFICATION OF HYDROLOGIC MODELS

In order to select procedures from among the many that are currently in use, it is useful to first establish a classification scheme for categorizing procedures that have common distinguishing characteristics. By grouping similar procedures, one or more procedures can be selected to represent each category and then the procedures can be tested and compared. If the procedures selected are representative of those in the category, the results may be used to make generalized inferences about the procedures in that category. The categories in the classification scheme should be different by at least one significant element. It is hoped that procedures assigned to a category would be similar in important characteristics, and differences in these characteristics should be apparent when procedures assigned to different categories are compared.

A number of schemes for classifying hydrologic methods have been developed. Classification schemes based on systems analysis concentrate on the three elements of the system black box: the input, transfer, and output functions. Systems are often characterized by the nature of the transfer function (i.e., model), which in systems theory is the function that transforms the input function into the output function. Systems are often categorized with the following sets of dichotomous terms: (a) deterministic versus stochastic, (b) static versus dynamic, (c) linear versus nonlinear, (d) lumped versus distributed, (e) time invariant versus time variant, and (f) conceptual versus empirical. Although these represent mutually exclusive categories, they are of limited value in classifying hydrologic models. They represent a limited scheme because there is wide variation in important characteristics of procedures that would fall within the same category. Thus, a classification scheme was developed that concentrated on the output function.

It is easiest to develop a classification scheme that concentrates on the hydrologic output. The classification system that is given in Table 1 identifies three forms of primary output: a peak discharge, a flood hydrograph, and a frequency curve; these outputs correspond to the three level-1 classes. After the primary output has been generated, a secondary output can be obtained. For example, when a peak-discharge formula is used, the frequency curve can be obtained by using the formula to compute an array of peak discharges for selected return periods. Similarly, a peak discharge for a selected return period can be obtained from a frequency curve obtained from multiple-event hydrograph analysis.

In addition to level 1, it is useful to define a second level. In level 2, the methods are separated on the basis of other factors, such as whether the method is based on calibration to measured data and the structure of the method. A third level of the classification scheme would consist of specific methods. For example, the Stanford watershed model is a continuous-record method, whereas the rational formula is an uncalibrated peak-discharge equation.

### Peak-Discharge Methods

For many hydrologic designs the only output required is a peak discharge for a selected return period. Thus, one category of the classification scheme is labeled peak-discharge methods. Many methods have been proposed for such design problems. The required peak discharge can be evaluated directly or by constructing the frequency curve and taking the value from the curve. Peak-discharge methods can be classified as belonging to one of four subgroups: single return period, index flood, moment estimation, and uncalibrated. Except for the uncalibrated equations, the other three level-2 methods in this class require fitting of empirical coefficients; the coefficients are most often obtained by regression.

#### Single-Return-Period Method

Single-return-period methods use watershed and precipitation characteristics to predict the peak discharge for a specific return period; a separate equation is usually calibrated for each return period. Most often, the single-return-period methods have the following form:

$$Q_p = b_0 X_1^{b_1} X_2^{b_2} \ldots X_p^{b_p} \quad (1)$$

Table 1. System for classifying hydrologic models.

| Primary Output | Secondary Output | Classification Level 1 | Classification Level 2 |
|---|---|---|---|
| Peak discharge | Frequency curve | Peak discharge | Single-return-period equations<br>Index-flood method<br>Moment estimation<br>Uncalibrated equations |
| Flood hydrograph | Peak discharge and frequency curve | Single-event hydrograph | Calibrated unit graph<br>Uncalibrated unit graph |
| Frequency curve | Peak discharge | Multiple-event hydrograph | Multiple event<br>Continuous record |

in which $X_i$ ($i = 1,2,\ldots,p$) are the watershed and precipitation characteristics, $b_j$ ($j = 0,1,2,\ldots,p$) are the coefficients, and p is the number of predictor variables used. A frequency curve can be derived by estimating the peak discharge with the equation for each of the necessary return periods. The U.S. Geological Service (USGS) state equations are examples of the single-return-period category.

### Index-Flood Method

The index-flood method is based on a single prediction equation and a series of index ratios. The prediction equation, which is usually calibrated by using regression, relates the peak discharge for a selected, or index, return period to both watershed and precipitation characteristics. The form of the index-flood equation is usually the same as that for the single-return-period method. Although the index-flood equation is usually calibrated for a 2-yr return period, the 10-yr event is sometimes used. Peak-discharge estimates for other return periods are obtained by multiplying the estimated peak discharge of the index-return period by a constant, which depends on the specific return period. The index ratios are often obtained by regression; therefore, the expected peak discharges computed by the index-flood method are unbiased.

### Moment-Estimation Methods

Moment-estimation methods usually relate the first three statistical moments, i.e., mean ($\bar{X}$), standard deviation (S), and skew (g), to watershed and precipitation characteristics; a separate prediction equation is used for each of the three moments. The peak discharge for a return period (p) is thus obtained by using the following relationship:

$$Q_p = \bar{X} + KS \quad (2)$$

where

$Q_p$ = peak discharge ($ft^3/sec$),
$\bar{X}$ = estimated mean value ($ft^3/sec$),
S = standard deviation ($ft^3/sec$), and
K = dimensionless value that is a function of both the skew and the return period.

In most cases, $\bar{X}$ and S are the mean and standard deviation of the logarithms of the annual maximum series; in such cases, it is necessary to use the antilogarithm of the $Q_p$ computed with Equation 2. The frequency curve can be evaluated by computing the value of $Q_p$ for selected return periods.

### Uncalibrated Equations

Although the single-return-period equation, index-flood method, and the moment-estimation method require fitting to measured hydrologic data, some peak-discharge methods are developed without fitting; these are called uncalibrated equations. The rational method and the TR-55 peak-discharge methods fall into this category. One would expect that the process of fitting would improve the accuracy of a method.

## Single-Event Hydrograph Methods

Although unit hydrograph models can be distinguished on the basis of more than one criterion, it is useful to limit the separation criterion to whether or not calibration was required. Calibrated unit hydrographs, such as the HEC-1 model, should provide more accurate estimates of runoff hydrographs than uncalibrated methods. Uncalibrated unit hydrograph models are desirable because they are designed to be used at ungaged locations; the Soil Conservation Service (SCS) TR-20 model is an example of this class. Although unit hydrograph methods provide a storm hydrograph as the primary output, they can also provide either a peak discharge or a frequency curve. Because urbanization causes significant changes in the volumes and timing of runoff, hydrograph models are becoming more widely used, especially where policies require storage of runoff to compensate for the effect of land use changes on the excess runoff volumes and rates.

## Multiple-Event Hydrograph Methods

Because the use of hydrograph methods has increased, there has been increased concern about some of the underlying assumptions. For example, the uncalibrated unit hydrograph models most often require acceptance of the assumption that the recurrence interval of the runoff equals that of the rainfall. Empirical evidence indicates that this is rarely the case. In addition, many argue that where data are available, the single-event hydrograph models make little use of the available data. Thus, multiple-event hydrograph models are sometimes recommended. Two subclasses of multiple-event models exist: multiple-event analysis and continuous-record analysis. A multiple-event analysis involves using the larger storm events of record as input to a conceptual hydrologic model. A frequency analysis is performed on the output to develop a frequency curve. A peak discharge can then be obtained from the frequency curve. This model type is based on at least two assumptions. First, it assumes that the largest rainfall event may not cause the greatest runoff; therefore, several storms for each year are used to ensure that the largest event for each year is included in the frequency analysis. Second, it assumes that the hydrometeorological data are sufficient input once the model has been fitted.

Continuous-record models are considered to be at least as accurate as the multiple-event models because they provide for continuous moisture accounting. On the other hand, they require considerably more technical expertise, time, and resources to calibrate and use. The continuous record of computed runoff is used to compute a frequency curve; because the peak-runoff rates are computed rather than measured, the frequency curve is often referred to as synthetic.

## CRITERIA FOR COMPARISON OF PROCEDURES

In making design estimates of flood peak discharges, accuracy is often considered the most important criterion. To characterize properly the accuracy of a hydrologic model, it is necessary to identify and to quantify factors that influence the accuracy of the model. That is, accuracy must be separated into its fundamental components. Definitions of precision and bias are needed to define accuracy. Precision is a measure of the random variation in a set of repeated estimates when the procedure is identically evaluated more than once. Bias is a measure of the systematic error in a set of estimates; it measures the deviation of the central tendency of these estimates from the true value. Given these definitions, accuracy can be defined as a measure of the closeness of the predicted values to the true value of the quantity being evaluated; it considers both precision and bias.

In statistical analyses, the mean square error (MSE) is used as the measure of accuracy. Accuracy

is a function of systematic and random error variation; accuracy can be separated into the precision and bias components as follows:

$$MSE = E(\hat{\theta} - \theta)^2 \quad (3a)$$

$$= E\left\{[\hat{\theta} - E(\hat{\theta})] + [E(\hat{\theta} - \theta)]\right\}^2 \quad (3b)$$

$$= E[\hat{\theta} - E(\hat{\theta})]^2 + E[E(\hat{\theta}) - \theta]^2 + 2E[\hat{\theta} - E(\hat{\theta})][E(\hat{\theta}) - \theta]^2 \quad (3c)$$

where $\theta$ is any parameter, $\hat{\theta}$ is an estimate of $\theta$, and E( ) denotes the expected value of the quantity enclosed in the parentheses or brackets. Given the above definitions for precision and bias and because $E[\hat{\theta} - E(\hat{\theta})] = 0$, MSE is the sum of the precision and the square of the bias:

$$MSE = E\left\{[\hat{\theta} - E(\hat{\theta})]^2\right\} + E[E(\hat{\theta}) - \theta]^2 \quad (4a)$$

$$= \text{precision} + \text{bias}^2 \quad (4b)$$

The variation of an estimated peak discharge from the true value can be represented by

$$(Y_{ijk} - Y_{0i}) = (Y_{ijk} - \overline{Y_{ik}}) + (\overline{Y_{ik}} - Y_{0i}) \quad (5)$$

where $Y_{0i}$ is the true estimate on watershed i, $Y_{ijk}$ is a value estimated by individual j on watershed i and by using procedure k, and $\overline{Y_{ik}}$ is the the mean of all estimates made on watershed i by using procedure k. The terms in the computational equation (Equation 5) correspond directly to the statistical definition of Equation 4.

To assess the precision of a hydrologic model, it would be necessary to make an estimate of the random error. In a strict sense, this requires repeated measurements. True repetition is not possible in hydrology, and thus a true measure of precision is not obtainable. A best estimate of precision can be obtained by using estimates of peak discharge made by different hydrologists. The variation of these estimates is a measure of the random variation. Because it is not a true estimate of precision, it is termed reproducibility. The term $(Y_{ijk} - \overline{Y_{ik}})$ represents the reproducibility of a procedure and is evaluated by repeated use of procedure k on the same watershed by different hydrologists; as such, it is as close as one can come to replication in hydrology. It is intended to provide an answer to the question, "How well can I expect to agree with other hydrologists?" Because replication is usually not available, only accuracy and bias are assessed.

By using the separation-of-variation concept of Equation 5, accuracy equals the variation of the predicted values from the true values. Because the true value differs for each watershed, it is necessary to standardize the differences when the accuracy of a method is evaluated. Thus, the accuracy is evaluated in the form of a standardized standard error:

$$A = \left\{[1/(n-1)] \sum_{i=1}^{n} [(Y_{ijk} - Y_{0i})/Y_{0i}]^2\right\}^{0.5} \quad (6)$$

The true peak discharge ($Y_{0i}$) is never known. For purposes of comparing hydrologic models where gaged data are available, the flood frequency analysis estimate of a particular exceedence probability can be used as the best estimate (1).

The term $(\overline{Y_{ik}} - Y_{0i})$ is the difference between the mean of all estimates on watershed i by using procedure k and the true value. It represents the systematic error variation of the procedure and identifies either overestimation or underestimation; a zero value indicates no systematic error. The bias of procedure k is estimated by

$$B_k = \left[\sum_{i=1}^{n} (Y_{ijk} * Y_{0i})^2 \Big/ \sum_{i=1}^{n} Y_{0i}^2\right] - 1.0 \quad (7)$$

## COMPARISON OF MODEL STRUCTURES AND INPUT REQUIREMENTS

The classification system of Table 1 is based on the primary output. This separation also represents different levels of design requirements. For example, it would not be practical to use a continuous-record model to design storm drain inlets. Similarly, it would not be rational to use an empirical peak-discharge equation to perform real-time flood forecasting. Because of the interest in comparing peak-discharge methods, the remainder of this study will focus on these methods; it is, however, important to recognize the classification system of Table 1 to maintain a proper perspective.

Most of the peak-discharge methods require quite similar input. The drainage area is a major input to most of the equations. An index of the rainfall depth is usually required; this is most often obtained from a curve of rainfall intensity, duration, and frequency for the site. When a rainfall depth or intensity is required, such as with the rational and SCS graphical methods, the product of the rainfall and drainage area reflects a supply of available water for runoff. The actual supply is a function of the return period, which is required by the peak-discharge methods. The reduction of rainfall supply to the volume of direct runoff is usually controlled by a runoff index that is primarily a function of land use; some methods use other factors such as slope or soil type in reducing the rainfall supply to a runoff volume. The slope and length are other watershed characteristics that serve as input to many peak-discharge methods.

### Calibrated Equations

#### Single-Return-Period Equations

The single-return-period equations, which have the structure of Equation 1, are nonlinear multiplicative because the variables have nonunit exponents; thus, the relative change in $Q_p$ due to a change in any of the variables depends on the value of the variables. In this sense, the model is nonlinear. For example, the three-parameter USGS urban peak-discharge equations (4) have the following form:

$$Q_p = b_0 A^{b_1} (13 - BDF)^{b_2} RQ_T^{b_3} \quad (8)$$

where A is the drainage area in square miles; BDF is the basin development factor, which represents the degree of land and channel development; $RQ_T$ is the peak discharge obtained from the USGS equation for rural watersheds within a state; and $b_i$ (i = 0,1,2,3) is the fitting coefficient dependent on the return period (T).

A separate equation is provided for the return periods of 2, 5, 10, 25, 50, 100, and 500 yr. The change in $Q_p$ due to a change in A for Equation 8 is given by

$$\partial Q_p / \partial A = b_0 b_1 A^{b_1 - 1} (13 - BDF)^{b_2} RQ_T^{b_3} \quad (9)$$

The rate of change for the USGS urban equations is nonlinear. It should be evident that the actual slopes of the relationships between $Q_p$ and A for the models will depend on the values of both the variables and the coefficients.

### Moment-Estimation Method

Thomas and Benson (5) derived the empirical coefficients of equations for predicting the mean and standard deviation of the logarithms of the annual peak-flow series; the regression equations for the skew coefficients were not statistically significant. Equations were derived for four regions of the United States. The regression equations for the mean ($\overline{X}$) and standard deviation (S) for rural watersheds in the eastern regions are

$$\overline{X} = 0.00264A^{1.01}P^{1.58} \quad (10)$$

$$S = 0.0142A^{0.99}P^{0.85} \quad (11)$$

in which P is the mean annual precipitation in inches. Skew coefficients for ungaged sites can best be estimated by averaging station values within the hydrologic vicinity of the ungaged site. McCuen (6) concluded that for the United States a mean skew value of zero was reasonable. In this case, the value of K of Equation 3 becomes the standardized normal variate and can be obtained from any basic textbook on statistical methods.

Equations 10 and 11 require only the drainage area and the mean annual precipitation to obtain an estimate of the peak discharge. In this respect, the input requirements are easier to obtain than those for the other methods described. Therefore, one would expect the accuracy to be less; nevertheless, because they were derived by regression, the estimates should be unbiased. The equations are nonlinear multiplicative in structure, although the exponents for the drainage area are nearly equal to unity.

### Index-Flood Method

The index-flood method requires the calibration of both the equation for the index return period and the ratios between the peak-flow rates for other return periods and the index return period. The structure of the index-flood equation is usually nonlinear multiplicative; watershed and precipitation characteristics are used as predictor variables. As an example, Trent (7) provided the following index-flood equation for estimating the 10-yr peak discharge from small rural watersheds:

$$Q_p = b_0A^{b1}R^{b2}DH^{b3} \quad (12)$$

in which R is an iso-erodent factor, defined as the mean annual rainfall kinetic energy times the annual maximum 30-min rainfall intensity, and DH is the difference in feet of the elevation of the main channel between the most distant point on the watershed boundary and the design point. The coefficients $b_i$ (i = 0,1,2,3) are a function of the hydrophysiographic zone. The estimated peak dicharge must be modified when the surface water storage in lakes, swamps, and ponds exceeds 4 percent. The 2-yr peak discharge is estimated by multiplying the 10-yr peak ($Q_{10}$) by the index ratio of 0.41. The 100-yr peak ($Q_{100}$) can be estimated by

$$Q_{100} = 1.64Q_{10}^{1.029} \quad (13)$$

If the index ratios are obtained by regression, the index-flood method should provide unbiased estimates of the peak discharge. Nevertheless, the accuracy of the estimates for return periods other than the index return period can be no greater than that obtained by the single-return-period equations; in most cases, the accuracy of the index-flood method will be less because the ratio represents a single fitting coefficient. For the single-return-period equation of the same return period, several coefficients are available for fitting.

## Uncalibrated Equations

The three methods discussed earlier, i.e., single-return-period equations, index-flood method, and moment estimation, require calibration; that is, the methods are fitted to peak-flow rates obtained from flood frequency analyses. Past empirical studies have indicated that the nonlinear multiplicative structure provides the greatest accuracy. Thus, this structure is usually chosen for these methods.

Uncalibrated equations are most often based on a conceptual framework. Therefore, the model structure is not simply chosen; instead, the structure is the result of the conceptual framework. Thus, the structure of uncalibrated equations shows wider variation than that of the calibrated methods.

### Rational Formula

The rational formula is the most widely used hydrologic equation. It has the following form:

$$Q_p = CiA \quad (14)$$

where

$Q_p$ = peak discharge ($ft^3$/sec),
C = runoff coefficient,
i = rainfall intensity (in./hr), and
A = drainage area (acres).

The form of the rational method results from the underlying conceptual framework. The method assumes a constant rainfall of intensity i for a duration of $t_c$ (hr); thus, the total rainfall depth is $it_c$. The product of the drainage area and the total rainfall depth is the volume of rainfall in inches that is available for runoff. The runoff coefficient (C) determines the proportion of the rainfall volume that appears as runoff. Conceptually, the runoff hydrograph for the rational method is triangular with a time base of $2t_c$, a time to peak of $t_c$, and a volume of runoff of $CiAt_c$; thus, 50 percent of the runoff lies under the rising limb of the runoff hydrograph.

The runoff coefficient is usually obtained from a table and is defined in terms of the land use. Some tables provide for selection of the value on the basis of return period and slope; the value of C increases for the less frequent events and with increasing slope. Some tables provide a range of C-values for each land use; although this permits the designer to select a value that reflects on-site conditions, it also leads to a lack of reproducibility. Poor reproducibility often creates difficulties between those proposing site development and those who are responsible for approving site-development plans. The rainfall intensity of Equation 14 is a function of the return period, the location, and the storm duration; the storm duration is most commonly taken as the time of concentration, although it has been shown that the critical storm duration may actually be shorter than the time of concentration (8). The value of i is obtained from a curve of rainfall intensity, duration, and frequency for the location. The relationship between the intensity and time of concentration ($t_c$) can be represented by an equation of the following form:

$$i = d_0t_c^{d1} \quad (15)$$

in which $d_0$ and $d_1$ are empirical coefficients

that reflect both the location and the units of i and $t_c$. The time of concentration is a function of the slope, length, and land cover; the value of $t_c$ has also been shown to be a function of rainfall intensity (9,10), although most methods for estimating $t_c$ are independent of i. When $t_c$ is a function of i, an iterative solution is necessary because i is also a function of $t_c$.

In summary, the basic input data required to use the rational method are the drainage area, the watershed slope, the hydraulic length, the return period, a nominal statement of the land cover, a table of C-values, and a curve of rainfall intensity, duration, and frequency for the site location. The drainage area, slope, and hydraulic length are obtained from either a site survey or a commercially available topographic map. For cases of nonhomogeneous land cover, the slope, length, and land cover are obtained for each flow segment to compute $t_c$.

### SCS TR-55 Graphical Method

The graphical method is quite similar in concept and structure to the rational formula and has the following form (11):

$$Q_p = q_u A Q/640 \quad (16)$$

where

$Q_p$ = peak discharge ($ft^3$/sec),
$q_u$ = unit peak discharge [$ft^3$/($mile^2$ • in.) of direct runoff],
A = drainage area (acres), and
Q = direct runoff (in.).

The unit peak discharge, which is obtained from Figure 5-2 of TR-55 (11), is a function of the time of concentration measured in hours. The runoff volume (Q) is a function of the SCS runoff curve number (CN) and the 24-hr rainfall depth ($P_{24}$) in inches. The curve number is a function of the land use, cover condition, and SCS soil type; CN is obtained from a table. The value of $P_{24}$ is a function of location and return period and is obtained from a volume-duration-frequency curve for the site location. The input requirements for the SCS graphical method are the drainage area, the watershed slope, the hydraulic length, the return period, a nominal statement of the land cover and condition, the soil type, a table of CN-values, the location, and the volume-duration-frequency curve for the location.

The graphical method of Equation 16 has a linear multiplicative structure, even though the equation for computing the runoff volume Q is nonlinear. The curve relating the unit peak discharge and the time of concentration is also nonlinear; actually, the structure of the curve of $q_u$ versus $t_c$ is quite similar to the structure of the intensity-duration-frequency curve used with the rational formula. It is evident that the rational method and the graphical method are almost identical in both structure and input requirements. The structures are classed as linear multiplicative because peak discharge is linearly related to each of the variables defined in the equation. For example, a change in the drainage area of 1 acre causes the same relative change in $Q_p$ regardless of the value of A. The two methods are multiplicative as opposed to being additive because the peak discharge is obtained by multiplying the values of the input variables.

The graphical method was formulated from numerous runs of the SCS TR-20 program (12). The TR-20 program uses a curvilinear unit hydrograph to compute the runoff hydrograph and thus the peak discharge. This curvilinear unit hydrograph has 37.5 percent of the volume under the rising limb. The time to peak of the unit hydrograph is two-thirds of the time of concentration. The runoff volume is a nonlinear function of the precipitation. It should be evident that conceptual differences exist between the graphical and the rational methods despite their use of similar input.

## Summary

It should be evident that the peak-discharge methods differ little in either their structure or their input requirements. The input usually consists of the drainage area, a precipitation characteristic, and one or more watershed characteristics. The main difference between methods, at least with respect to input requirements, is the number of predictor variables used. The accuracy of prediction does not appear to improve when variables are added beyond the drainage area, the precipitation index, a land use index, and a watershed characteristic such as the slope.

The structures of the methods are also quite similar. Although linear multiplicative structures are often used for the uncalibrated equations, the other peak-discharge methods usually rely on nonlinear multiplicative form, which is a more flexible structure. For the uncalibrated methods, the linear multiplicative structure is used because empirical evidence indicates a wide range of values for the exponents. For example, for estimating peak discharges in Iowa, Lara (13) reported exponents for the drainage-area variable from 0.42 to 0.70. Sauer and others (4) reported values from 0.15 to 0.41 for nationwide urban peak-discharge equations. For estimating floods in Maryland, Walker (14) reported values from 0.8585 to 0.947. Trent (7) reported values from 0.23 to 1.31. It is evident that the empirical coefficients are highly variable and depend on factors such as location, type of watershed (urban or rural), and the range of watershed sizes.

Given that the structures and input requirements are similar, is there any reason to believe that one method is any better than the others? The major difference certainly is that which exists between the calibrated and the uncalibrated methods. Calibrated methods should provide unbiased estimates; they will also provide more accurate estimates when the test watersheds are similar to those used in calibrating the equation. Accuracy can be expected to decrease significantly as the coefficients become less applicable to the watersheds being tested.

Among the calibrated methods (i.e., single return period, index flood, and moment estimation), the major difference lies in the number of coefficients calibrated. For example, the single-return-period method required 24 coefficients for the 3-parameter models for the 2-, 5-, 10-, 25-, 50-, and 100-yr peaks. The moment-estimation technique would probably require fewer because there are only three equations to calibrate. The index flood would require one set for the index flood and at least five for the index ratios. Although the larger number of coefficients should lead to greater accuracy for the single-return-period method, the increased accuracy may not be statistically significant. Nevertheless, the independent calibration of single-return-period equations for different return periods may not preserve the skew of the individual station frequency curves. The moment-estimation method would be expected to best replicate the shape characteristics of the frequency curve.

## ACCOUNTING FOR FLOW IN CHANNEL SYSTEMS IN MAKING PEAK-DISCHARGE ESTIMATES

Hydrograph and multiple-event methods almost always include one or more input variables or parameters that reflect flow in channel systems. For example, the SCS TR-20 model uses the channel length and convex method routing coefficient to reflect channel characteristics. Channel system characteristics are not handled in such a direct manner with most of the peak-discharge methods. The uncalibrated equations such as the rational formula and SCS TR-55 graphical method do not include specific variables to reflect channel characteristics; nevertheless, flow in channel systems can be partly accounted for by including channel-flow characteristics in the computation of the time of concentration. This indirect method of accounting for channel characteristics limits the potential accuracy of the methods for watersheds where channel flow is significant. The uncalibrated equations should not be used where channel storage effects are significant. That is, where flow rates are significantly affected by channel characteristics, adjustment of the time of concentration may not be adequate for handling the effects of channel characteristics on peak-discharge rates.

Conceptually, the product of the intensity and the drainage area in the rational formula represents the supply rate of water; the runoff coefficient represents the portion of the supply rate that is converted into direct runoff; the proportion (1 - C) represents the losses due to interception and other overland flow processes, such as depression storage and infiltration. When the time of concentration is adjusted to reflect channel runoff, it is not totally reasonable that the shape of the intensity-duration-frequency curve, from which the value of i is obtained, reflects the sensitivity of peak discharge to channel characteristics. A similar argument can be made for the graphical method. If the effect of channel characteristics is accounted for in the time of concentration, it is not totally reasonable that the shape of the unit peak-discharge curve of TR-55 reflects the sensitivity of peak discharge to channel characteristics.

The three types of peak-discharge methods that usually require calibration most often account for flow in channel systems differently than do the uncalibrated equations. Specifically, the single-return-period equations, the moment-estimation methods, and the index-flood methods are often calibrated by using data obtained from stream gages. In such cases, the log Pearson type III estimates of the peak discharge and the statistical moments of the annual maximum series reflect the effects of the channel system. Thus, the values of the fitting coefficients reflect the channel system. For example, the three-parameter USGS urban equation (Equation 8) contains four coefficients that are directly affected by the channel characteristics of the urban watersheds that were used to calibrate the model. Also, the coefficients in the equations that are used to estimate $RQ_T$ contain fitting coefficients that reflect the channel characteristics of the rural watersheds that were used to calibrate the models for predicting $RQ_T$.

The point of this discussion is that methods calibrated with data obtained from stream gages should be expected to perform differently from those in which the characteristics of the channel system must be reflected indirectly, such as through the time of concentration. When models calibrated with data from stream gages are compared with peak discharges obtained from stream-gage records, one would expect such models to perform better, in terms of accuracy and bias, than models that were not calibrated. Similarly the calibrated models might not perform as well as the uncalibrated models when the models are compared with data obtained from watersheds where channel systems are nonexistent or minor. In summary, it is important for a model to be used under conditions similar to those used in the development or calibration of the model.

## COMPARISONS WITH MEASURED DATA

Because the peak-discharge methods are so widely used, comparisons of the methods are of special interest. Two studies have recently been undertaken that illustrate the concepts discussed earlier. The Water Resources Council (WRC) study (1) compared nine methods on 70 rural watersheds. Because the USGS single-return-period equations for each state, the rational method, and the SCS graphical method are widely used, it is of interest to compare the results from the WRC study for these three methods. The mean bias of the 100-yr event was 10, 80, and 75 percent, respectively, for the three methods. The interquartile ranges of the percentage of deviation from the gage estimate were 45, 180, and 165 percent, respectively. Given that the USGS equations are intended for rural watersheds and were calibrated from similar data, it is not surprising that these equations produced the smallest bias and the smallest dispersion. The rational and graphical methods were intended to be used on watersheds that were smaller than most of the watersheds included in the study. In addition, these two methods are used mostly to estimate inlet peak discharges rather than peaks on streams of significant channel storage where gages would likely be located. Thus, the large positive biases and large ranges should not have been unexpected.

Rawls, Wong, and McCuen (15) compared several peak-discharge methods on 40 small urban watersheds. The watersheds included in this data set had drainage areas less than 4,000 acres. The methods included the USGS urban equations (Equation 8), the rational method (Equation 14), and the graphical method (Equation 16). By using the bias and accuracy statistics of Equations 6 and 7, the three methods resulted in bias values of -0.11, -0.49, and -0.07, respectively, and accuracy values of 0.66, 0.68, and 1.17, respectively, for the 100-yr events. Because the data base that was used for testing was part of the data base used to calibrate the USGS equation, the bias and accuracy values of -0.11 and 0.66 can be used as standards of comparison. The graphical method is relatively unbiased, whereas the rational method still tended to overpredict. The graphical method showed somewhat greater scatter (i.e., poorer accuracy) than that of the USGS equations, whereas the scatter for the rational method was comparable with that of the USGS equation. The low bias of the graphical method indicates that, on the average, the method provides reasonable agreement to peak discharges computed by using log Pearson type III analyses. The higher variability in comparison with that of the USGS method probably results because it was not calibrated from such data. The tendency of the rational method to overpredict may indicate that it was applied to watersheds that are too large; that is, the conceptual framework and runoff coefficients may not be applicable to watersheds as large as 4,000 acres.

## DISCUSSION AND CONCLUSIONS

Despite empirical studies comparing peak-discharge methods, the debate continues over which method should be used in design. Although the comparison studies have suggested that calibrated equations are

relatively unbiased and have the smallest error variation, all of the studies have avoided defining what represents a significant difference. Furthermore, the WRC study (1) suggested that the sample sizes used in these comparison studies were inadequate for making conclusive statements. If the empirical evidence is inadequate, it is possible to combine the results of the empirical studies with a rational analysis of the conceptual framework, structure, and input requirements of the methods.

When the peak-discharge methods are compared on the basis of their input requirements, there is little difference; drainage area is usually the most important input variable; a rainfall characteristic and a time characteristic are other common, important input variables. The methods also differ little in structure. Although the methods calibrated are usually nonlinear, the variation in the coefficients from one empirical study to another is sufficiently large that the results do not suggest that a linear structure is unreasonable.

The greatest difference between the methods is their conceptual framework. The calibrated equations emphasize channel characteristics, whereas the uncalibrated equations emphasize surface-runoff characteristics. The input variables for the calibrated methods are often similar to those for the uncalibrated equations, but the fitting coefficients provide a conceptual mechanism for incorporating channel characteristics into the estimated peak discharges. Although the uncalibrated equations can attempt to account for channel flow by modifying the time of concentration, the use of Manning's equation for computing channel velocities cannot totally reflect channel-storage characteristics. Thus, for watersheds where the flow in channels is significant, the calibrated methods have a distinct advantage.

The uncalibrated methods also differ conceptually among themselves. For example, although both the graphical and the rational methods are based on unit hydrograph concepts, the rational method assumes a much larger portion of flow within the rising limb of the hydrograph than the graphical method (i.e., 50 percent versus 37.5 percent). Thus, one would expect that the rational method would be more appropriate for small watersheds where the land cover conditions cause a rapid response. The graphical method appears to be more appropriate for slightly larger watersheds where surface runoff storage effects are more evident.

Where it is necessary to formulate design standards as part of stormwater management or drainage policies, how does this rational comparison provide insight concerning which method to select? Both the empirical evidence and the rational analysis suggest that a single-return-period equation should be used where a peak discharge is needed on a stream having significant storage. If an entire frequency curve is required, the moment estimation may be preferable. For small watersheds where surface runoff dominates, the uncalibrated equations may be preferred. Selection of the uncalibrated equation should depend on the similarity of the watershed characteristics to the characteristics of the site. For small inlet areas, the rational method may be preferred; selection of this method, however, would assume that the watershed response is rapid. Thus, the rational method may not be appropriate for low sloped areas such as coastal watersheds.

To summarize, in formulating policy adequate consideration should be given to the agreement between the conceptual framework of the design method and the characteristics of the design problem for which the policy is intended.

## REFERENCES


1. Estimating Peak Flow Frequencies for Natural Ungaged Watersheds. Hydrology Committee, Water Resources Council, Washington, D.C., 1981, 346 pp.
2. G. Fleming and D.D. Franz. Flood Frequency Estimating Techniques for Small Watersheds. Journal of the Hydraulics Division of ASCE, Vol. 97, 1971, pp. 1441-1460.
3. R.H. McCuen, W.J. Rawls, G.T. Fisher, and R.L. Powell. Flood Flow Frequency for Ungaged Watersheds: A Literature Evaluation. Agricultural Research Service, U.S. Department of Agriculture, Beltsville, Md., Rept. ARS-NE-86, 1977, 136 pp.
4. V.B. Sauer, W.O. Thomas, Jr., V.A. Strickler, and K.V. Wilson. Flood Characteristics of Urban Watersheds in the United States--Techniques for Estimating Magnitude and Frequency of Urban Floods. FHWA, Rept. FHWA/RD-81/178, 1981.
5. D.M. Thomas and M.A. Benson. Generalization of Streamflow Characteristics from Drainage-Basin Characteristics. U.S. Geological Survey, Reston, Va., USGS Water Supply Paper 1975, 1970.
6. R.H. McCuen. Map Skew??? Journal of the Water Resources Planning and Management Division of ASCE, Vol. 105, Sept. 1979, pp. 269-277.
7. R.E. Trent. FHWA Method for Estimating Peak Rates of Runoff from Small Rural Watersheds. FHWA, March 1978.
8. T.R. Bondelid and R.H. McCuen. Critical Storm Duration for the Rational Method. Journal of Civil Engineering Design, Vol. 1, No. 3, 1979, pp. 273-286.
9. R.M. Ragan and J.O. Duru. Kinematic Wave Nomograph for Times of Concentration. Journal of the Hydraulics Division of ASCE, Vol. 98, 1972, pp. 1765-1771, Proc. Paper 9275.
10. R.H. McCuen, S.L. Wong, and W.J. Rawls. Estimating the Time of Concentration in Urban Areas. Journal of the Water Resources Planning and Management Division of ASCE, to be published.
11. Urban Hydrology for Small Watersheds. Soil Conservation Service, U.S. Department of Agriculture, Tech. Release 55, 1975.
12. O.G. Lara. Floods in Iowa: Technical Manual for Estimating Their Magnitude and Frequency. Iowa Natural Resources Council Bull. 11, March 1973.
13. P.N. Walker. Flow Characteristics of Maryland Streams. Maryland Geological Survey, Rept. of Investigations 16, 1971.
14. W.J. Rawls, S.L. Wong, and R.H. McCuen. Comparison of Urban Flood Frequency Procedures. Journal of the Hydraulics Division of ASCE, to be published.

# Predicting Hydrologic Effects of Urbanization by Using Soil Conservation Service Methods

RICHARD H. McCUEN AND NORMAN MILLER

A recent study by the Water Resources Council indicated that the methods of the Soil Conservation Service (SCS) are among the most widely used hydrologic design methods. The TR-55 graphical and chart methods are used to predict peak discharge. The TR-55 tabular method and the TR-20 computer package can be used to generate entire storm hydrographs. Because the methods are widely used for design in urban areas, it is important to understand exactly how the effects of urbanization should be assessed by using the SCS methods. Changes in land use affect the flood runoff through both the time of concentration and the SCS runoff-curve number. The effect of urbanization on peak discharges indicated by SCS methods is compared with the effect indicated by other peak-discharge methods.

Hydrologists have demonstrated major concern over the hydrologic effects of urbanization for at least three decades. During this period, a wide array of hydrologic models has been developed to predict the effects of urbanization on runoff characteristics. Even in 1983 more models are being developed. It appears reasonable, therefore, to examine some of these models and to assess the range of predicted effects of urbanization on runoff characteristics.

Urbanization is a process that affects a number of components of the hydrologic cycle. The clearing of vegetated land cover reduces the interception storage. Often, development of land involves significant amounts of grading. The grading usually causes significant decreases in the depression storage. After clearing and grading, parts of the developing area are covered with impervious surfaces. In addition, the previously sinuous drainageways are straightened; the result is a decrease in both the roughness and natural storage. The impervious surfaces decrease the potential for infiltration, and the modifications to the drainageways change the storage effects on runoff. In many localities, storm-water detention facilities are required to compensate for the natural storage that is lost during urbanization; however, studies have shown that detention storage does not return the runoff and storage characteristics to their predevelopment status (1,2).

The hydrologic effects of urbanization are most often assessed by using the change in peak discharge as the sole criterion. Nevertheless, other runoff characteristics are important. In addition to peak discharge, urbanization causes changes in both the volume of direct runoff and the various time characteristics of the runoff, including the time of concentration, the time to peak, and the duration of flow at various flood stages. These other runoff characteristics are recognized as being important, especially because of their effects on water quality. In summary, when the hydrologic effects of urbanization are evaluated, it is important to view the problem from a multicriterion standpoint.

Although the hydrologic concepts used by the Soil Conservation Service (SCS) (3,4) have been in existence for some time, their use gained widespread acceptance when SCS TR-55 was published in 1975 (5). The TR-55 methods have been included in the design sections of many drainage and storm-water management policies and are widely used. In many states, the TR-55 methods are replacing the rational formula as the recommended technique for peak-discharge estimation on small watersheds.

The objective of this paper is to demonstrate how the SCS methods can be used to evaluate the hydrologic effects of urbanization and to compare the predicted effects with the results of other studies.

## EFFECT ON RUNOFF VOLUMES

The reductions in interception storage, depression storage, and infiltration that accompany urbanization cause increases in runoff volumes. The increased volume of direct runoff is partly responsible for both the degradation of channels and the decreases in groundwater recharge. In recognition of the detrimental effects of increases in runoff volume, one purpose of storm-water management is to replace the natural storage that is lost due to urbanization.

The SCS methods use the following equation to compute the depth of runoff (Q) in inches that results from a 24-hr rainfall depth (P) in inches:

$$Q = (P - 0.2S)^2/(P + 0.8S) \quad (1)$$

in which S is the potential maximum retention,

$$S = (1{,}000/CN) - 10 \quad (2)$$

where CN is the SCS curve number for runoff. The rainfall depth is for a specified return period. The SCS methods are most often applied by using the 24-hr rainfall depth.

The runoff CN is an index that reflects the land use, treatment, hydrologic condition, and hydrologic soil group. CN increases as the pervious land covers are changed to impervious land covers. SCS assumes a CN of 98 for impervious surfaces. Thus, a composite CN can be obtained by weighting the impervious and pervious land cover CNs by using the fraction of the total area in each land cover:

$$CN = 98f + (1 - f)CN_P \quad (3)$$

where f is the fraction of imperviousness and $CN_P$ is the CN for the pervious portion of the watershed. Because the CN is a function of f, the change in the runoff volume (Q) due to a change in f is obtained as follows:

$$\partial Q/\partial f = (\partial Q/\partial S) \cdot (dS/dCN) \cdot (\partial CN/\partial f) \quad (4a)$$

$$\partial Q/\partial f = \{(98 - CN_P)[400(P - 0.2S) + 800Q]\}/[(CN)^2 (P + 0.8S)] \quad (4b)$$

Equation 4 indicates that the sensitivity of Q to changes in f is a direct function of Q and is inversely related to the pervious-area CN. Figure 1 shows the relationship between the rate of change of the runoff and the fraction of imperviousness for the pervious surface CNs of 60, 70, 80, and 90 and a rainfall of 5 in. To illustrate the use of Equation 4b, if P is 5 in., $CN_P$ is 70, and f is 0.9, then $\partial Q/\partial f = 3.15$. If a proposed development would increase the fraction of imperviousness by 0.05, the change in the runoff volume would be 3.15 (0.05) = 0.16 in., which is the product of $\partial Q/\partial f$ and $\Delta f$.

Figure 1. Sensitivity of runoff volume to fraction of imperviousness for selected pervious area CNs.

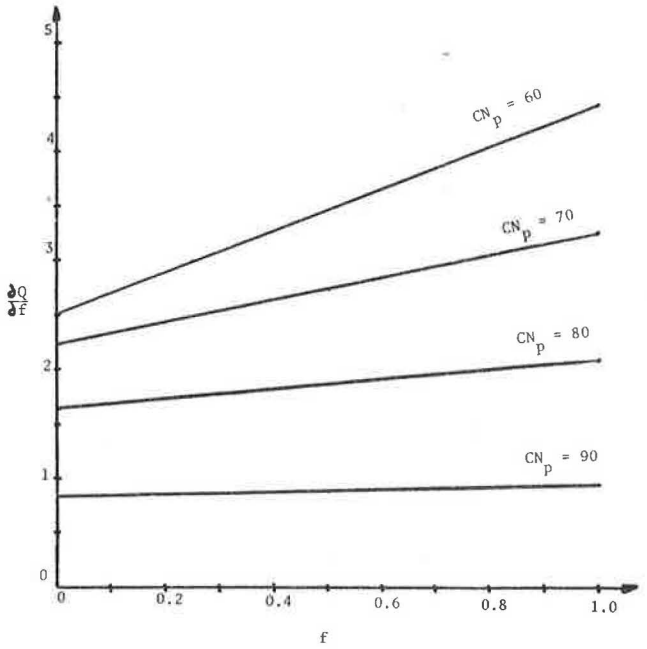


EFFECT ON TIME PARAMETERS

Time is an important parameter in most hydrologic models, including the SCS methods. The time of concentration ($t_c$) and the lag time (L) are the two most frequently used time parameters. SCS computes the lag time as follows:

$$L = \ell^{0.8}(S + 1)^{0.7}/1{,}900Y^{0.5} \quad (5)$$

where

L = lag time (hr),
$\ell$ = watershed length (ft),
Y = watershed slope (%), and
S = potential maximum retention, which is defined by Equation 2.

SCS provides the following relationship between L and $t_c$:

$$t_c = 1.67L \quad (6)$$

SCS provides a second method, which is called the velocity method, for computing the time of concentration. Although the lag equation (Equation 5) is recommended only for small rural drainage areas, the velocity method can be used with all land covers. When the velocity method is used, the time of concentration is defined as follows:

$$t_c = \left[\sum_{i=1}^{n} (\ell_i/V_i)\right]/3{,}600 \quad (7)$$

in which $\ell_i$ is the length of the ith flow segment in feet, $V_i$ is the velocity in feet per second of flow through flow segment i, and n is the number of flow segments. The velocity for overland flow segments can be estimated by using a graph of the watershed slope and the velocity; different relationships are given for different surface types. Manning's equation can be used to estimate the velocity of flow in channels.

When the lag method is used and part of the watershed is urbanized, SCS provides two graphs of lag factors for correcting the lag estimated with Equation 5. In one graph the percentage of imperviousness is related to a lag correction factor, which can vary from 0 to 1. In the other graph the percentage of the hydraulic length modified is related to a lag correction factor. The lag factor in both graphs is a function of CN. These lag factors are approximations of the effect of urbanization on the time parameters.

If the more exact evaluation of the effect of urbanization on the time of runoff cannot be evaluated by using the velocity method, the effect can be estimated by examining the change in the lag time with respect to change in the fraction of the watershed that is impervious. By using Equations 5, 2, and 3, it can be shown that $\partial L/\partial f$ is given as follows:

$$\partial L/\partial f = (\partial L/\partial S) \cdot (dS/dCN) \cdot (\partial CN/\partial f) \quad (8)$$

From Equation 5, the partial differential of L with respect to S is

$$\partial L/\partial S = 0.7\ell^{0.8}(S + 1)^{-0.3}/1{,}900Y^{0.5} \quad (9)$$

From Equation 2, the differential of S with respect to CN is

$$dS/dCN = -1{,}000/(CN)^2 \quad (10)$$

From Equation 3, the partial differential of CN with respect to f is

$$\partial CN/\partial f = 98 - CN_P \quad (11)$$

Therefore, the following expression results for the partial differential of Equation 8:

$$\partial L/\partial f = [-700\ell^{0.8}(98 - CN_P)]/[1{,}900(S + 1)^{0.3}(CN)^2Y^{0.5}] \quad (12)$$

The second derivative is

$$\partial^2 L/\partial f^2 = \left\{700\ell^{0.8}(98 - CN_P)^2\,[2CN(S + 1)^{0.3} - 300(S + 1)^{-0.7}]\right\} \div [1{,}900(S + 1)^{0.6}CN^4\,Y^{0.5}] \quad (13)$$

The change in the lag time due to change in the percentage of imperviousness can be evaluated by using a Taylor expansion:

$$L_a = L + (\partial L/\partial f) \cdot df + (1/2!)(\partial^2 L/\partial f^2) \cdot df^2 + (1/3!)(\partial^3 L/\partial f^3) \cdot df^3 + \ldots \quad (14)$$

in which L is the lag time at f = 0, and $L_a$ is the lag time at f = df. The lag factor can be obtained by dividing Equation 14 by L:

$$L_a/L = 1 + (\partial L/\partial f) \cdot (df/L) + (1/2!)(\partial^2 L/\partial f^2) \cdot (df^2/L) + (1/3!)(\partial^3 L/\partial f^3) \cdot (df^3/L) + \ldots \quad (15)$$

For the range of values for CN and f that are usually of interest, the second-order Taylor series is sufficient. Then Equation 15 reduces to the following:

$$L_a/L = 1 + (\partial L/\partial f) \cdot (df/L) + (1/2!)(\partial^2 L/\partial f^2) \cdot (df^2/L) \quad (16)$$

The first-order Taylor series is acceptable when CN is greater than 85 and f is less than 0.3. For a CN of 70 and an f of 0.6, the error in using the second-order Taylor series (Equation 16) is about 0.05. Figure 2 shows the peak-factor relationships obtained by using the second-order Taylor series (solid lines) and the peak-factor relationships of TR-55 (broken lines). The noticeable differences between the two sets of lines indicate that the lag formula, which was derived for use on rural water-

Figure 2. Variation of lag factor with CN and fraction of imperviousness.

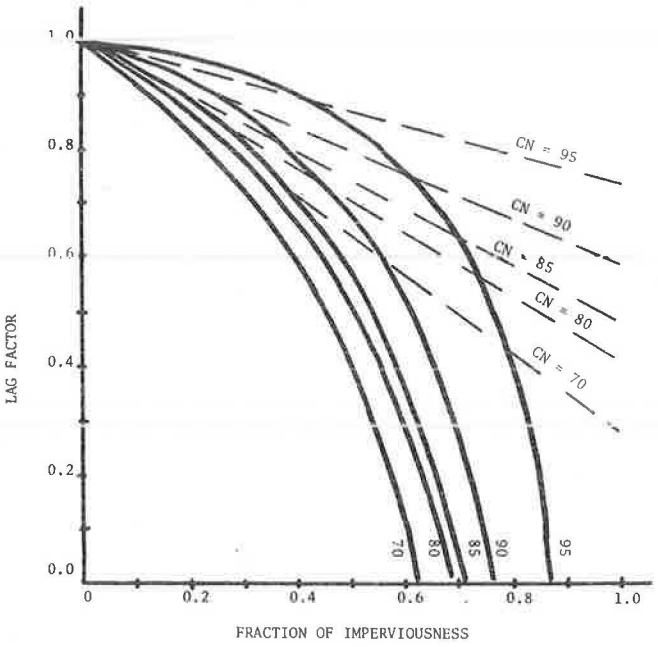


sheds, should not be used with the lag factors of TR-55 for even moderate levels of imperviousness, for example, greater than 30 percent; i.e., f = 0.3. Beyond this value, which actually varies with CN, the sensitivity of the lag formula to changes in imperviousness may not be rational. When the percentage of imperviousness exceeds this value, the velocity method should be used to examine the effect of urbanization on time parameters.

To illustrate the use of Equation 12 for evaluating the effect of urbanization on the timing of runoff, the effect of a change in imperviousness on the time of concentration can be computed by multiplying the constant 1.67 from Equation 6 by Equation 12 to give $\partial t_c/\partial f$. For a watershed with a flow length of 1,000 ft, a pervious-area CN of 70, and a slope of 2 percent, $\partial t_c/\partial f = 0.379$ when f = 0. Therefore, if development were to increase f to 10 percent, the time of concentration would decrease by 0.379 (0.1) = 0.038 hr, which is the product of the change in f and $\partial t_c/\partial f$.

## SCS METHODS

The SCS has developed an array of hydrologic methods. The simplified methods described in TR-55 can be used to compute either a peak discharge or an entire hydrograph. Two peak-discharge methods are provided in TR-55--the graphical method and the chart method. When an entire hydrograph is needed, the TR-55 tabular method can be used. A simplified method for determining the required volume of detention storage is also given in TR-55.

The TR-20 computer program (4) can be used for more complex watershed analyses. TR-20 can be used to generate runoff hydrographs, route the hydrographs through either channel reaches or reservoirs, and combine hydrographs at stream confluences.

### Graphical Method

Chapter 5 in TR-55 describes a method for estimating the peak discharge. The method, which is referred to as the graphical method, derives its name from a graph that relates the time of concentration in hours and the unit peak discharge inch cubic feet per second per square mile per inch of runoff. The input data requirements, which are minimal, are the return period in years (T); the 24-hr, T-yr precipitation in inches (P); the CN; the drainage area in square miles (A); and the time of concentration in hours ($t_c$).

The procedure requires the volume runoff to be estimated by using P and CN as input to Equation 1. The time of concentration can be estimated by using either the lag method or the velocity method; however, the velocity method is preferred for the graphical method. The unit peak discharge is estimated from Figure 5-2 of TR-55, which relates the unit peak discharge and the time of concentration. The peak discharge equals the product of the unit peak discharge, the drainage area, and the volume of runoff.

The graphical method is recommended (a) where valley routing is not required; (b) for watersheds where land use, soil, and cover are uniformly distributed throughout the watershed; and (c) where runoff can be represented by one CN. Also, the graphical method should not be used when runoff volumes are less than about 1.5 in. for CNs less than 60 and the drainage area should be less than 20 miles$^2$. These limitations are given in TR-55.

### Chart Method

Another procedure for computing the peak discharge, which is called the chart method, is described in TR-55. The chart method was designed for use in estimating the effect of development on the peak-discharge rate. The input data are the same as those for the graphical method (except for $t_c$) with the addition of the hydraulic length in feet, the percentage of ponds and swampy area, the watershed slope in percent, and the percentage of both the impervious area and the hydraulic length modified. Not all the data are necessary for all cases because some of the options are not mandatory. Application of the method is limited to watersheds from 1 acre to 2,000 acres. The method is based on a 24-hr storm volume and a SCS type II storm distribution.

The hydraulic length (HL) is used when it is desired to make a shape adjustment. The hydraulic length is entered and used to compute the effective area (EA):

$$EA = 0.00013586HL^{3/5} \quad (17)$$

If a watershed shape adjustment is not desired, the HL is not necessary and EA should be set equal to the drainage area (A).

If a significant portion of the watershed is swampy or in ponds or both, the pond and swamp adjustment factor can be obtained from a table. The value depends on the location of the ponds or swampy area within the watershed, the return period (T) (or storm frequency), and the percentage of ponding and swampy area.

The unit peak discharge, which will be discussed below, is obtained from charts designed for index slopes of 1, 4, and 16 percent. For slopes other than those for these three index values, a slope-adjustment factor can be obtained from a table. The following table indicates the slope designations:

| Slope Designation | Index Slope (%) | Slope Range (%) |
|---|---|---|
| Flat | 1 | SP $\leq$ 2.5 |
| Moderate | 4 | 2.5 < SP $\leq$ 7.5 |
| Steep | 16 | 7.5 < SP |

The effective area and slope are used as input to the appropriate part of a table in TR-55, and the slope-adjustment factor is obtained.

The unit peak discharge is then obtained from one of three figures in TR-55, which is separated on the basis of the three index slopes. The unit peak discharges are given in units of cubic feet per second per inch of runoff. The figures define the unit peak discharges for the SCS type II storm. The CN is used with the effective area to get the unit peak discharge.

By using the depth of precipitation and the CN, the volume of runoff (in inches) can be determined. If an adjustment is to be made for the percentage of imperviousness, the peak-adjustment factor (FIMP) is obtained from a figure. The percentage of imperviousness (IMP) and the CN are used as input. A similar adjustment is used when the hydraulic flow pattern has been or will be modified. The percentage of the hydraulic length modified (HLM) and the CN are used as input to a figure from which the peak-adjustment factor (HLMF) is obtained.

### Tabular Method of TR-55

The tabular method, which is discussed in Chapter 5 of TR-55, was designed for use in the following circumstances:

1. For developing composite flood hydrographs at any point within a watershed,
2. For measuring the effects of changes in land use of one or more subwatersheds, and
3. For assessing the effects of structures or combinations of structures.

In general, the procedure was intended for measuring the effect on the composite flood hydrograph of changes within subwatersheds of a larger drainage area.

The input requirements for the tabular method for each subwatershed are the same as those needed in the graphical method. In addition, the travel time for each channel reach is necessary.

Before the method is applied, the user should be familiar with several constraints. The constraints that were used in developing the method are important when applying the method. The tabular method was developed by making numerous computer runs with the TR-20 program. In each case, a CN of 75 was used and the rainfall volumes were selected to yield 3 in. of runoff. When the tabular method is applied to cases having characteristics that are significantly different from the conditions used in developing the method, the resulting hydrograph may not provide close agreement with the hydrograph that would result from a TR-20 analysis. These assumptions are not considered to be critical when the sole purpose in using the method is to assess the effect of changes in a watershed, such as land use or structure changes. The difference in the before and after hydrographs is relatively insensitive to the assumption of a CN of 75.

In order to make accurate assessments of watershed changes, there are certain limitations that should be adhered to in applying the method. First, within any subwatershed there should be little variation in CN; this does not mean that subwatersheds should have similar CNs but that each subwatershed should have little variation in soil and land use characteristics. Second, the area of each subwatershed should be less than 20 miles$^2$. Third, the precipitation should be sufficient to yield runoff volumes greater than 1.5 in., especially when CNs are less than 60.

The solution methodology centers about the tabular discharge values, which are given in a set of tables in TR-55. A table segment is given for selected times of concentration ($t_c$): 0.1, 0.2, 0.3, 0.4, 0.5, 0.75, 1.0, 1.25, 1.5, and 2.0 hr. For values other than these, the closest value can be used; further precision can be achieved through interpolation.

Each table segment is further subdivided by the total travel time ($T_t$) from the subwatershed outlet to the design point. For each $t_c$ and $T_t$, discharge rates are given in cubic feet per second per square mile per inch of runoff for hydrograph times (i.e., the time from the beginning of precipitation) ranging from 11.0 to 20.0 hr in various time increments; these hydrograph times correspond to time in the 24-hr SCS type II rainfall distribution.

The procedure used in solving problems with the tabular discharge hydrograph method is to segment the watershed into appropriate subareas and identify the necessary input for each subarea and channel reach. The hydrograph at the design point due to runoff from any subarea is determined by entering the tables for the subarea $t_c$ and the total travel time from the outlet of the subarea to the design point. The total hydrograph is determined by summing the subarea hydrographs.

### SCS TR-20 Computer Program

TR-20 is a computerized method for solving hydrologic problems by using the concepts outlined in Section 4 of the SCS National Engineering Handbook. The program was formulated to develop runoff hydrographs, to route hydrographs through both channel reaches and reservoirs, and to combine or separate hydrographs at confluences. The program is designed to make multiple analyses in a single run so that various alternatives can be evaluated in one pass through the program; this leads to more efficient use of computer time.

Even though a computer is used to solve problems, the input data requirements are surprisingly minimal; the amount of data depends on the complexity of the problem to be solved. If actual rainfall events are not going to be used, the total depth of precipitation is the only meteorological input. For each subarea, A, CN, and $t_c$ are required; the SCS antecedent soil moisture condition (I, II, or III) must also be specified. For each channel reach, the length is required along with the channel cross-section description, which includes the elevation, discharge, and end-area data; although it is optional, a routing coefficient may also be used as input. If the streamflow routing coefficient is not given as input, it will be computed by using the cross-section data. For each structure it is necessary to describe the outflow characteristics with the elevation-discharge-storage relationship. The time increment for all computations must be specified, and any baseflow in a channel reach must be identified.

## EFFECT ON PEAK DISCHARGES COMPUTED WITH SCS METHODS

When SCS hydrologic methods are used, the effect of urbanization on peak discharges is assessed by the joint effect of urbanization on $t_c$ and CN. For the chart method, the computed peak discharge will increase as either the runoff volume or the peak factors increase. The peak factors are a function of CN and the percentage of change in either the imperviousness or the hydraulic length modified. The tabular method will show an increase in the peak discharge when either the runoff volume increases or the time of concentration or the channel-reach

Table 1. Effect of urbanization on 10-yr peak discharge.

| IMPA (%) | CN | Q (in.) | $q_u$ [(ft$^3$/sec)in.] | FIMP | QP (ft$^3$/sec) | $\Delta QP/QP_0$ (%) | $\Delta Q/Q_0$ (%) | $\Delta q_u/q_{uo}$ (%) | $\Delta$IMPF (%) |
|---|---|---|---|---|---|---|---|---|---|
| 0 | 60 | 1.30 | 42 | 1.00 | 54.6 | – | – | – | – |
| 10 | 64 | 1.58 | 46 | 1.06 | 77.0 | 41.0 | 21.5 | 9.5 | 6 |
| 20 | 68 | 1.88 | 50 | 1.13 | 106.2 | 94.5 | 44.6 | 19.0 | 13 |
| 30 | 71 | 2.12 | 54 | 1.20 | 137.4 | 151.6 | 63.1 | 28.6 | 20 |

travel time or both decrease. For the RUNOFF subprogram of the TR-20 program, changes in urbanization will be reflected by changes in CN and $t_c$, both of which are necessary input.

The chart method is easily used to demonstrate the effect of urbanization on peak discharge. For a 100-acre, wooded (fair condition) watershed with a slope of 4 percent and type-B soil, CN is 60. The 10-yr 24-hr rainfall depth is assumed to be 5 in. The results in Table 1 show the effect of increases in the percentage of imperviousness on the 10-yr peak discharge. By using Equation 2 to compute CN, the change in CN is a prime input to each of the steps. CN is used to obtain the runoff volume (Q), the unit peak discharge ($q_u$), and the peak factor (FIMP). The change in peak discharge is 151.6 percent for a change of 30 percent in imperviousness.

The effect of a change in the fraction of imperviousness on the peak discharge can be computed analytically for the graphical method. The peak discharge will change in accordance with the changes to $t_c$ and Q; the change in the runoff volume results from a change in CN. The graph in TR-55 that relates the unit peak discharge in cubic feet per second per square mile per inch of runoff can be represented by a function having the following form:

$$q_u = b_0 t_c^{b_1} \tag{18}$$

in which $b_0$ and $b_1$ are coefficients that must be determined for small ranges of $t_c$. The peak discharge ($q_p$) is computed by

$$q_p = q_u A Q \tag{19}$$

The effect of urbanization is then determined analytically by

$$\partial q_p/\partial f = [(dq_u/dt_c)(\partial t_c/\partial f)]\,AQ + q_u A(\partial Q/\partial f) \tag{20}$$

The derivative $dq_u/dt_c$ can be obtained by differentiating Equation 18 as follows:

$$dq_u/dt_c = b_1 b_0 t_c^{b_1-1} = b_1 q_u/t_c \tag{21}$$

The partial derivative $\partial t_c/\partial f$ equals 1.67 times the value of Equation 12, and the partial derivative $\partial Q/\partial f$ is computed with Equation 4. The first term on the right-hand side of Equation 20 represents the effect of change in f on $q_p$ because of the effect of change in f on $t_c$; the second term represents the effect of change in $q_p$ due to the effect of f on Q.

## ADVANTAGES AND DISADVANTAGES OF SCS METHODS

As have all hydrologic methods, the SCS methods have been criticized. A major concern of practicing engineers has been the inadequate form of the documentation of the methods. Before worksheets were made available in 1981 for the TR-55 methods, many applications were incorrectly made. The TR-20 documentation is not a good learning tool for someone interested in making a first application of the computer program. Also, the documentation does not make the limitations of the methods sufficiently clear. These problems are currently being addressed. Revised manuals will be available in the near future.

Several elements of the methods have been criticized as not being rational; however, this is to be expected for any simplified method. The two most frequent criticisms appear to be the assumed initial abstraction relationship and the infiltration relationship that is imbedded within the methods. Although these elements are criticized, it is not clear that they contribute to any inaccuracies; that is, these assumptions may not affect the accuracy of the methods when the methods are used for the purposes for which they were intended.

The methods have also been criticized because of the apparent lack of an empirical basis. Although some effort has been made to document the empirical as well as the conceptual basis for the SCS methods (6, pp. 353-364), recent empirical studies have shown the accuracy of the methods to be similar to that of other widely used hydrologic methods. The most recent study (7) comparing hydrologic methods on small urban watersheds indicated that the TR-55 methods were relatively unbiased but showed slightly more error variation than both the rational method and the new USGS urban-peak formula.

In spite of these criticisms, the SCS hydrologic methods have numerous advantages. First, they have been widely used and no major problems have been reported. Second, the input data are easily obtained, and the methods are simple to apply. Recent studies (8,9) have shown that reasonably accurate estimates of the input can be obtained by using remotely sensed data. Third, the SCS methods represent an array of procedures, including peak-discharge methods, simple hydrograph methods, methods for analyzing complex watersheds, and methods for sizing storm-water detention facilities. The array of procedures enables the planner and designer to solve various elements of a problem by using procedures based on the same concepts. Such integrated design eliminates problems associated with the use of different methods. Also, the methods can be used for analyzing runoff problems for both urban and rural land covers. The SCS methods are also popular because they have eliminated the reproducibility problem that is associated with many of the empirical formulas such as the rational method; regulatory agencies that must review and approve design plans are often confronted with the problems created by the range of values provided with empirical coefficients such as the runoff coefficient of the rational method.

An important advantage of the SCS methods is the continued research that is being undertaken to improve and diversify the methods. For example, a two-stage riser design method was developed because hydrologists recognized that one-stage risers in detention ponds did not adequately control the runoff frequency curve. Similarly, CNs were developed for new agricultural practices.

## PEAK DISCHARGE: COMPARISON OF SCS METHODS WITH OTHER MODELS

Leopold (10, pp. B9-B11) provided a graph of the ratio of the mean annual discharges after and before development versus the percentage of the area served by storm sewers and percentage of the area that was urbanized (according to Leopold, 100 percent urbanization corresponds to 50 percent imperviousness). The values of the ratio ranged from 1 to 6. As an example, when 50 percent of the area was served by sewers and 50 percent was urbanized, the ratio value was about 2.85.

Dunne and Leopold (11), after Carter (12) and Anderson (13), provided the following relationship between the percentage of imperviousness (I) and the ratio of the after- to the before-urbanization peak discharges:

$$Q_q \text{ (after urbanization)}/Q_p \text{ (before urbanization)} = (0.30 + 0.0045I)/0.30 \quad (22)$$

Thus, the ratio would vary from 1 to 2.5 for values of I from 0 to 100 percent.

Sarma, Delleur, and Rao (14) provided the following relationship for computing peak discharges on urban basins:

$$Q_p = 484.1A^{0.723}(1 + I/100)^{1.516}P_E^{1.113}T_R^{-0.403} \quad (23)$$

where

$Q_p$ = peak discharge (ft³/sec),
A = drainage area (miles²),
I = percentage of imperviousness,
$P_E$ = volume of excess rainfall (in.), and
$T_R$ = duration of excess rainfall (hr).

It is evident that the effect of urbanization will vary with the values of A, $P_E$, and $T_R$. For example, for a 1-mile² watershed in which 1 in. of precipitation excess occurs during 1 hr, the ratio of the after-urbanization to the before-urbanization peak discharges ranged from 1.0 at I equal to zero to 2.86 at I equal to 100 percent. This range agrees favorably with the range resulting from Equation 22.

The USGS urban peak-flow formula (14) has the following form:

$$UQ_T = b_0A^{b1}SL^{b2}(RI2 + 3)^{b3}(ST + 8)^{b4}(13 - BDF)^{b5}I^{b6}RQ_T^{b7} \quad (24)$$

where

$UQ_T$ = urban peak discharge for return period T (ft³/sec),
A = drainage area (miles²),
SL = channel slope (ft/mile) with a maximum value of 70 ft/mile,
RI2 = 2-yr, 2-hr rainfall intensity (in.),
ST = basin storage (%),
BDF = basin development factor,
I = percentage of imperviousness,
$RQ_T$ = rural watershed peak discharge (ft²/sec) for the T-yr event (i.e., before development peak discharge), and
$b_i$ (i = 0, 1, ..., 7) = regression coefficients, which vary with the return period of the discharge.

Assuming that A, SL, RI2, and ST remain constant with development, the increase in peak discharge due to urbanization is a function of BDF and I. Sauer and others (15) indicated that the ratio of peak discharges after to those before development will range from 1 to 4.5 for the 2-yr event and from 1 to 2.7 for the 100-yr event as the value of BDF varies from 0 to 12 and I varies from 0 to 100 percent.

Although the SCS peak-discharge methods use CN and the percentages of imperviousness and hydraulic length modified to account for the effects of urbanization on peak discharge, other methods use either the imperviousness alone or a combination of other factors. Methods that use more than one factor, such as the SCS methods, the USGS urban equations, and Leopold's relation between percentage of area served by sewers and percentage urbanized, are certainly more flexible and provide more opportunity to adapt the procedures for different watershed modifications than methods based solely on the percentage of imperviousness. Urbanization of a watershed can take many forms, from land cover changes such as residential development to the installation of a sewer system and modification of the channel system. Because the hydrologic effects of each of these factors are different, it is important to have a model that is sensitive to the type of urbanization and will reflect the hydrologic effects of the watershed change. However, as the number of factors in a model that relate to a specific process, such as urbanization, increases, it becomes increasingly difficult to calibrate the model and separate the effects of the factors. The problem is compounded because the change of the peak discharge results from changes to various factors such as the level of natural storage, the timing of the runoff, the volume of runoff, and the drainage density. Conceptual models attempt to reflect the effect of changes in each of these factors on the runoff.

## DISCUSSION

A variety of hydrologic models has been developed to represent each of the components of the hydrologic cycle. Models of groundwater flow, evapotranspiration, channel flow, and infiltration are used for decision making; surface-runoff models are probably the most widely used. Because of the diversity of surface-runoff regimes, several surface-runoff models have been developed. In many cases, the models have been fitted with measured data from the site or region where the model was intended to be used. Other models have been developed without fitting to measured data and are recommended for general use at all sites within a large region. Such uncalibrated models are widely used because of the generality of their conceptual framework and their operational simplicity.

The SCS concepts were initially developed for estimating surface runoff from agricultural areas. TR-55, which was published in 1975, provided methods for estimating surface runoff from urban watersheds. The methods recognize the effect of urbanization on all elements of surface runoff, including the peak discharge, the runoff volume, and the time characteristics of both surface runoff and channel flow. Thus, the methods permit the evaluation of the effects of urbanization on all of the major aspects of surface runoff in urban areas. Because of this flexibility and the computational simplicity of the methods, TR-55 has been widely adopted as part of drainage and storm-water management policies.

The true hydrologic impact of urbanization cannot be known because the processes involved and their interaction are too complex to be represented mathematically, especially when one considers the diversity in urban watersheds. This has led to the development of a number of urban surface-runoff models. Problems are created when different models are used by different hydrologists at the same site. This is sufficient reason for adopting one

method, even when we recognize that if we knew the true effect of urbanization, the model selected might not be the most accurate. What criteria should be used in selecting one design method? First, the conceptual framework of the model should be rational. Second, the model should be flexible so that it can be used for a variety of design problems. Third, the model should be applicable to large regions, not just sites within a single county. Fourth, the input data requirements should be minimal and easily obtainable. Fifth, the method should be highly reproducible; that is, different hydrologists should get the same design at a given location. Sixth, a model should be simple to apply.

In summary, the SCS methods appear to satisfy the six criteria for model selection (i.e., conceptually rational, flexible in design, widely applicable, requiring minimal input, highly reproducible, and computationally simple). Studies have also shown that the methods are reasonably accurate and relatively unbiased when they are applied under the conditions for which they were developed.

REFERENCES


1. R.H. McCuen. A Regional Approach to Urban Stormwater Detention. Geophysical Research Letters, Vol. 1, No. 7, Nov. 1974, pp. 321-322.
2. R.H. McCuen. Downstream Effects of Detention Basins. Journal of Water Resources Planning and Management Division of ASCE, Vol. 105, 1979.
3. Hydrology. In National Engineering Handbook, Section 4, Soil Conservation Service, U.S. Department of Agriculture, 1969.
4. Computer Program for Project Formulation: Hydrology. Soil Conservation Service, U.S. Department of Agriculture, Tech. Release 20, 1969.
5. Urban Hydrology for Small Watersheds. Soil Conservation Service, U.S. Department of Agriculture, Tech. Release 55, 1975.
6. R.E. Rallison and N. Miller. Past, Present, and Future SCS Runoff Procedure. Proc., International Symposium on Rainfall-Runoff Modeling, Water Resources Publications, Littleton, Colo., 1982.
7. W.J. Rawls, S.L. Wong, and R.H. McCuen. Comparison of Urban Flood Frequency Procedures. Journal of the Hydraulics Division of ASCE (to be published).
8. R.M. Ragan and T.J. Jackson. Runoff Synthesis Using Landsat and the SCS Model. Journal of the Hydraulics Division of ASCE, Vol. 106, 1980.
9. T.R. Bondelid, T.J. Jackson, and R.H. McCuen. A Computer-Based Approach to Estimating Runoff Curve Numbers Using Landsat Data. AgRISTARS, 1981, pp. 1-72.
10. L.B. Leopold. Hydrology for Urban Land Planning: A Guidebook on the Hydrologic Effects of Urban Land Use. U.S. Geological Survey, Reston, Va., Circ. 554, 1968.
11. T. Dunne and L.B. Leopold. Water in Environmental Planning. W.H. Freeman and Co., San Francisco, 1978.
12. R.W. Carter. Magnitude and Frequency of Floods in Suburban Area. U.S. Geological Survey, Reston, Va., Professional Paper 424-B, 1961.
13. D.G. Anderson. Effects of Urban Development on Floods in Northern Virginia. U.S. Geological Survey, Reston, Va., Water Supply Paper 2001-C, 1970.
14. P.B.S. Sarma, J.W. Delleur, and A.R. Rao. A Program in Urban Hydrology, Part II. Water Resources Research Center, Purdue Univ., West Lafayette, Ind., Oct. 1969, 240 pp.
15. V.B. Sauer, W.O. Thomas, Jr., V.A. Stricker, and K.V. Wilson. Magnitude and Frequency of Urban Floods in the United States. U.S. Geological Survey, Reston, Va., 1981.


# Simple Methods to Evaluate Relative Effects of Longitudinal Encroachments

LEON A. TRAILLE AND DONALD L. CHERY, JR.

**To aid highway planners and others who must site structures and fills in natural floodplains, simplified graphical solutions were developed that provide short-cut methods for easy assessment of encroachment impacts. Changes in stage (water-surface elevation) and hydrograph peak discharge due to encroachments were determined. The discussion is limited to encroachments that parallel the channel.**

Construction in floodplains of highway fills and other types of built-up areas with alignments generally parallel to the main channel of a river or stream constitutes longitudinal or lateral encroachment. Such encroachments usually reduce storage and conveyance available for passing flood flows and generally alter the characteristics of flooding at the affected site.

The impact of encroachments can be determined by using existing techniques that include an assortment of computer models and other methods. These techniques are complex, however, require costly and time-consuming field data collection and preparation, and are therefore unsuitable at the preliminary design phase for assessing relative impact of encroachment alternatives on flooding. In this paper results are presented from a study that developed simple procedures to evaluate impacts of encroachment options on flood depths and peak-discharge rates. Sample problems are presented to illustrate the procedures developed.

RESEARCH APPROACH

To develop the simplified procedures, representative channel cross sections were selected and a controlled series of tests with existing mathematical models produced a set of predicted changes that were used to develop the graphic plots of relationships among groups of significant variables. The entire range of graphs developed and step-by-step proce-

dures for using them are presented in a user's manual (1).

Two aspects of flooding modified by longitudinal encroachments that were addressed in this study are (a) changes in water-surface profile and (b) changes in hydrograph peak-discharge rate. Figure 1 shows schematically the entire range of encroachment conditions with respect to the symmetry of the main channel and overbanks. The simplified procedures can accommodate an asymmetrical channel and overbank cross section.

## ASSUMPTIONS AND LIMITATIONS

To develop simple procedures with a minimum of input requirements and field data-collection tasks, the following assumptions were made:

1. A single representative cross section and encroachment width can be used to model subreaches.
2. Flow is subcritical before and after encroachment; there is a Froude number of 0.6 or less.
3. Base flow that exists before the arrival of a flood wave is small relative to the amplitude of the flood wave; i.e., the event is single-peaked.
4. Flow does not overtop levees or embankments along its length whenever the water-surface elevation increases; the result is complete blockage of the flow beyond the limits of the constriction (no storage or conveyance).
5. Flow is confined from transverse spreading beyond the outer fringe of the unencroached floodplain when a single floodplain is encroached on.

Figure 1. Longitudinal-encroachment configurations.

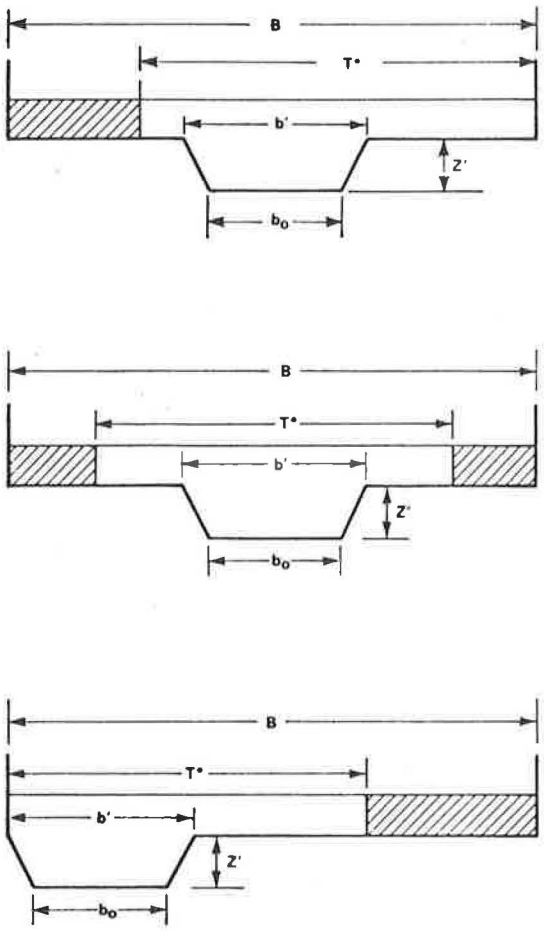


6. Natural reaches to be constricted are unaffected by downstream controls such as bridge sites, spillways, or stream junctions.
7. Effects of encroachment are independent of valley symmetry or encroachment symmetry.

## CHANGES IN WATER-SURFACE PROFILE

For flood flows with a steady or near-steady discharge rate, the floodplains provide added conveyance for passing the flood. For such flow conditions, flood profiles are governed by the principle of energy and mass conservation and can be solved entirely by using Bernoulli's equation (2). The resulting loss of floodplain conveyance due to longitudinal encroachment causes increased flood stages within the constriction. The relative change in flood stage due to encroachment is a function of the distribution of the total conveyance between the main channel and the floodplains and of the degree of constriction caused by encroachment. This relationship is used to develop the simplified procedures for estimating flood-elevation changes due to a longitudinal encroachment by employing the step-backwater flood-routing program HEC-2 (3). The difference in water-surface elevation is expressed functionally by using the significant variables that govern the flood profile:

$$\Delta H = f(H', K, K_{mc}, \Delta K_0, K_0, F_r) \quad (1)$$

where

$\Delta H$ = increase in water-surface elevation due to encroachment,
$H'$ = flow depth above bank-full stage,
$K$ = total conveyance for design flow at cross section without encroachment,
$K_{mc}$ = main-channel conveyance,
$K_0$ = total overbank conveyance,
$\Delta K_0$ = conveyance loss due to encroachment, and
$F_r$ = Froude number at the cross section.

$F_r$ is computed by using the following relationship:

$$F_r = (\alpha Q^2 B/g A^3)^{1/2} \quad (2)$$

where

$$\alpha = \sum_1^N (K_N^3/A_N^2)/(K^3/A^2) \quad (3)$$

and where

subscript N = Nth segment in cross section,
g = acceleration due to gravity,
B = unencroached top width of cross section, and
A = total flow area.

Conveyance is computed as follows:

$$K = (1.49/n)(A^5/P^2)^{1/3} \quad (4)$$

where n is Manning roughness coefficient and P is the wetted perimeter.

Making the variable grouping in Equation 1 dimensionless gives the following:

$$\Delta H/H' = f[(K_{mc}/K)(\Delta K_0/K_0) F_r] \quad (5)$$

## CHANGES IN HYDROGRAPH PEAK-DISCHARGE RATE

The high frictional resistance and obstruction to the relatively shallow flow depths in floodplains

distort a transient (unsteady) flood wave as it travels through natural stream reaches. This additional storage serves to dampen the flood wave in the direction of flow, resulting in hydrograph attenuation (4). The construction of longitudinal fills within the floodplains results in a loss of overbank storage with consequent reduction in the attenuating potential provided by natural conditions, which causes amplification of the outflow hydrograph peak.

DAMBRK, the National Weather Service model of dynamic wave unsteady flow routing (5), was used to generate the data base for simple procedures to assess changes in hydrograph peak-discharge rate. The DAMBRK model is based on the one-dimensional flow continuity and momentum equations, commonly referred to as the Saint Venant equations for unsteady flows (6). A finite difference scheme is used to solve the equations (7, pp. 16-35). This model was chosen because of its capability to simulate stream reaches that have different roughness properties and reach lengths in the main channel and overbanks. Also, the overbanks and the main channel are treated independently in the solution scheme to account for the variation that usually occurs in natural stream reaches. The theoretical basis and capabilities of the model have been described by Fread (5).

The constricted outflow hydrograph peak $Q_{m_c}$ was taken to be functionally related to the following significant physiographic and hydrologic variables:

$$Q_{m_c} = f(Q_{m_0}, Q_{m_n}, t_p, L, B, b', Q_{nB}, n_{c_p}, n_{mc}, T^*) \quad (6)$$

where

$Q_{m_c}$ = outflow peak for the constricted reach,
$Q_{m_0}$ = inflow peak,
$Q_{m_n}$ = outflow peak for the unconstricted reach,
$t_p$ = time to peak of the inflow hydrograph,
$L$ = reach length of constriction measured along the channel,
$B$ = top width of the natural floodplain,
$b'$ = top width of main channel,
$Q_{nB}$ = normal flow bank-full capacity of channel,
$n_{c_p}$ = equivalent Manning roughness coefficient of floodplains (overbanks),
$n_{mc}$ = Manning roughness coefficient of main channel, and
$T^*$ = encroached top width of cross section.

The bank-full depth of the main channel ($Z'$), the bottom width ($b_0$), and the bed slope ($S_0$) were lumped together and incorporated in the variable $Q_{nB}$. Making the variables in Equation 6 dimensionless gives

$$Q_{m_n}/Q_{m_c} = f[(L/B)(B/b')(T^*/B)(Q_{m_0}/Q_{nB})(n_{mc}/n_{cp})(Q_{m_0} t_p/B^3)] \quad (7)$$

Figure 2 shows schematically the channel variables used in the analysis. Two distinct situations, case 1 and case 2 in Figure 2, were considered in development of the simplified graphical solution scheme for Equation 7. Case 1 applies to conditions of negligible floodplain velocities, and therefore the overbanks are treated as off-channel storage. Case 2 applies to conditions for which overbank velocities are significant and therefore incorporates conveyance as well as storage effects.

## EXAMPLES

To illustrate the application of the simplified estimation procedures, three sample problems are presented. One example estimates the change in

Figure 2. Encroachment and channel schematic.

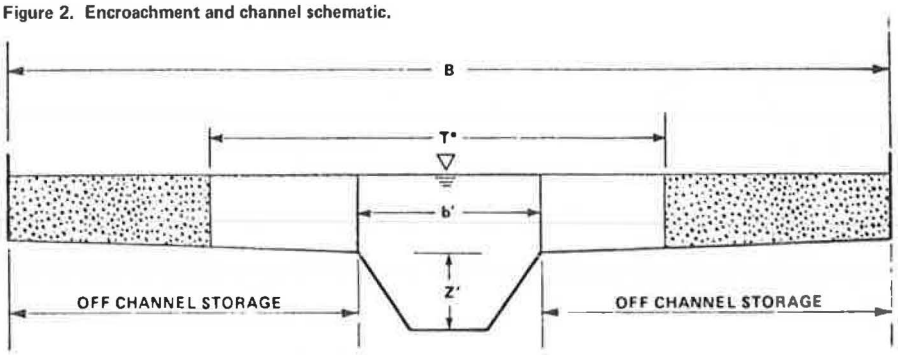


CASE 1

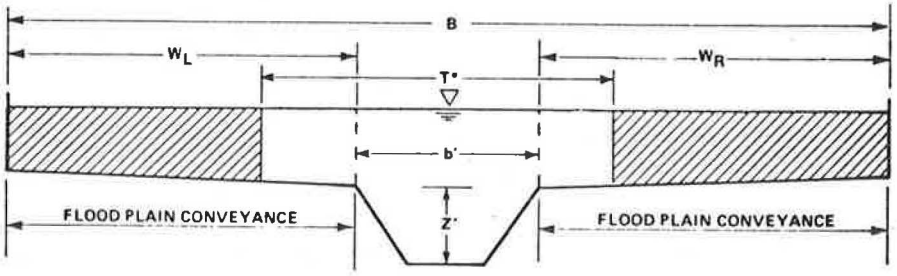


CASE 2

Figure 3. Sample cross section.

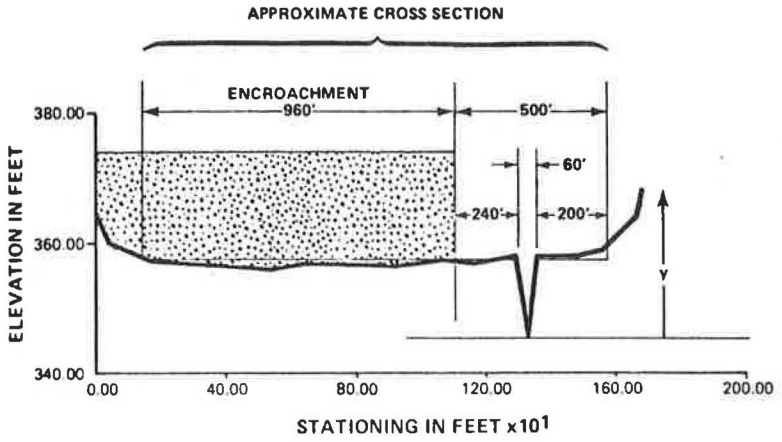


water-surface elevation given the width of the encroachment. The next estimates an allowable encroachment given a limit to the increase in water level. The third example estimates the change in peak discharge for a given width of encroachment.

Example 1: Change in Water-Surface Profile for a Given Width of Encroachment

A proposed 960-ft encroachment is placed in a representative stream cross section as shown in Figure 3. The resulting change in water-surface elevation is estimated by a simple procedure given the following information:

| Parameter | Amount |
|---|---|
| Design flow peak (Q) | 12,000 ft³/sec |
| Main channel slope ($S_0$) | 0.0014 |
| Left overbank roughness ($n_L$) | 0.12 |
| Right overbank roughness ($n_R$) | 0.09 |
| Main channel roughness ($n_{mc}$) | 0.06 |

The rectangular approximation to the overbanks uses as datum the bank-full elevation of the channel shoulders (which have the same elevation) and ends where the overbanks begin to depart significantly from the horizontal plane. For the rectangular approximation of the overbank and an approximate triangular shape of the main channel (assuming an isosceles triangle), shown in Figure 3, the following parameters were determined:

| Parameter | Amount (ft) |
|---|---|
| Left overbank top width ($W_L$) | 1,200 |
| Right overbank top width ($W_R$) | 200 |
| Top width of main channel (b') | 60 |
| Bank-full depth (Z') | 12 |
| Top width of section (B) | 1,200 + 200 + 60 = 1,460 |

With these parameters the following steps give the desired estimate of the increase in water-surface elevation.

Step 1

Compute the normal flow depth ($y_n$) from Manning's equation, expressed as follows:

$$Q = 1.486 S_0^{1/2} (1/n_{mc})\, A_{mc}(y)\, R_{mc}(y)^{2/3} + \Sigma (1/n_{ob})\, A_{ob}(y) R_{ob}(y)^{2/3} \quad (8)$$

where

Q = design discharge rate,
$A_{ob}$ = flow area of one overbank,
$R_{ob}$ = hydraulic radius of one overbank, and
$R_{mc}$ = hydraulic radius of main channel determined at $A_{mc}/P_{mc}$.

$$12{,}000 = 1.486 \times (0.0014)^{1/2} \left[ (1/0.06) \left( [1/2\,(60 \times 12) + 60\,(y_n - 12)]^{5/3} / \left\{ 2[(30^2 + 12^2)^{1/2} + (y_n - 12)] \right\}^{2/3} \right) + [(1{,}200/0.12) + (200/0.09)]\,(y_n - 12)^{5/3} \right] \quad (9)$$

The hydraulic radius of each overbank is approximated by the depth of flow in the rectangular overbanks; i.e., $R_{ob} = y_n - 12$. Successive estimates of $y_n$ by trial and error eventually give $y_n \approx 17$ ft.

Alternatively, the conveyance in the subsections can be computed independently by using Manning's equation and plotted graphically. From this procedure, the normal flow depth ($y_n$) can be determined. The main channel conveyance as a function of depth ($K_{mc}$) can be determined from Equation 4 as follows:

$$K_{mc} = (1.486/0.06) \left\{ [1/2(60 \times 12) + 60(y - 12)]^5 / 2[(30^2 + 12^2)^{1/2} + (y - 12)]^2 \right\}^{1/3} \quad (10)$$

where y is total flow depth. For three trial solutions (y = 12, 15, and 18 ft) $K_{mc}$ = 28,018, 51,907, and 82,680 ft³/sec, respectively.

Assuming that the hydraulic radius of the overbanks can be estimated by the depth of flow y - z', the overbank conveyances ($K_L'$) are determined as follows:

$$K = (1.486/n_{ob})\, W_{ob}\, (y - z')^{5/3} \quad (11)$$

Therefore, the left overbank conveyance ($K_L'$) is determined as follows:

$$K_L' = (1.486/0.12) \times 1{,}200 \times (y - 12)^{5/3} \quad (12)$$

For y = 15 and 18 ft, $K_L'$ = 92,730 and 294,400 ft³/sec, respectively. The right overbank conveyance ($K_R$) is determined as follows:

$$K_R = (1.486/0.09) \times 200\,(y - 12)^{5/3} \quad (13)$$

For y = 15 and 18 ft, $K_R$ = 20,607 and 65,461 ft³/sec, respectively.

Plots of $K_{mc}$, $K_L'$, $K_R$, and total K as a function of depth y are shown in Figure 4, where

$$K = K_{mc} + K_L' + K_R \quad (14)$$

Figure 4. Conveyance versus depth for cross section.

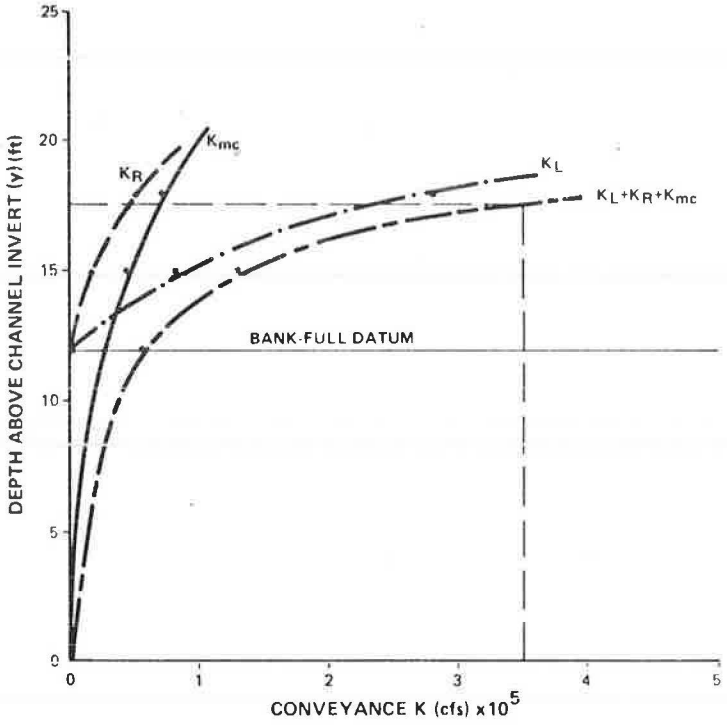


$y_n$ is determined for the depth that satisfies Equation 8; i.e., $K = 12{,}000/0.0014^{1/2} = 3.1 \times 10^5$ ft$^3$/sec. From Figure 4, the depth at which the value of K computed above is satisfied is 17 ft. Therefore, $y_n$ = 17 ft.

Step 2

Determine the weighted Froude number from the conveyance and area distribution derived in step 1 and Equations 2 and 3. From Figure 4, the conveyance distribution is as follows: $K_L = 2.0 \times 10^5$ ft$^3$/sec, $K_R = 3.5 \times 10^4$ ft$^3$/sec, and $K_{mc} = 7.0 \times 10^4$ ft$^3$/sec.

From Equation 3,

$$\alpha = \Big( [(2.0 \times 10^5)^3/(1{,}200 \times 5)^2] + [(3.5 \times 10^4)^3/(200 \times 6)^2] + \{(7 \times 10^4)^3/[60 \times 6 + 1/2\,(60 \times 12)]^2\} \Big) / \{(3.1 \times 10^5)^3 \div [5(1{,}200 + 200 + 60) + 1/2(60 \times 12)]^2\} = 2.07 \quad (15)$$

From Equation 2,

$$F_r = \Big( (2.07 \times 12{,}000^2 \times 1{,}460)/\{32.2(1{,}460 \times 5) + [1/2(60 \times 12)]\}^3 \Big)^{1/2}$$

$$F_r \simeq 0.17 \quad (16)$$

Step 3

Determine $\Delta K_0/K_0$.

From Equation 9,

$$\Delta K_0 = (1.486/0.12) \times 960 \times 5^{5/3} = 1.74 \times 10^5 \text{ ft}^3/\text{sec} \quad (17)$$

From step 2,

$$K_0 = 3.05 \times 10^5 - 7 \times 10^4 \text{ ft}^3/\text{sec} = 2.35 \times 10^5 \text{ ft}^3/\text{sec} \quad (18)$$

$$\Delta K_0/K_0 = 1.74/2.35 = 0.74 \quad (19)$$

Step 4

Determine $\Delta H/H'$. Figure 5 [taken from the user's manual by Traille and others (1, p. 37)] provides an estimate of the surcharge for values of $F_r$, $K_{mc}/K$, and $\Delta K_0/K_0$ determined in steps 1-3. From step 1, $K = 3.1 \times 10^5$ ft$^3$/sec and from step 2, $K_{mc} = 7.0 \times 10^4$ ft$^3$/sec.

$$K_{mc}/K = (7.0 \times 10^4)/(3.1 \times 10^5) = 0.22 \quad (20)$$

From Figure 5 at $K_{mc}/K = 0.22$, $\Delta K_0/K_0 = 0.70$, and for $F_r = 0.1$, $\Delta H/H' = 0.7$, where H' is the depth of flow above bank-full stage or 17 minus 12.

$$\Delta H = 0.7 \times 5.0 = 3.5 \text{ ft} \quad (21)$$

## Example 2: Maximum Encroachment for a Given Permissible Increase in Flow Level

Determining the maximum encroachment for a specified rise in water-surface elevation (for example, 1.0 ft) requires first determining the following ratio:

$$\Delta H/H' = 1/5 = 0.20 \quad (22)$$

From Figure 5 for $\Delta H/H' = 0.20$, and $K_{mc}/K$ as determined in Example 1, step 4, $\Delta K_0/K_0 = 0.29$. For the rectangular approximation to the overbank, the conveyance can be assumed to be linearly distributed in each overbank. Therefore, the allowable constriction width $T_Z$ for $\Delta K_0/K_0 = 0.29$ is computed as follows:

$$T_Z/W_L = (\Delta K_0/K_0)\,(K_0/K'_L) \quad (23)$$

or

$$T_z = 0.29 \times [(2.4 \times 10^5)/(2.0 \times 10^5)] \times 1{,}200 = 417 \text{ ft} \quad (24)$$

Figure 5. Changes in water-surface elevation.

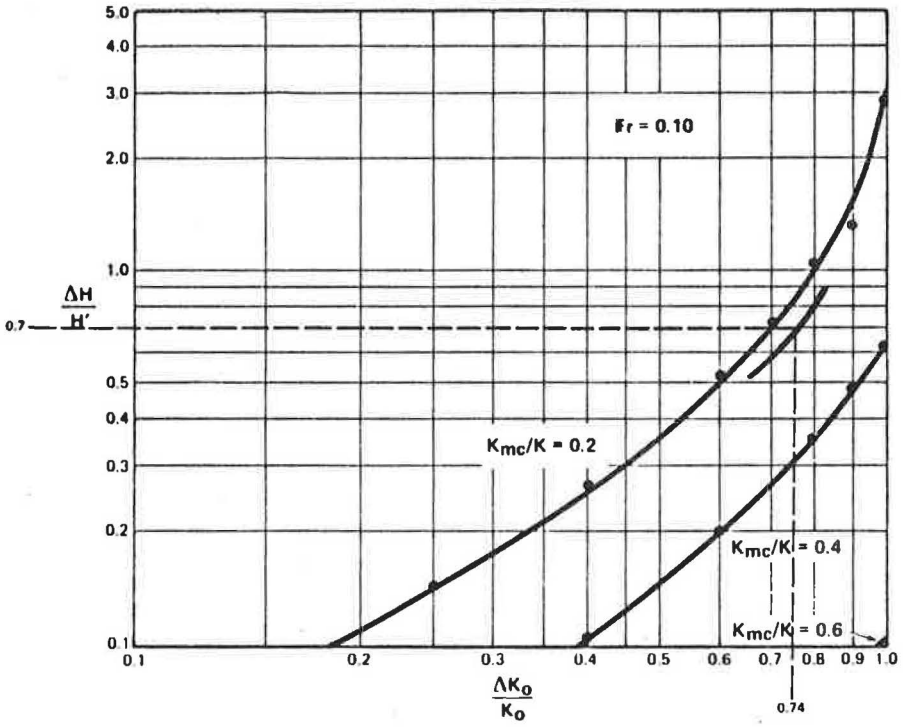


Figure 6. Dimensionless plot of peak-flow changes due to lateral encroachment: case 1.C.1.

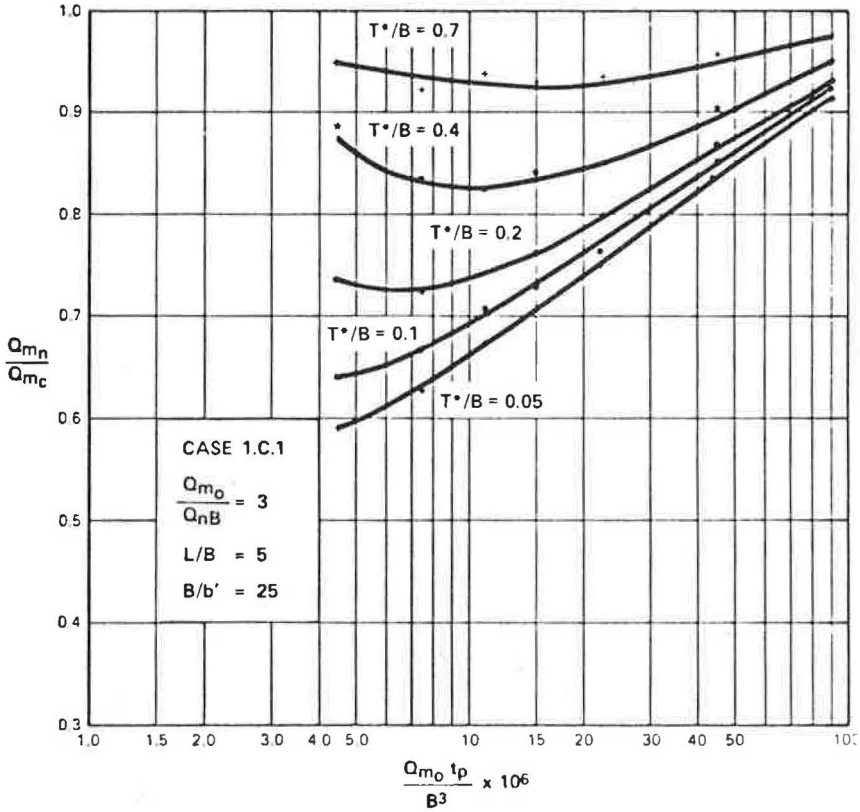

Figure 7. Dimensionless plot of peak-flow changes due to lateral encroachment: case 1.D.1.

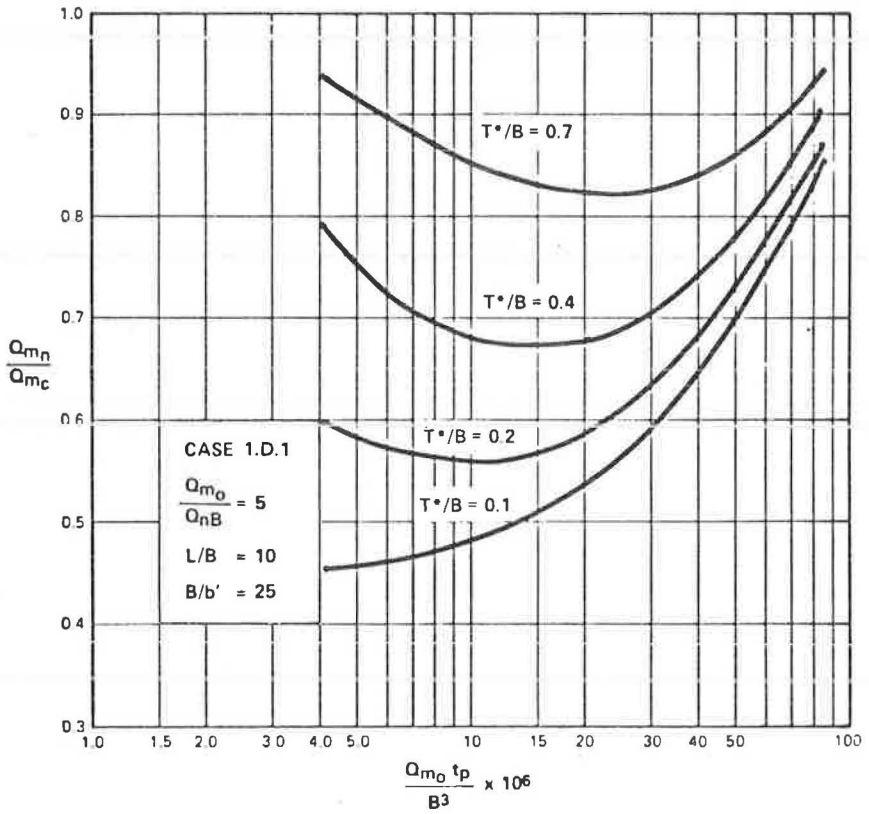


Figure 8. Dimensionless plot of peak-flow changes due to lateral encroachment: case 1.D.2.

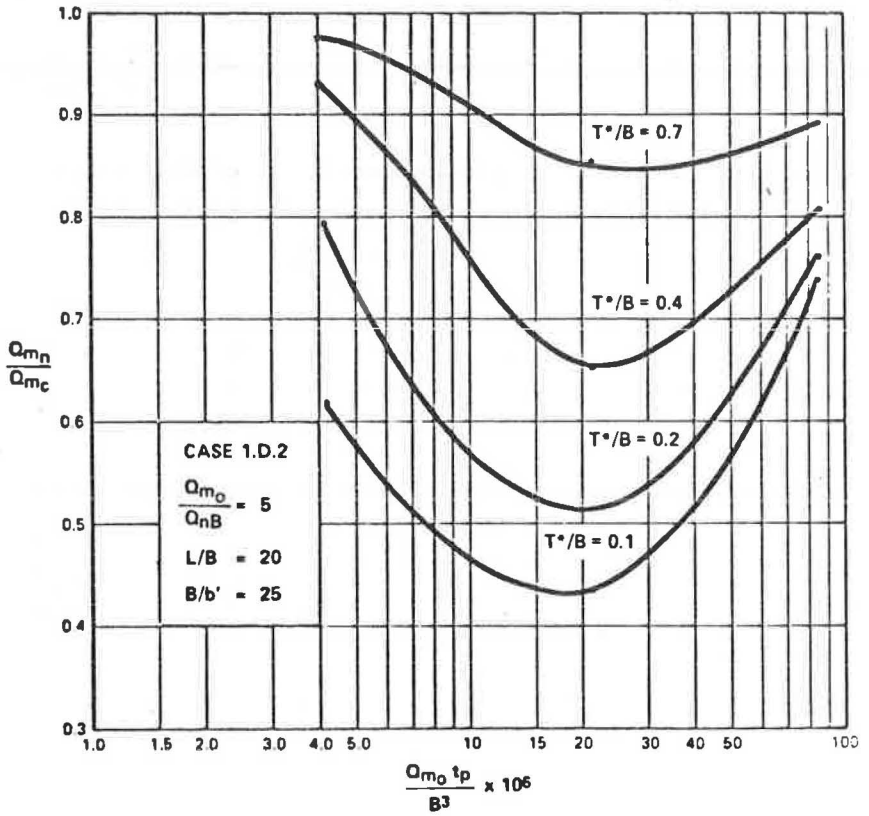

Example 3: Change in Hydrograph Peak Flow Rate (No Overbank Conveyance)

Values for the input variables of Equation 6 are required. Determine a representative trapezoidal approximation of the channel cross-section geometry for the selected subreach. The next step establishes whether the flow condition is based on the obstruction in the floodplains. The parameters in Equation 7 are established next. These parameters can be adjusted to account for the effects of meanders and the variable overbank roughness coefficient (1).

The following data are given for a heavily vegetated overbank channel (i.e., no overbank conveyance):

| Parameter | Amount |
|---|---|
| Width of cross section (B) | 200 ft |
| Width of main channel (b') | 10 ft |
| Depth of main channel (Z') | 10 ft |
| Main channel roughness ($n_{mc}$) | 0.025 |
| Main channel slope ($S_0$) | 0.0015 |
| Encroached top width (T*) | 40 ft |
| Time to hydrograph peak ($t_p$) | 0.30 hr |
| Inflow hydrograph peak ($Q_{m_0}$) | 2,000 $ft^3/sec$ |
| Reach lengths of channel and overbanks ($L_C = L_R = L_L$) | 1,200 ft |

Follow the next two steps to estimate the percentage of increase in the flow rate.

Step 1

Calculate values for the parameters in Equation 7, excluding the roughness ratio. Normal bank-full flow ($Q_{nB}$) is computed by using Equation 8:

$$Q_{nB} = (1.486/0.025)\{(10 \times 10)^5/[10 + 2(10)^2]\}^{1/3}(0.0015)^{1/2} = 514\ ft^3/sec$$

$$Q_{m_0}/Q_{nB} = 2{,}000/514 = 4$$

$$B/b' = 200/10 = 20$$

$$Q_{m_0}t_p/B^3 = (2{,}000 \times 0.30)/200^3 = 75 \times 10^{-6}$$

$$L/B = 1{,}200/200 = 6$$

$$T^*/B = 40/200 = 0.2 \qquad (25)$$

Step 2

Figure 6 approximately satisfies all the variable groupings except $Q_{m_0}/Q_{nB}$. Extrapolation of Figures 7 and 8 for L/B = 6 gives $Q_{m_n}/Q_{m_c} = 0.88$. From Figure 6 read $Q_{m_n}/Q_{m_c}$ as 0.92. Averaging with 0.88 to determine the value at $Q_{m_0}/Q_{nB} = 4$ gives 0.90. The amount of amplification to the outflow hydrograph is therefore $Q_{m_c}/Q_{m_n} = 1/0.90 = 1.11$. Thus, the outflow peak of the encroached reach $Q_{m_c}$ is magnified 11 percent.

## CONCLUSIONS

The simulation results indicate that the change in water-surface profile can be expressed as a function of the valley section's conveyance distribution in the main channel and floodplains, the average flow depth in the overbanks (expressed as a depth above bank-full stage), the Froude number of the flow in the unencroached condition, and the degree of constriction (conveyance reduction) in the overbanks due to the encroachment.

Constricting the natural channel valley by encroaching laterally was found to decrease the rate of hydrograph attenuation and thus to increase the natural peak-outflow hydrograph. The characteristic shape of the inflow hydrograph, as defined by the peak-discharge rate and the time of rise of the inflow hydrograph, was found to exert considerable influence on the attenuation of a flood.

## REFERENCES


1. L.A. Traille, D.L. Chery, Jr., H.W. Shen, and S. Taylor. Flow Modifications by Storage Loss Through Flood Plain Encroachment--User's Manual. NCHRP, Project 15-7 (unpublished report available from NCHRP), Aug. 1982.
2. V.T. Chow. Open Channel Hydraulics. McGraw-Hill, New York, 1959.
3. HEC-2 Water Surface Profiles: User's Manual. U.S. Army Corps of Engineers, Davis, Calif., Hydrologic Engineering Center Computer Program 723-02A, 1979.
4. S. Hayami. On the Propagation of Flood Waves. Disaster Prevention Research Institute, Kyoto Univ., Japan, Bull. 1, 1951.
5. D.L. Fread. DAMBRK: The NWS DAM-BRK Flood Forecasting Model. Office of Hydrology, National Weather Service, Washington, D.C., Nov. 1979.
6. F.M. Henderson. Open Channel Flow. Macmillan, New York, 1966.
7. D.L. Fread. Flood Routing in Meandering Rivers with Flood Plains. In Rivers '76: Proc., Symposium on Inland Waterways for Navigation, Flood Control, and Water Diversion, Vol. 1, ASCE, New York, 1976.

# Simple Methods for Estimating Backwater and Constriction Scour at Bridges and Abrupt Encroachments

STEWART W. TAYLOR AND HSIEH WEN SHEN

Analytic expressions for bridge backwater and constriction scour are presented for subcritical flow through five commonly occurring bridge crossings. To assess the effects of constriction scour on bridge backwater, a known cross-section technique is employed. Based on the analytic expressions, bridge backwater and constriction scour are numerically simulated over a wide range of flow conditions. Regression analysis is used to develop simplified explicit relations for bridge backwater as a function of Froude number, pier energy-loss coefficient, constriction ratio, and conveyance ratio. The resulting regression equations are sufficiently accurate for preliminary hydraulic analyses of bridge waterways in a feasibility study. Simplified expressions are not intended for detailed design analysis. Practical application of the simplified expressions is illustrated through a step-by-step design procedure.

In a feasibility or preliminary design phase of a bridge, highway engineers are faced with estimating bridge backwater, scour of the bridge waterway, and the effects of scour on the bridge backwater. Extensive literature has been written on these subjects; many rigorous methods are available for detailed analysis. The existing methods or models often require access to a computer and a large amount of detailed data, such as river channel geometry, sediment data, geometry of the bridge, and so forth. At the feasibility or preliminary level, detailed data are often nonexistent and often estimated; hence, a detailed analysis is not justified in terms of accuracy or in the time required for the lengthy computations. Highway engineers must explore many options in the feasibility or preliminary phase. A simple yet reasonably accurate hydraulic analysis, given the data constraints, is presented here and is intended to guide highway engineers' decision making before a detailed analysis is made. The advantages of this analysis over other short-cut methods are as follows: (a) bridge backwater is functionally related to easily computed uniform-flow properties and bridge characteristics; and (b) bridge backwater is computed explicitly, whereas other procedures involve a trial solution.

## ANALYSIS OF BACKWATER AND CONSTRICTION SCOUR

Simple methods are based on the detailed analysis of flow modification by bridges and abrupt encroachments presented by Taylor (1); highlights are given below. Bridge crossings are grouped into five categories, shown in Figure 1, and are described as follows: case I, bridge piers crossing a river channel; case II, bridge piers crossing a river channel with floodplains; case III, abrupt width encroachment of a river channel; case IV, total abrupt encroachment of floodplains; and case V, partial abrupt encroachment of floodplains. These five cases were selected to represent commonly occurring bridge crossings. Additional cases could be created by introducing bridge piers in the width encroachment; our studies, however, indicate that additional backwater caused by piers in such cases is small when compared with the magnitude of the backwater due to width encroachment.

### Assumptions

Some assumptions are made to generalize and simplify the analysis with the knowledge that only rough estimates are obtainable from simple solutions.

Figure 1. Nomenclature.

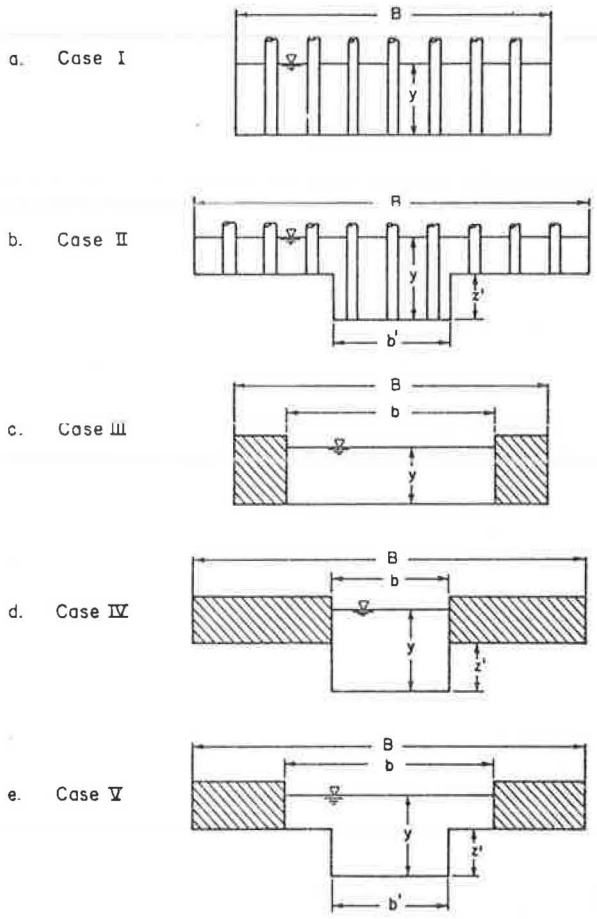


1. Flow is subcritical.
2. Bridge crossings are normal to the flow (nonskew), and floodplains are symmetrical around the river channel (noneccentric). Although bridge openings are often skew or eccentric in practice, introducing these variables, given the degree to which the flood discharge, channel roughness, and so on are known, defeats the whole purpose of a simple analysis.
3. Flow never overtops the lowest elevation of the encroachment embankment (no weir flow) and never contacts the bottom of the bridge deck (no orifice flow); occurrence of either of these phenomena could cause a bridge failure. This study assumes that sufficient freeboard will be incorporated into the bridge design to prevent weir flow or orifice flow.
4. Flow is uniform before the construction of a bridge crossing; i.e., flow at the future bridge site is not strongly influenced by some downstream control. Uniform-flow conditions are easily calculated and are useful parameters on which simple solutions may be based.
5. Constriction scour occurs uniformly within

Figure 2. Definition sketch for bridge piers: cases I and II.

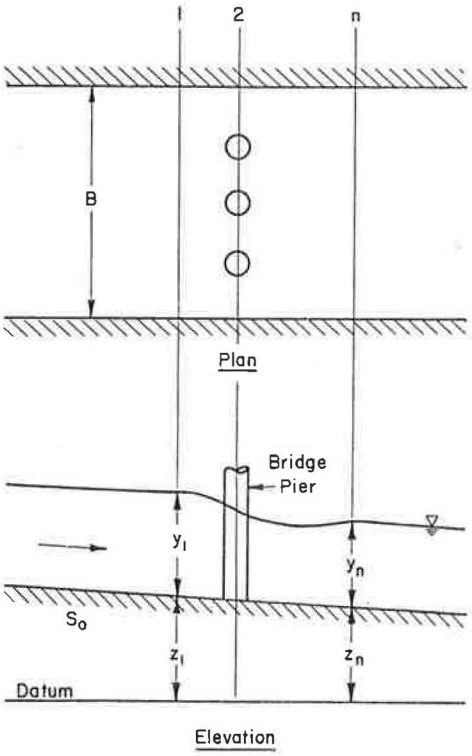


Figure 3. Definition sketch for abrupt encroachment: cases III, IV, and V.

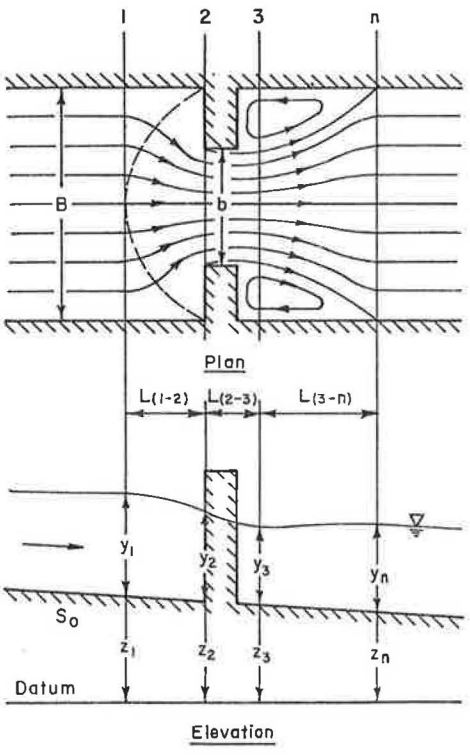


the bridge opening, and local scour is neglected. Without detailed knowledge of sediment sizes and the lateral distribution of bed shear stress, it is not possible to predict the lateral distribution of constriction scour. Local scour around piers may be estimated from any of the numerous pier-scour equations and superimposed onto the constriction scour depth to estimate the total depth of scour.

6. There is no change in river regime; i.e., the river is quasi-stable from a geomorphic point of view. Potential changes in the river regime should be studied once the final bridge site has been chosen and more data are available.

## Backwater Analysis

The steady-state backwater, or increase in stage upstream from a bridge crossing, is found by applying the energy equation across the control volumes shown in Figures 2 and 3. For valid application of the one-dimensional energy equation, control volumes are selected so that the flow at a given cross section is nearly one-dimensional in the longitudinal direction and the pressure distribution is nearly hydrostatic in the vertical direction.

With reference to Figure 2, the backwater for the bridge piers of cases I and II is found by considering the energy balance between sections 1 and n. For uniform flow without bridge piers, flow velocity and depth are by definition constant in the longitudinal direction. The energy equation for uniform flow may be written as follows:

$$\alpha_n (U_n^2/2g) + y_n + z_1 = \alpha_n (U_n^2/2g) + y_n + z_n + h_{f(1-n)} \quad (1)$$

where

$\alpha$ = kinetic energy coefficient,
U = mean flow velocity,
g = acceleration of gravity,
y = flow depth,
z = bed elevation, and
$h_{f(1-n)}$ = energy loss due to friction.

With bridge piers the energy balance is expressed as follows:

$$\alpha_1 (U^2/2g) + y_1 + z_1 = \alpha_n (U_n^2/2g) + y_n + z_n + h'_{f(1-n)} + h_{L(1-n)} \quad (2)$$

where the energy loss due to piers is assumed to be of the form

$$h_{L(1-n)} = K_L \alpha_n (U_n^2/2g) \quad (3)$$

Subtracting Equation 1 from Equation 2 and rearranging yields

$$y_1 - y_n = \alpha_n (1 + K_L)(U_n^2/2g) - \alpha_1 (U_1^2/2g) + h'_{f(1-n)} - h_{f(1-n)} \quad (4)$$

The upstream velocity $U_1$ may be written in terms of $U_n$ by using the relation for mass conservation,

$$Q = A_1 U_1 = A_n U_n \quad (5)$$

Because the friction losses with and without bridge piers are approximately equal, i.e., $h'_{f(1-n)} = h_{f(1-n)}$, Equation 4 becomes

$$y_1 - y_n = [\alpha_n (1 + K_L) - \alpha_1 (A_n/A_1)^2](U_n^2/2g) \quad (6)$$

Dividing by the normal hydraulic depth ($A_{n/B}$, where B is the channel top width) results in the nondimensional backwater expression

$$y^*/(A_n/B) = 1/2\,[\alpha_n (1 + K_L) - \alpha_1 (A_n/A_1)^2]\, F_n^2 \quad (7)$$

where $F_n = U_n/(gA_n/B)^{1/2}$ is the Froude number and $y^* = y_1 - y_n$ is the backwater. The pier energy-loss coefficient ($K_L$) is generally a function of the pier shape and degree of pier constric-

tion. As an approximation, the $\Delta K_p$ of Bradley (2), which is equivalent to $K_L$, may be used to evaluate $K_L$. Equation 7 requires a trial-and-error solution for $y_1$ that is easily computed in three to four iterations by using the Newton-Raphson convergence scheme once $A_1$ and $\alpha_1$ are in terms of $y_1$.

Backwater associated with the abrupt encroachments of cases III, IV, and V is found by applying the energy equation in a stepwise fashion to the control volumes shown in Figure 3. Given the downstream boundary condition $y_n$, the energy equation is applied between section n and section 3, where flow depth is a minimum, to solve for $y_3$. Data of Liu, Bradley, and Plate (3) indicate that section 3 roughly coincides with the downstream face of the embankment. Once $y_3$ has been determined, the energy equation is written from section 3 to section 1 and solved for $y_1$. The two energy expressions are thus

$$\alpha_3(U_3^2/2g) + y_3 + z_3 = \alpha_n(U_n^2/2g) + y_n + z_n + h_{f(3-n)} + h_{L(3-n)} \quad (8)$$

$$\alpha_1(U_1^2/2g) + y_1 + z_1 = \alpha_3(U_3^2/2g) + y_3 + z_3 + h_{f(1-3)} \quad (9)$$

where

$h_{f(3-n)}$ = friction loss occurring in the control volume bounded by sections 3 and n,
$h_{L(3-n)}$ = eddy loss occurring in the control volume bounded by sections 3 and n, and
$h_{f(1-3)}$ = friction loss occurring in the control volume bounded by sections 1 and 3.

Schneider and others (4) define the friction losses as follows:

$$h_{f(3-n)} = L_{(3-n)}Q^2/K_3K_4 \quad (10)$$

$$h_{f(1-3)} = [L_{(1-2)}Q^2/K_1K_3] + [L_{(2-3)}Q^2/K_3^2] \quad (11)$$

where K is the conveyance. Reach lengths $L_{(1-2)}$, $L_{(2-3)}$, and $L_{(3-n)}$ are determined as follows. The accelerating flow upstream from the abrupt encroachment may be studied by using potential-flow analysis. Figure 3 shows the streamlines that result from a Schwarz-Christoffel transformation of a potential source in a half-plane with boundaries representing those in open channel flow. Schneider and others (4) locate section 1 of the intersection of the center streamline and the equipotential line emanating from the points where the water edge and embankments intersect. Section 2 is located at the upstream face of the embankment. As demonstrated by Schneider and others (4), the straight-line distance between sections 1 and 2 is not representative of the average streamline length. Instead, the lengths of all streamlines are averaged to find $L_{(1-2)}$ as a function of the straight-line distance and the constriction ratio. The length $L_{(2-3)}$ is approximately the length of the abrupt encroachment, simply the bridge embankment width. As seen in Figure 3, the reach between sections 3 and n is characterized by large eddies downstream from the encroachment that result from flow separation occurring at or slightly upstream from section 3. The length of the separation zone, approximately $L_{(3-n)}$, is the distance from the efflux of the abrupt expansion to the point where flow reattaches to the sidewalls of the channel. For case III, measurements by Abbott and Kline (5) are used to estimate $L_{(3-n)}$ as a function of the area ratio. Field observations by Schneider and others (4) suggest that $L_{(3-n)}$ is one encroachment width b for cases IV and V.

Energy loss due to lateral mixing in the expansion reach is given by Taylor (1) as follows:

$$h_{L(3-n)} = K_L(H/b)(U_3^2/2g) \quad (12)$$

where H = (B - b)/2, the step height. For case III, $K_L$ is obtained by numerically integrating velocity-profile data for abrupt channel expansions, given by Lokrou (6). The relation between $K_L$ and the constriction ratio $\sigma$ = b/B is shown in Figure 4 (6). A different relation for $K_L$ is derived for cases IV and V based on the observed field data of Schneider and others (4); it is given in Figure 5.

With all energy-loss terms defined, Equation 8 is solved by trial and error for $y_3$; Equation 9 is then solved by trial and error for $y_1$ given $y_3$. A Newton-Raphson convergence scheme may be used to speed computations.

## Constriction Scour

The constriction scour resulting from bridge piers, cases I and II, was found to be negligibly small when compared with local scour. By using a physical model study, Laursen and Toch (7) found that the effect of pier contraction on scour will seldom be important in modern bridge design. They indicated that in order for the depth of scour to be appreciably affected, the contraction would have to be about 10 percent, an amount seldom attained in current bridge design practice. Although constriction scour is small for bridge piers, local scour may be substantial. The mechanics of local scour around piers has been discussed by Shen (8) and by Richardson and others (9).

Constriction scour for cases III, IV, and V is estimated by considering the equilibrium scour depth in a long constriction. The constriction-scour depth ($\Delta y_s$), shown in Figure 6, is found by

Figure 4. Coefficient of energy loss due to lateral mixing: case III.

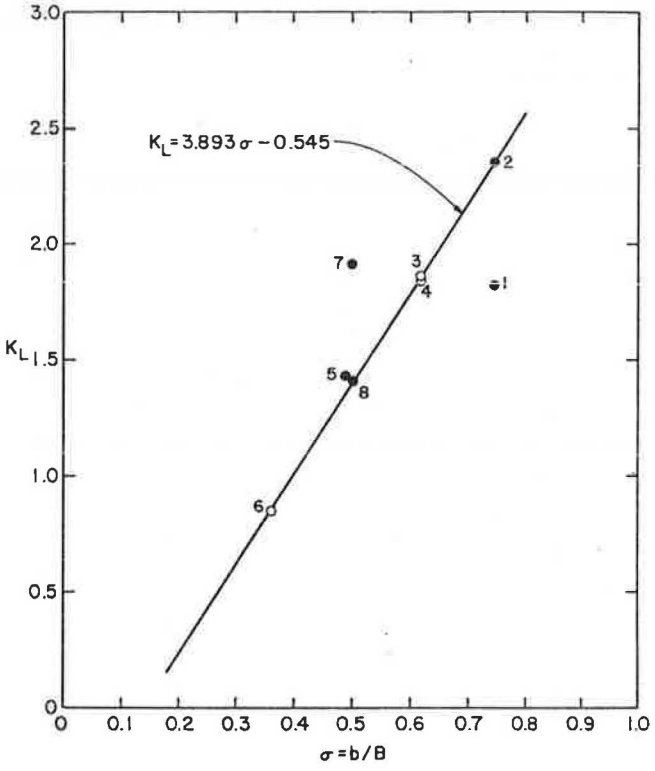

Figure 5. Coefficient of energy loss due to lateral mixing: cases IV and V.

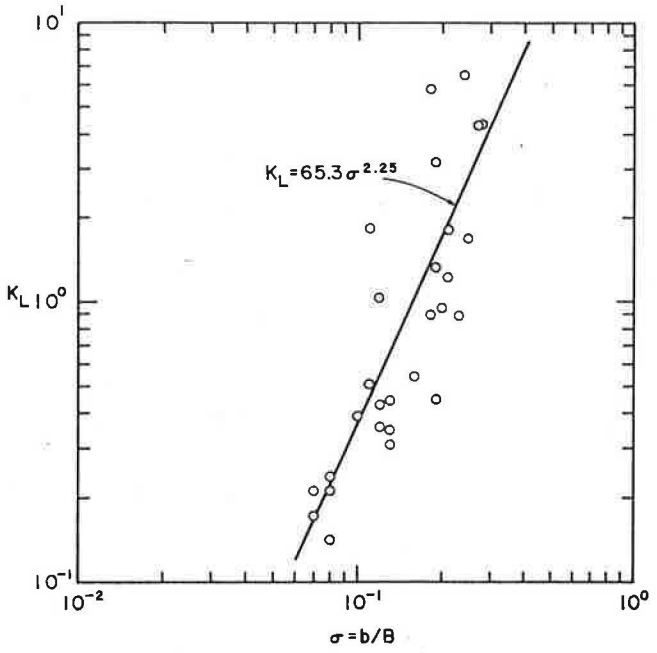


Figure 6. Definition sketches for constriction scour.

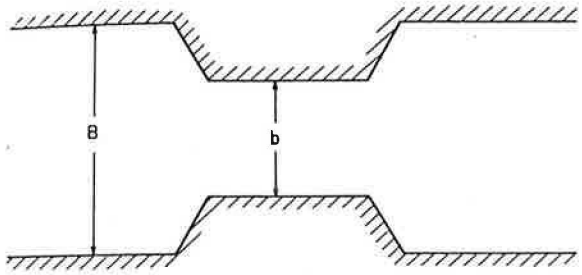


a. Plan View – Cases I, II and III

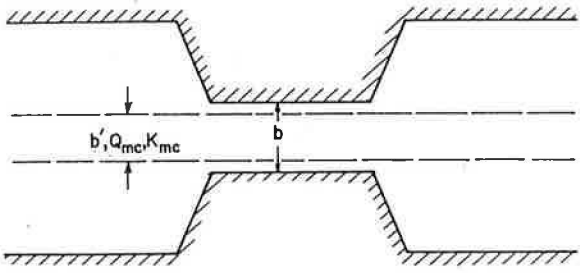


b. Plan View – Cases IV and V

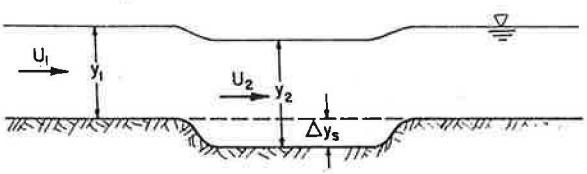


c. Profile View

Figure 7. Constriction scour: case III.

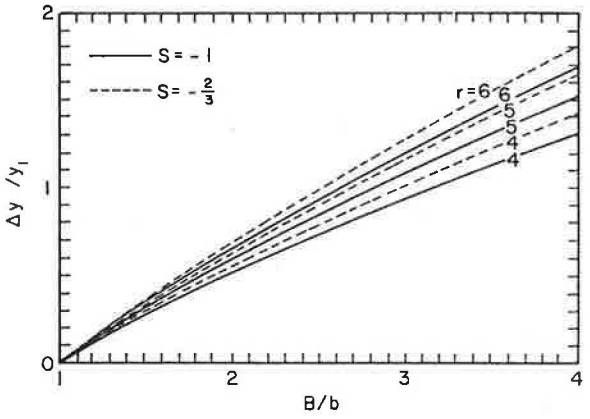


solving the equations of water continuity, sediment continuity, and sediment transport simultaneously. When the sediment transport into the constriction is the same as the transport out of the constriction, the scour hole achieves the dynamic equilibrium

$$Q_s = q_{s_1} B = q_{s_2} b \tag{13}$$

where $Q_s$ is the sediment discharge and $q_s$ is the sediment discharge per unit width.

For case III, a simple sediment transport function is chosen:

$$q_s = K U^r y^s \tag{14}$$

where K is an empirical coefficient, and the exponent $r > 0$ and $s < 0$. Laursen (10) has shown that the bed-load equations of Duboys, Shields, Schoklitsch, Meyer-Peter and Muller, and Brown-Einstein can be reduced to Equation 14. The coefficient K is generally a function of channel characteristics, channel roughness, and bed-material size. The exponent r ranges between 4 and 6, whereas the exponent s varies between -2/3 and -1. Solving Equations 5, 13, and 14 simultaneously and letting $\Delta y_s = y_2 - y_1$ gives

$$\Delta y_s / y_1 = (B/b)^{(1-r)/(s-r)} - 1 \tag{15}$$

Equation 15 is plotted in Figure 7 for r = 4, 5, 6, and s = -2/3, -1. In the absence of better data, choosing r = 6 and s = -2/3 will give a conservative estimate of constriction scour.

Constriction scour for cases IV and V is found by using the analysis by Laursen (11). Assuming that no sediment is transported over the floodplains, the Manning resistance equation, the water and sediment continuity equations, and the sediment transport relation given by Laursen (12) may be solved simultaneously to give

$$y_2/y_1 = (Q/Q_{mc})^{6/7} (b'/b)^{6/7\,[(2+a)/(3+a)]} (n_2/n_1)^{6/7\,[a/(3+a)]} \tag{16}$$

where $Q_{mc}$ is the discharge conveyed in the main channel, b' is the main-channel width, and a is the exponent depending on the ratio of shear velocity to fall velocity ($u_*/w$). Laursen's analysis (11) suggests that the maximum scour depths occur for large values of $u_*/w$. Assuming $a = 9/4$ ($u_*/w > 2$), $n_1 = n_2$, and $Q/Q_{mc} = K/K_{mc}$, Equation 16 may be written

$$\Delta y_s / y_1 = (K/K_{mc})^{0.86} (b'/b)^{0.69} - 1 \tag{17}$$

Negative values of $\Delta y_s/y_1$ may be obtained from Equation 17 but have no physical meaning. If negative values are computed, it is assumed that $\Delta y_s = 0$. For case IV, b'/b = 1 so that

$$\Delta y_s/y_1 = (K/K_{mc})^{0.86} - 1 \quad (18)$$

Equations 17 and 18 are plotted in Figure 8.

## Effects of Constriction Scour on Backwater

Constriction scour enlarges the bridge opening, which in turn relieves or reduces the backwater. Although the development of scour is a time-dependent process, the backwater in such a case may be estimated by assuming that the scour develops instantly. This is reasonable, because the time required for the constriction scour hole to achieve its full equilibrium depth is short, probably less than an hour for a sand-bed stream. To assess the effect of scour on backwater, the backwater is first computed based on the preceding energy analysis for the case of no scour, i.e., a rigid boundary assumption. The depth of constriction scour ($\Delta y_s$) is estimated from the appropriate scour relation--Equation 15, 17, or 18--and is subtracted from $z_3$ to obtain the elevation of the scoured bed. Backwater is then recomputed for the fully scoured condition. This procedure is termed the known cross-section method. The difference $y^* - y_s^*$, where $y_s^*$ is the backwater associated with constriction scour, reflects the amount that the backwater has been reduced by the scour.

# SIMPLE METHODS FOR ESTIMATING BACKWATER

The backwater equations presented in the previous section, with or without constriction scour, require an iterative solution for $y^*$ or $y_s^*$, which makes them impractical for quick, preliminary estimates of backwater. To avoid the trial-and-error procedure inherent in this or any other bridge backwater analysis, the backwater equations are formulated into an iterative computer model, which is used to synthesize a large data base. The synthesized backwater data, generated over a wide range of flow conditions and channel constrictions, are nondimensionalized. Regression analysis is used to fit a model from which backwater may be determined explicitly. Although the regression model may not be able to reproduce the results from the analytic expression exactly, the approximate nature and need for quick backwater estimates at the feasibility study level justify the approach.

Figure 8. Constriction scour: cases IV and V.

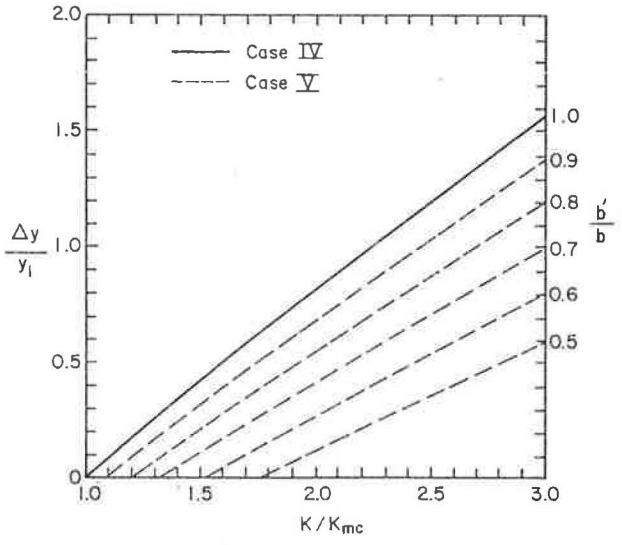


## Dimensional Analysis

Grouping variables nondimensionally into physically meaningful parameters is a useful way of reducing the number of independent variables describing bridge backwater. The analysis of backwater and constriction scour indicates that the general relation (cases I-V) for backwater is of the form

$$y^* = f(\alpha_n, Q, A_n, g, b, B, K, K_{mc}, K_L, n_{ob}, n_{mc}, \Delta y_s) \quad (19)$$

where $n_{ob}$ is the overbank and $n_{mc}$ is the main-channel Manning roughness coefficient. By inspection, Equation 19 is nondimensionalized to give

$$y^*/y_n = f[\alpha_n, Q/(g A_n^3/B)^{1/2}, b/B, K_{mc}/K, K_L, n_{mc}/n_{ob}, \Delta y_s/y_n] \quad (20)$$

in which

$$F_n = Q/(g A_n^3/B)^{1/2} \quad (21)$$

is recognized as the Froude number.

## Regression Analysis

The synthesized data base was nondimensionalized according to Equation 20 and transformed into logarithms. Stepwise (forward) regression analyses of the transformed data were made based on the following criteria: F-level for inclusion = 0.01; F-level for deletion = 0.005; and tolerance level = 0.001. Results of the regression analysis, including regression statistics of the transformed data, are given in Figures 9-16. For the sake of brevity, the extensive plotted results of case IV, rigid boundary, are not included. The complete results are discussed elsewhere (1). The regression equations may be easily solved for backwater by using a hand-held calculator, or if a graphical solution is desired, the figures may be used directly. The range of flow conditions, channel properties, and bridge opening widths for the data base is summarized in Figure 17. For the rigid boundary condition of case III (Figure 12), laboratory data of Liu, Bradley, and Plate (3) were used in the analysis rather than synthesized data.

## Discussion of Results

For the bridge piers of case I, the regression analysis indicated that the backwater ratio is a function of $F_n$ and $K_L$ only. For the case II bridge piers, regression analysis indicated that the product $(\alpha_n)^{1/2}F_n$ and $K_L$ describe the backwater ratio in nonuniform channels. The influence of pier width and spacing and pier shape is absorbed into the loss coefficient $K_L$. Because constriction scour was shown to be negligible for bridge piers, the results are applicable to both rigid- and movable-boundary conditions.

Laboratory data (simple normal crossing, vertical board abrupt encroachment) of Liu, Bradley, and Plate (3) were used in the case III rigid-boundary regression analysis. By combining $F_n$ and b/B into one term, the backwater was found to be a function of a single parameter. Because $K_L$ is a linear function of b/B (Figure 4), energy losses in terms of $K_L$ are contained implicitly in the denominator of $F_n/(b/B)$. For case III, movable-boundary backwater data were numerically simulated. The regres-

**Figure 9. Results of regression analysis.**

| Case | Boundary Type | Equation | | N | $R^2$ | S | Error |
|---|---|---|---|---|---|---|---|
| I | Rigid or Movable | $\frac{y^*}{y_n} = F_n^{[3.300+\log F_n(1.281+0.406\log F_n)]} K_L^{0.974}$ | (22) | 120 | 0.99 | 0.014 | ±3% |
| II | Rigid or Movable | $\frac{y^*}{A_n/B} = 0.815\,(\sqrt{\alpha_n}F_n)^X K_L^{0.615}$ | (23) | 189 | 0.99 | 0.026 | ±6% |
| | | $X = 2.434+0.223 \log \sqrt{\alpha_n}F_n+\log K_L(-1.152-0.759 \log \sqrt{\alpha_n}F_n)$ | (24) | | | | |
| III | Rigid | $\frac{y^*}{y_n} = 0.661\left(\frac{F_n}{b/B}\right)^{2.064}$ | (25) | 57 | 0.94 | N/A | |
| | Movable | $\frac{y^*_s}{y_n} = 0.181\left(\frac{F_n}{b/B}\right)^{2.208}$ | (26) | 360 | 0.98 | 0.090 | -19%, +23% |
| IV | Rigid | $\frac{y^*}{y_n} = 1.123\,F_n^{1.871}\left(\frac{K_{mc}}{K}\right)^{-3.116}\left(\frac{b}{B}\right)^{0.553}\left(\frac{n_{mc}}{n_{ob}}\right)^{-0.805}$ | (27) | 225 | 0.96 | 0.16 | -31%, +45% |
| | Movable | $\frac{y^*_s}{y_n} = 1.173\,F_n^{1.148}\left(\frac{y^*}{y_n}\right)^{0.413}$ | (28) | 225 | 0.97 | 0.13 | -26%, +35% |
| V | Rigid | $\frac{y^*}{y_n} = 1.123\,F_n^{1.871}\left(\frac{K_{mc}}{K}\right)^{-3.116}\left(\frac{b'}{B}\right)^{0.553}\left(\frac{n_{mc}}{n_{ob}}\right)^{-0.805}$ | (29) | 675 | — | — | |
| | Movable | $\frac{y^*_s}{y_n} = 1.218\,F_n^{0.795}\left(\frac{y^*}{y_n}\right)^{0.566}$ | (30) | 675 | 0.97 | 0.15 | -29%, +41% |

N = number of samples
$R^2$ = coefficient of determination
S = standard error of estimate
Error: 2/3 of the data fell within this error range

sion analysis indicated that the movable-boundary backwater could also be expressed as a function of the single variable $F_n/(b/B)$. The constriction scour depth ($\Delta y_s$) is included implicitly in b/B, as suggested by Equation 15. Although exponents r and s were varied in the simulation ($4 < r < 6$ and $-2/3 < s < -1$), the backwater was found to be insensitive to these parameters. An expression relating the movable-boundary backwater to the rigid-boundary backwater is found by dividing Equation 25 by Equation 24, or

$$y_s^*/y^* = 0.274\,[F_n/(b/B)]^{0.144} \quad (30)$$

This relation indicates the degree to which constriction scour will relieve the backwater from the rigid-boundary condition.

Backwater for case IV, rigid boundary, was found to be a function of four variables, as given by Equation 26. Stepwise regression showed that $F_n$ and $K_{mc}/K$ accounted for 95 percent of the variation in $y^*/y_n$, although b/B and $n_{mc}/n_{ob}$ were significant at an F-level for inclusion of 0.01. The standard error of the estimate (S = 0.16) suggests that the error associated with Equation 26 is -31 to +45 percent. The kinetic energy correction factor ($\alpha_n$) was not found to be a significant parameter, even though $\alpha_n$ varied over a wide range ($1 < \alpha_n < 9$). A simple model for case IV, movable boundary, was developed by relating the movable-boundary backwater to the rigid-boundary backwater so that $y_s^*/y_n = f(F_n, y^*/y_n)$. Constriction scour ($\Delta y_s$) as given by Equation 18 is a function of $k_{mc}/K$ and is thus contained implicitly in $y^*/y_n$. The standard error of the estimate (S = 0.13) suggests that the absolute error in using the movable-boundary relation (Equation 27) is -26 percent, +35 percent. A more accurate estimate of the movable-boundary backwater may be obtained from

$$y_s^*/y_n = 8.93F_n^{1.93}\,(\Delta y_s/y_n)^{0.650}\,(b/B)^{0.921}\,(n_{mc}/n_{ob})^{-1.06} \quad (31)$$

in which $R^2 = 0.99$ and S = 0.061; the absolute error is -13 to +15 percent. For the sake of brevity, no graphical solution of Equation 31 is given.

For the range of conditions investigated, the backwater for the partial floodplain encroachment case V, rigid boundary, was found to be of the same order as that for case IV. A comparison of the case V backwater against case IV backwater is shown in Figure 16. Evidently the backwater is nearly the same for both cases over the investigated range of b'/b, although the expected decreasing trend for case V is somewhat apparent. More data are required to assess the flow distribution and energy losses for case V, because Figure 16 indicates that in some instances the backwater for case V is greater than that for case IV, a physical impossibility. For practical purposes, however, the rigid-boundary backwater of case V may be conservatively evaluated by using the relation for case IV. The movable-boundary backwater relation for case V is similar to that developed for case IV, i.e., $y_s^*/y_n = f(F_n, y^*/y_n)$, although the numerical constants differ in magnitude. The standard error of the estimate (S = 0.15) suggests that the absolute error in using the movable-boundary backwater relation (Equation 29) is -29 percent, +41 percent.

## PRACTICAL APPLICATION

Practical application of the simplified backwater and constriction scour relations is demonstrated as follows:

Step 1: Estimate the uniform-flow conditions of the river reach under consideration for the design discharge. If a rating curve does not exist, the Manning equation may be used to derive the rating curve. Cross-sectional area, wetted perimeter, and top width may be tabulated from river cross sections. The river slope may be computed from river cross sections or topographic maps. Studies by Chow (13) and Barnes (14) are useful references for estimating Manning n-values.

Step 2: After the river configuration has been studied, use Figure 1 to categorize the river crossing as case I, case II, and so on. Enter Figure 9

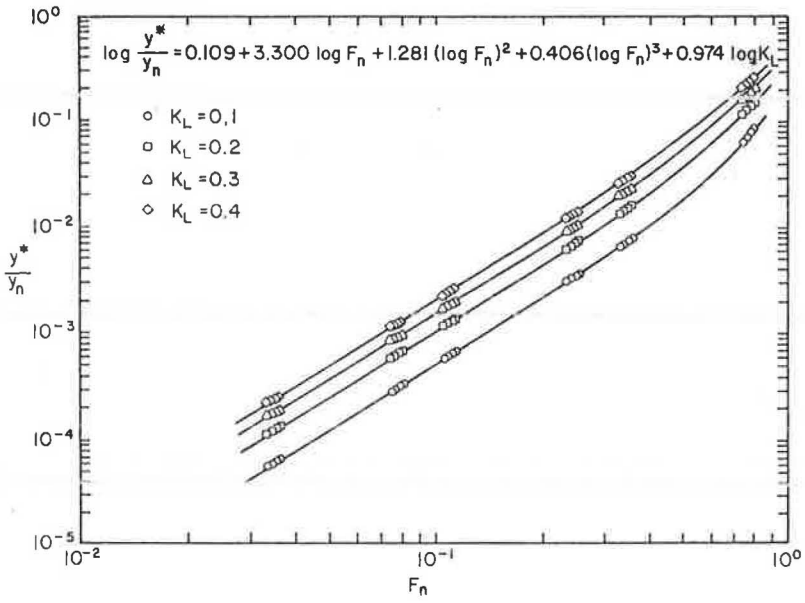


Figure 10. Change in water-surface elevation: case I, rigid boundary.

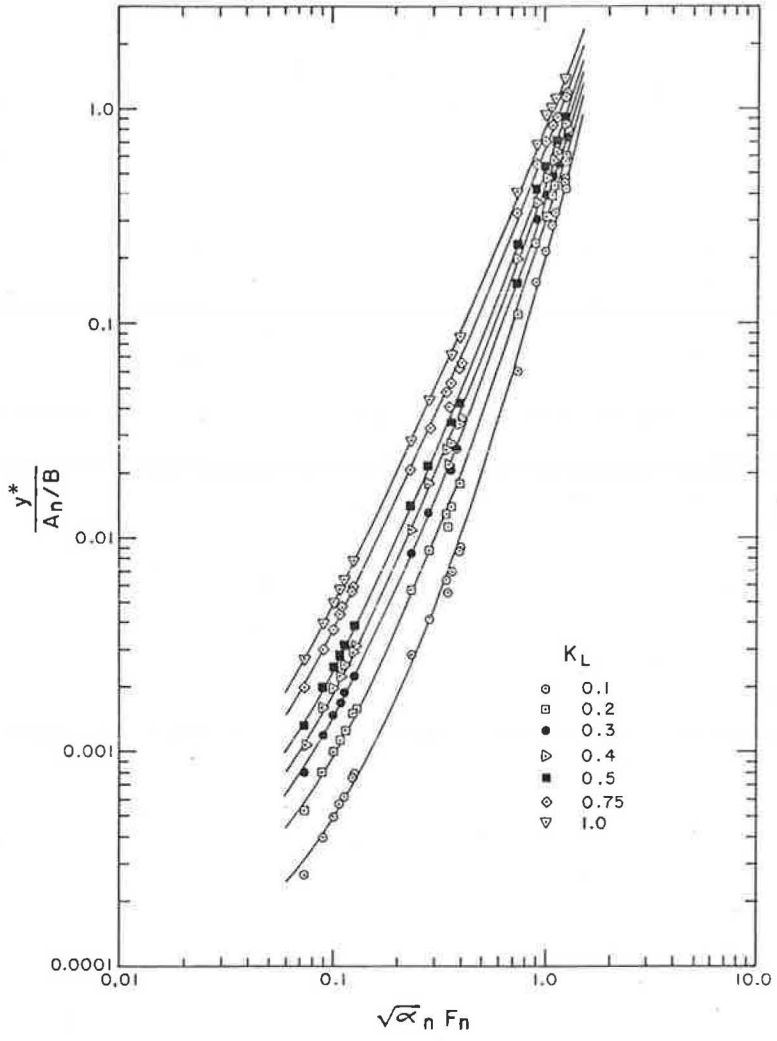


Figure 11. Change in water-surface elevation: case II, rigid boundary.

Figure 12. Change in water-surface elevation: case III, rigid boundary.

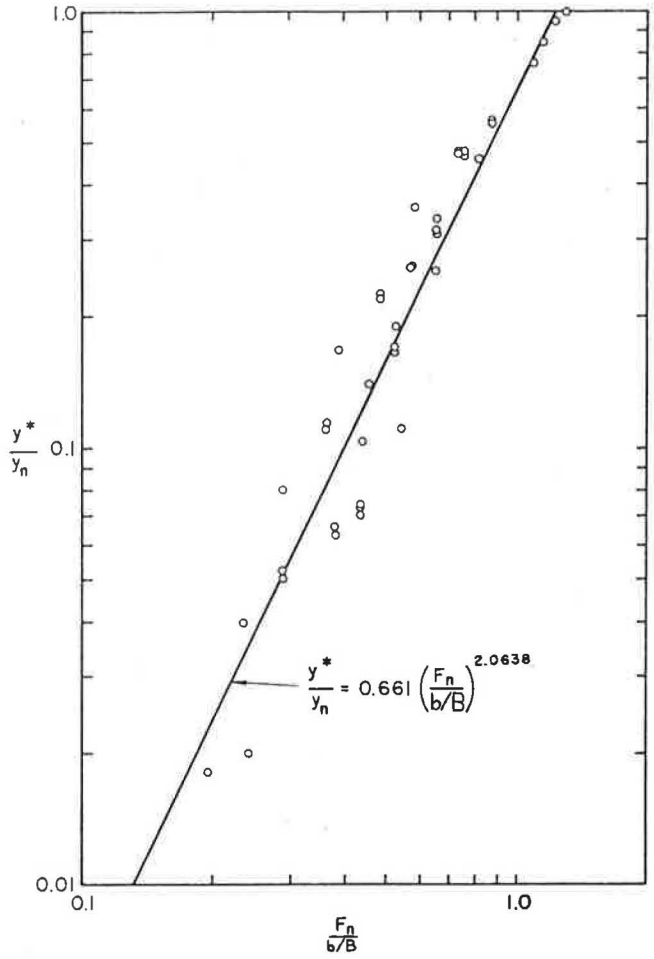


Figure 13. Change in water-surface elevation: case III, movable boundary.

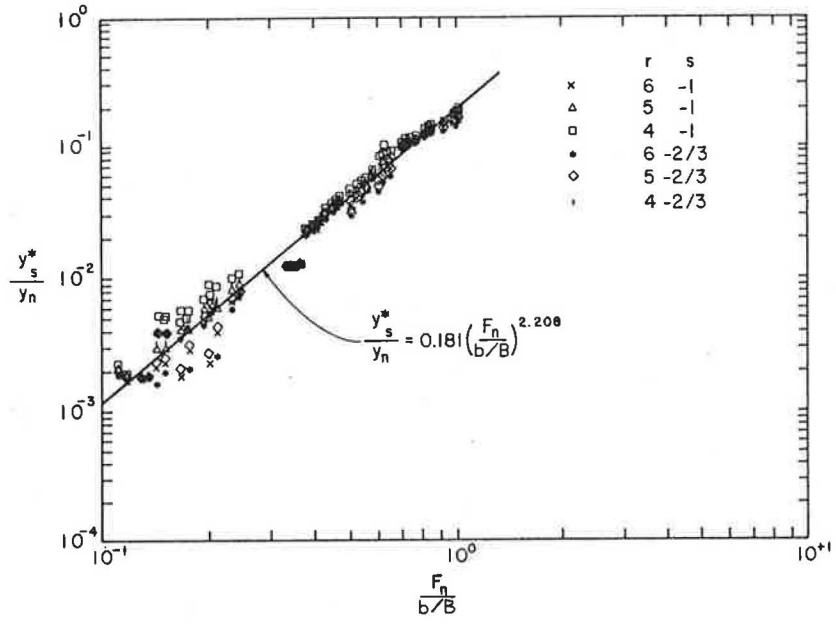

to locate the appropriate backwater relations. Estimate the required nondimensional independent variables ($F_n$, b/B, $K_{mc}/K$, $n_{mc}/n_{ob}$, $K_L$).

Step 3: Compute the backwater ratio $y^*/y_1$ by assuming rigid-boundary hydraulics from the appropriate relation in Figure 9.

Step 4: Compute the constriction scour ratio $\Delta y_s/y_1$. If the bridge category is case I or case II, constriction scour is assumed to be negligible. For the remaining cases compute $\Delta y_s/y_1$ as follows: case III, Equation 15; case IV, Equation 18; and case V, Equation 17.

Step 5: Compute the backwater ratio $y_s^*/y_1$ by assuming movable boundary hydraulics from the appropriate relation in Figure 9.

Step 6: If the increase in stage ($y^*$ or $y_s^*$, depending on whether the boundary is rigid or movable) is unacceptable, assume a new bridge opening and recompute $y^*$ or $y_s^*$.

As with all regression-based equations, extrapolation outside the data range over which the equations were developed may give erroneous results.

## SUMMARY AND CONCLUSIONS

### Analysis of Backwater and Constriction Scour

Expressions for backwater based on the conservation of energy in open-channel flow were presented for five commonly occurring bridge crossings. To satisfy the one-dimensional flow assumption, the theories of potential flow and empirical results were used to locate cross sections in zones of nearly one-dimensional flow. An expression for constriction scour was derived as a function of the ratio of channel width to bridge opening width and exponents describing the bed-load transport rate. A procedure referred to as the known cross-section method was

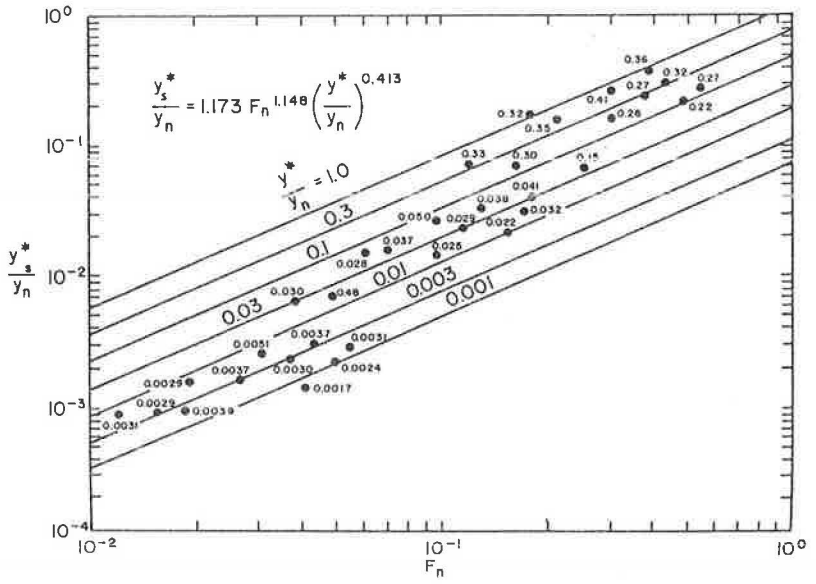


Figure 14. Change in water-surface elevation: case IV, movable boundary.

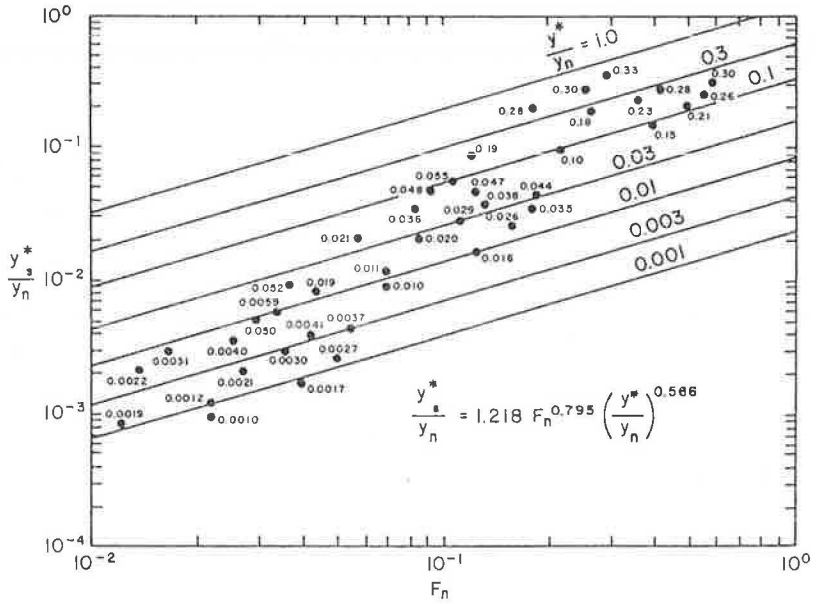


Figure 15. Change in water-surface elevation: case V, movable boundary.

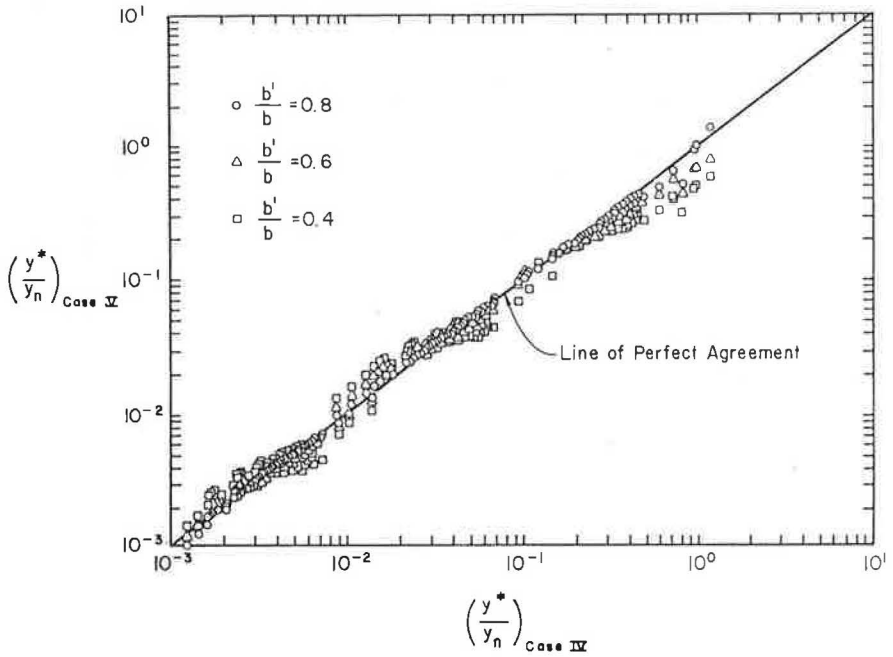


Figure 16. Comparison of changes in water-surface elevation for cases IV and V, rigid boundary.

Figure 17. Range of data used in regression analysis.

| Case | $y_n$(ft) | b(ft) | b'(ft) | B(ft) | z'(ft) | $S_o$ | $n_{mc}$ | $n_{ob}$ | Q($ft^3/s$) | $K_r$ | $F_n$ |
|---|---|---|---|---|---|---|---|---|---|---|---|
| I | 10–50 | 82–98 | — | 100 | — | 0.00001–0.005 | 0.030 | — | 640–150,000 | 0.1 –0.4 | 0.033–0.81 |
| II | 3–20 | 82–98 | 10–30 | 100 | 1–15 | 0.0001 –0.01 | 0.030 | 0.01 | 69– 15,200 | 0.1 –1.0 | 0.04 –0.91 |
| III Rigid | 0.33–0.72 | 2– 6 | — | 7.9 | — | 0.001 –0.0012 | 0.022 | — | 2.5–5.0 | — | 0.065–0.29 |
| III Movable | 1–52 | 50–90 | — | 100 | — | 0.00014–0.0019 | 0.030 | — | 57– 99,000 | 1.4 –3.0 | 0.1 –0.5 |
| IV | 12–80 | 50–250 | 50–250 | 1000 | 10–50 | 0.00001–0.001 | 0.030 | 0.075–0.15 | 490–590,000 | 0.077–2.9 | 0.12–0.59 |
| V | 12–80 | 62.5–625 | 50–250 | 1000 | 10–50 | 0.00001–0.001 | 0.030 | 0.075–0.15 | 490–590,000 | 0.13 –23 | 0.12–0.59 |

developed for easily assessing the effects of constriction scour on backwater.

## Simple Methods for Estimating Backwater

Through numerical simulation, dimensional analysis, and regression analysis, explicit relations for bridge backwater were developed for both rigid- and movable-boundary conditions. For bridge piers, it was found that the backwater is a function of the Froude number, the kinetic-energy coefficient, and a pier energy-loss coefficient. The Froude number and the ratio of bridge opening width to channel width were found to describe the backwater in a channel abrupt encroachment. In the case of floodplain encroachments, the Froude number and the ratio of main channel conveyance to total conveyance were found to be the primary parameters controlling backwater. These solutions are of an accuracy suitable for use in a bridge feasibility or preliminary design study; the backwater regression equations, however, are not intended for detailed analyses.

## Practical Application

Step-by-step procedures were given to demonstrate how the simple backwater and constriction scour relations may be applied to feasibility studies.

## Recommendations

Further studies are necessary to quantify the multidimensional flow phenomena resulting from floodplain encroachment. The time dependence of bridge scour and development of armor layers within the bridge waterway also need further investigation. Last, both analytic and simplified procedures need to be verified against field data.

## REFERENCES

1. S.W. Taylor. Flow Modification by Bridges and Abrupt Encroachments. Department of Civil Engineering, Colorado State Univ., Fort Collins, Colo., M.S. thesis, 1982.
2. J.N. Bradley. Hydraulics of Bridge Waterways. FHWA, Hydraulic Design Series 1, 1978.
3. H.K. Liu, J.N. Bradley, and G.J. Plate. Backwater Effects of Piers and Abutments. Colorado State Univ., Fort Collins, Colo., Rept. CER57HKL10, 1957.
4. V.R. Schneider, J.W. Board, B.E. Colson, F.H. Lee, and L. Druffel. Computation of Backwater and Discharges at Width Constrictions of Heavily Vegetated Flood Plains. U.S. Geological Survey, Reston, Va., Water Resources Investigation 76-129, 1977.
5. D.E. Abbott and S.J. Kline. Experimental Investigation of Subsonic Turbulent Flow Over Single and Double Backward Facing Steps. ASME Journal of Basic Engineering, Series D, Vol. 84, 1962, pp. 317-325.

6. V.P. Lokrou. Characteristics of Flow in Channel Abrupt Expansions. Department of Civil Engineering, Colorado State Univ., Fort Collins, Colo., Ph.D. thesis, 1979.
7. E.M. Laursen and A. Toch. Scour Around Bridge Piers and Abutments. Iowa Highway Research Board, Bull. 4, May 1956, pp. 36-38.
8. H.W. Shen. Scour Near Piers. In River Mechanics (H.W. Shen, ed.), Volume 2, Chapter 23, Colorado State Univ., Fort Collins, Colo., 1971.
9. E.V. Richardson, D.B. Simons, S. Karaki, K. Mahmood, and M.A. Stevens. Highways in the River Environment: Hydraulic and Environmental Design Considerations. FHWA, Training and Design Manual, May 1975.
10. E.M. Laursen. The Application of Sediment Transport Mechanics to Stable Channel Design. Journal of the Hydraulics Division of ASCE, Vol. 82, No. HY4, 1956.
11. E.M. Laursen. Scour at Bridge Crossings. Journal of the Hydraulics Division of ASCE, Vol. 86, No. HY2, Proc. Paper 2369, Feb. 1960, pp. 39-54.
12. E.M. Laursen. The Total Sediment Load of Streams. Journal of the Hydraulics Division of ASCE, Vol. 84, No. HY1, Proc. Paper 1530, Feb. 1958, pp. 1530-1 through 1530-36.
13. V.T. Chow. Open-Channel Hydraulics. McGraw-Hill, New York, 1959.
14. H.H. Barnes. Roughness Characteristics of Natural Channels. U.S. Geological Survey, Reston, Va., Water-Supply Paper 1849, 1977.